

UNDERSTANDING THE ROLE OF AKAP150 PALMITOYLATION IN SYNAPTIC
PLASTICITY

by

ALICIA MAE PURKEY

B.A. University of Colorado, Boulder 2011

A thesis submitted to the
Faculty of the Graduate School of the
University of Colorado in partial fulfillment
of the requirements for the degree of
Doctor of Philosophy
Pharmacology Program

2019

This thesis for the Doctor of Philosophy degree by

Alicia Mae Purkey

has been approved for the

Pharmacology Program

by

Matthew J. Kennedy, Chair

K. Ulrich Bayer

Timothy Benke

Angeles Ribera

Katharine Smith

Mark L. Dell'Acqua, Advisor

Date: 08/09/2019

Purkey, Alicia Mae (Ph.D., Pharmacology)

Understanding the Role of AKAP150 Palmitoylation in Synaptic Plasticity

Thesis directed by Professor Mark L. Dell'Acqua

ABSTRACT¹

Ca²⁺-permeable AMPA-type glutamate receptors (CP-AMPA) containing GluA1 but lacking GluA2 subunits contribute to multiple forms of synaptic plasticity, including long-term potentiation (LTP), but mechanisms regulating CP-AMPA are poorly understood. A-kinase anchoring protein (AKAP) 150 scaffolds kinases and phosphatases to regulate GluA1 phosphorylation and trafficking, and trafficking of AKAP150 itself is modulated by palmitoylation on two Cys residues. Here, we developed a palmitoylation-deficient knock-in mouse to show that AKAP150 palmitoylation regulates CP-AMPA incorporation at hippocampal synapses. Using biochemical, super-resolution imaging, and electrophysiological approaches, we found that palmitoylation promotes AKAP150 localization to recycling endosomes and the postsynaptic density (PSD) to limit CP-AMPA basal synaptic incorporation. In addition, we found that AKAP150 palmitoylation is required for LTP induced by weaker stimulation that recruits CP-AMPA to synapses but not stronger stimulation that recruits GluA2-containing AMPA. Thus, AKAP150 palmitoylation controls its subcellular localization to maintain proper basal and activity-dependent regulation of synaptic AMPA subunit composition.

¹ Portions of this chapter were previously published in *Cell Reports* and are included with permission of the copyright holder.¹

The form and content of this abstract are approved. I recommend its publication.

Approved: Mark L. Dell'Acqua

ACKNOWLEDGEMENTS

I am incredibly thankful for many individuals and their support throughout the process of graduate school. First, thank you Mark Dell'Acqua for accepting me into your lab and being an excellent mentor. Not only did you give me the opportunity to thrive in a remarkable scientific environment but you also allowed me the opportunity to travel, meet new people and advance my career. You are so highly respected in the field and I aspire to be like you; thank you for teaching me how to write grants and papers, conduct meaningful and thorough science, and be a collaborative coworker. Also, thanks to the past and present members of the Dell'Acqua lab. I would especially like to acknowledge Emily Gibson, Kevin Woolfrey, and Kevin Crosby; thank you Emily for your lab/life support, Kevin Woolfrey for co-piloting the CS project (Chapter III: APEGs assays, SEP-TfR imaging) and for being my in-lab mentor/sibling for the entirety of my graduate career, and Kevin Crosby for general wisdom and help with super resolution imaging troubleshooting and analysis (Chapter III: STED image analysis). I would also like to thank Dominik Stich in the Advanced Light Microscopy Core for helping maintain the STED microscope and acquiring images (Chapter III: STED imaging). Additionally, thank you to Wallace Chick in the Transgenic and Gene Targeting Core for helping develop the AKAP CS mouse that became the focus of my thesis work.

Thanks to my thesis committee for continuous support and engagement. Thank you for being around to answer questions outside of committee meetings and writing me letters of recommendation for grant and job applications. Specifically, thanks to Matt for keeping things on track and always providing excellent support, Angie for going the extra mile in preparation for my NRSA and post-doc interviews, Tim for always helping

with excellent ephys questions, Ulli for his fantastic grantsmanship and advice, and Kate for being a role model colleague and friend. I am thankful for all of your extended mentorship.

The Synaptic Plasticity Group deserves many thanks including: Drs. Jason Aoto, Ulli Bayer, Tim Benke, Chris Forde, Matt Kennedy, Won Chan Oh, Kate Smith and their lab members. Thank you all for creating a family-like environment at work, where support is always close. I will sincerely miss the ability to just walk down the hall to ask questions, get a reagent or talk science with you. Especially, thanks are due to Jason Aoto for allowing me to be an honorary member of the Aoto lab for a while and teaching me patch clamping. Thank you for the resources and technical support. I'd also like to thank my past labs for instilling in me a love of research and allowing me to gain skills that have led to my success in graduate school and beyond. Thank you to the Keller lab at CU Boulder (especially Dorian Mitchem and Matt Keller) and the Messersmith lab at CU Anschutz (especially Stacey Bagby and John Arcaroli).

Thanks to the Pharmacology Graduate Training Program, Dr. Port, Elizabeth Bowen and Shanelle Felder. You all believe in the students and tirelessly work for us to succeed. Thank you for always putting us first and providing a perfect example of how a graduate program should be run. Thanks to the student cohort (current and previous), especially Brooke Sinnen. Graduate school would have been much more difficult and lonely without you. I continue to learn from you every day in science and life. Thank you for always believing in me and supporting me, be it through extended conversations about science, watching me give every talk of my graduate school career, editing my grants and papers, and even being my roomie for every conference and retreat ever. I

am grateful to call you a colleague and a true friend/homomeric complex. Thanks to the Department of Pharmacology, especially Catherine Lambert. Thank you Cathy for always having your door open and for holding my hand through grant applications. I only hope there is something close to a “Cathy” at every institute I go in the future. And speaking of grant applications, I would also like to acknowledge my funding sources, NINDS and AHA, which supported my graduate school education and science.

And ultimately, without the support of my family I would not have made it to graduate school, let alone through graduate school. First and foremost, thank you to my parents Robert and JoAnne Purkey. You have always supported me in everything I have done and, truly, my success is your success. I love and appreciate my husband and best friend Josh Hulstrom. Thank you for being the calming and grounding influence I desperately need. Thanks to all of my family, especially my immediate family (including but certainly not limited to Ariana Alberici, Kaila Alberici, Delane Moehring, Annette Purkey, Carey Purkey, Jake Purkey, Luke Purkey, and Rob Purkey) for always showing a sincere interest in my research and general well-being. Thank you to my grandparents, especially Richard and Patricia Robb. Your support sustains me and reminds me of what matters most. And, finally, thank you to anyone reading this thesis!

TABLE OF CONTENTS

<u>CHAPTER</u>	<u>Page</u>
I INTRODUCTION	1
Hippocampus: circuitry and relevance in learning and memory	1
Excitatory synapses	3
Pre-synaptic terminal	5
Synaptic cleft.....	6
Post-synaptic compartment.....	6
Glutamate receptors	9
AMPA receptors	9
AMPA receptor properties and assembly	9
AMPA variable CTD contributes to subunit regulation	15
AMPA synaptic organization	18
Auxiliary proteins	19
Outstanding questions	20
NMDA receptors.....	21
Synaptic plasticity	23
Long-Term Potentiation (LTP).....	23
History of LTP in the hippocampus.....	23
Calcium-permeable AMPARs and LTP	25
Controversy surrounding CP-AMPA involvement in LTP	27
LTP mechanisms: AMPAR recruitment hypotheses.....	28
AMPA insertion models: trafficking and lateral diffusion	28

AMPA synaptic recruitment by means of phosphorylation	32
AMPA organization within the synapse during LTP.	33
Other LTP phenomena: structural plasticity and LTP in vivo.....	37
Structural plasticity.....	37
LTP correlates to learning and memory in vivo.....	37
Long Term Depression (LTD)	39
Additional LTD happenings: structural plasticity and LTD <i>in vivo</i>	41
Plasticity and learning and memory in disease	42
A-kinase anchoring proteins	43
AKAP79/150.....	44
AKAP79/150 mutation studies	46
AKAP150 knockout (KO)	47
AKAP150-PKA binding deficient mutants Δ PKA and D36	49
AKAP150-CaN binding deficient mutant Δ PIX.....	50
Protein palmitoylation	50
Palmitoylation, the dynamic post-translational lipidation	50
Enzymes governing palmitoylation.....	53
DHHCs.....	53
PPTs.....	56
Detecting palmitoylation in cells	59
Metabolic labeling.....	59
Biochemical approaches to palmitoylation detection.....	61
Synaptic protein palmitoylation	64

Palmitoylation in neuronal pathology	65
AKAP79/150 palmitoylation.....	69
II THESIS STATEMENT	71
Rationale.....	71
Research question.....	71
Specific aims	72
Hypotheses.....	72
III AKAP150 PALMITOYLATION REGULATES SYNAPTIC INCORPORATION OF CA2+-PERMEABLE AMPARS BASALLY AND DURING LTP	73
Introduction	73
Aims	76
Materials and methods	76
Generation of AKAP150 CS knock-in mice	76
Primary mouse hippocampal neuron culture.....	77
Fractionation and immunoblotting of brain tissue.....	78
APEGs palmitoylation assay	78
Extracellular fEPSP recordings	79
Whole-cell electrophysiology.....	80
TF-488 feeding to label REs	82
SEP-TfR imaging.....	83
Immunocytochemistry on mouse primary hippocampal neuron cultures for dendritic spine analysis.....	83
Dendritic spine analysis by Dil labeling	84

Surface GluA1 antibody labeling	84
Super-resolution stimulated emission depletion (STED) nanoscopy	85
STED image analysis	85
Quantification and statistical analysis	87
Results	87
AKAP CS palmitoylation-deficient knock-in mice exhibit reduced AKAP150 levels in PSD-enriched fractions.	87
AKAP CS dendritic spines contain smaller AKAP150 nanodomains that exhibit reduced overlap with the PSD.....	91
AKAP CS localization to recycling endosomes is decreased.....	93
AKAP CS mice exhibit enhanced CP-AMPA-mediated basal synaptic transmission.	94
AKAP150 palmitoylation is required for expression of CP-AMPA-dependent but not CP-AMPA-independent LTP.....	104
AKAP CS mice exhibit enhanced, CP-AMPA-dependent de-depression after prior induction of LTD.	105
Summary and discussion	108
AKAP150 palmitoylation and PKA/CaN anchoring in control of basal CP-AMPA incorporation	111
AKAP150 palmitoylation and PKA/CaN anchoring in CP-AMPA meta-plasticity that controls LTP/LTD balance.....	112
AKAP palmitoylation and signaling in multiple locations during LTP and LTD.....	114

IV EXPLORING FURTHER MECHANISMS OF AMPAR REGULATION IN AKAP CS	
MICE.....	117
Introduction.....	117
Aims	118
Materials and methods	119
Results	121
AKAP CS animals have normal extrasynaptic receptor composition.....	121
CP-AMPA involvement in basal transmission in AKAP CS animals.....	121
Impaired response to cLTP in AKAP CS mouse cultures.....	123
Conclusions and discussion	125
V CONCLUSIONS AND FUTURE DIRECTIONS	128
Broad implications.....	128
Key findings	128
Remaining questions and future directions.....	129
AMPA trafficking and the recycling endosome	129
The CS frequency dilemma.....	131
Age-dependent and behavioral outcomes of AKAP palmitoylation disruption	131
Intact LTD: AKAP's palmitoylation state and signaling mechanisms during LTD .	132
Spatial and temporal control of AKAP palmitoylation.....	132
REFERENCES	135

LIST OF TABLES

Table 1.1 CP-AMPA plasticity studies	29
Table 1.2 AMPAR studies in transgenic mice	34
Table 1.3 AKAP150 transgenic mouse model studies	51
Table 3.1: Key resources table.....	86
Table 4.1: Key resources table.....	120

LIST OF FIGURES

Figure 1.1: Structure of the rodent hippocampus.	2
Figure 1.2: Excitatory synapses in CA1 of the hippocampus.	4
Figure 1.3: Ionotropic glutamate receptor structure.	10
Figure 1.4: AMPAR structure and characteristics.	13
Figure 1.5: AKAP150 WT and binding-deficient mutants.	48
Figure 1.6: The DHHC proteins and palmitoylation mechanism.	58
Figure 1.7: Palmitoylation detection techniques.	62
Figure 3.1: AKAP150 and PKA-RII levels are reduced in PSD-enriched fractions from AKAP CS palmitoylation-deficient mice.	88
Figure 3.2: Additional characterization of AKAP CS mice and cultured neurons.	89
Figure 3.3: AKAP150 CS localization to the PSD is reduced.	92
Figure 3.4: AKAP150 CS endosome localization and RE exocytosis.	95
Figure 3.5: AKAP CS mice exhibit slightly increased AMPAR mEPSC amplitude and decreased frequency but normal evoked basal transmission at hippocampal CA1 synapses.	97
Figure 3.6: Electrophysiological characterization of AKAP CS cultures.	98
Figure 3.7: AKAP CS mice have elevated basal CP-AMPA activity at CA1 synapses.	101
Figure 3.7: AKAP CS mice have elevated basal CP-AMPA activity at CA1 synapses.	102
Figure 3.8: Analysis of GluA1 S845 phosphorylation.	103

Figure 3.9: CP-AMPA-dependent LTP at CA1 synapses is impaired in AKAP CS mice.
..... 106

Figure 3.9: CP-AMPA-dependent LTP at CA1 synapses is impaired in AKAP CS mice.
..... 107

Figure 3.10: AKAP CS mice can undergo CP-AMPA-dependent de-depression at CA1
synapses. 109

Figure 3.11: Summary of findings from Chapter III. 110

Figure 4.1: Normal TBOA response in AKAP CS mice. 122

Figure 4.2: AMPAR-minis after chronic CP-AMPA blockade and cLTP. 124

ABBREVIATIONS

ABE	acyl biotinyl-exchange
ABHD	alpha/beta-hydrolase fold domain
ABP	AMPA-binding protein, also known as GRIP-2
AC	adenylyl cyclase, also known as adenylyl cyclase and adenylylate cyclase
ACSF	artificial cerebrospinal fluid
acyl-RAC	acyl resin-assisted capture
AD	Alzheimer's disease
AKAP	A-kinase anchoring protein
AKAP CS	palmitoylation-deficient AKAP79 or 150
AMPA	α -amino-3-hydroxy-5-methyl-4-isoxazolepropionic acid receptors
AP	action potential
APE	acyl polyethylene glycol exchange
APEGs	acyl-PEG exchange gel-shift
APP	amyloid precursor protein
APT1	acylprotein thioesterase-1
APV/AP5	(2R)-amino-5-phosphonopentanoate/(2R)-amino-5-phosphonovaleric acid
AZ	active zone
A β	beta-amyloid
BAC	bacterial artificial chromosome
BACE1	beta-secretase
BAPTA	1,2-bis(o-aminophenoxy)ethane-N,N,N',N'-tetraacetic acid
BiP	immunoglobulin binding protein
BSA	bovine serum albumin
C-terminal	carboxy terminal
C57BL/6	C57 black 6 inbred strain of laboratory mice
CA	cornu ammonis
CA1	cornu ammonis area 1
CA3	cornu ammonis area 3
CALI	chromophore-assisted light inactivation
CAM	cell adhesion molecule
CaMKII	calcium/calmodulin-dependent protein kinase II
cAMP	cyclic adenosine monophosphate
CaN	calcineurin
CDK5	cyclin dependent kinase 5
CI-AMPA	calcium-impermeable AMPA
cLTD	chemical LTD
cLTP	chemical LTP
CMP	chloroform-methanol precipitation
CNS	central nervous system

CP-AMPA	calcium-permeable AMPAR
CRD	cysteine rich domain
cTBS	compressed theta burst stimulation
CTD	carboxy-terminal domain
D36	AKAP PKA binding mutant via a 36 amino acid C-terminal truncation
DAG	diacylglycerol
DG	dentate gyrus
DHHC	aspartate-histidine-histidine-cysteine
DHPG	dihydroxyphenylglycine
Dil	1,1'-Dioctadecyl-3,3',3',3'-Tetramethylindocarbocyanine Perchlorate ('Dil'; DiIC18(3))
DIV	days in vitro
EC	entorhinal cortex
ECL	enhanced chemiluminescence
ECR	extracellular region
EDTA	ethylenediaminetetraacetic acid
EEA1	early endosome antigen 1
EM-CCD	electron-multiplying charge-coupled device
ER	endoplasmic reticulum
ES cell	embryonic stem cell
F-actin	filamentous actin
fEPSP	field excitatory post-synaptic potential
FYN	proto-oncogene tyrosine-protein kinase Fyn
GABA	gamma-Aminobutyric acid
GluA1	AMPA-type glutamate receptor subunit 1
GluA2	AMPA-type glutamate receptor subunit 2
GluA3	AMPA-type glutamate receptor subunit 3
GluA4	AMPA-type glutamate receptor subunit 4
GluN1	NMDAR-type glutamate receptor subunit 1
GluN2	NMDAR-type glutamate receptor subunit 2
GluN2A	NMDAR-type glutamate receptor subunit 2A
GluN2B	NMDAR-type glutamate receptor subunit 2B
<i>Gria1</i>	glutamate receptor 1 gene
<i>Gria2</i>	glutamate receptor 2 gene
<i>Gria3</i>	glutamate receptor 3 gene
<i>Gria4</i>	glutamate receptor 4 gene
<i>Grin1</i>	glutamate receptor subunit zeta-1 gene
<i>Grin2A</i>	glutamate receptor subunit epsilon-1 gene
<i>Grin2B</i>	glutamate receptor subunit epsilon-2 gene
<i>Grin2C</i>	glutamate receptor subunit epsilon-3 gene
<i>Grin2D</i>	glutamate receptor subunit epsilon-4 gene
GRIP	glutamate receptor-interacting protein

GSK3	glycogen synthase kinase 3
HAM	hydroxylamine
HD	Huntington's Disease
HDFP	hexadecylfluorophosphonate
HFS	high frequency stimulation
HIP14	Huntingtin-interacting-protein-14
HRP	horseradish peroxidase
I/O	input/output
ID	intellectual disability
IEM1460	N,N,N-Trimethyl-5-[(tricyclo[3.3.1.1 ^{3,7}]dec-1-ylmethyl)amino]-1-pentanaminiumbromide hydrobromide
INCL	infantile neuronal ceroid lipofuscinosis
JNK	c-Jun N-terminal kinase
KO	knockout
Kv4.2	voltage-gated potassium channel 4.2
Kv7.2/3	voltage-gated potassium channel 7.2/3
LBD	ligand binding domain
LFS	low frequency stimulation
LTCC	L-type Ca ²⁺ channel
LTD	long-term depression
LTP	long-term potentiation
LTR	long-terminal repeat
LZ	leucine zipper
MAGUK	membrane-associated guanylate kinase
mEPSC	miniature excitatory post-synaptic current
mGluR	metabotropic glutamate receptor
mRNA	messenger ribonucleic acid
MS	mass spectrometry
MWM	Morris water maze
N-terminal	amino terminal
NA	numerical apterature
NASPM	1-naphthylacetyl spermine
NBQX	2,3-dihydroxy-6-nitro-7-sulfamoyl-benzo[f]quinoxaline
NEM	N-ethylmaleimide
NIH	National Institutes of Health
NMDAR	N-methyl-D-aspartate receptors
NMJ	neuromuscular junction
NSF	N-ethylmaleimide-sensitive factor
NTD	amino-terminal domain
P	post-natal day
P2	crude synaptosomal pellet
p38 MAPK	p38 mitogen-activated protein kinase
PALM	photoactivated light microscopy

Palmitoyl-CoA	palmitoyl-coenzyme A
PAT	palmitoyl-acyl transferase
PB	piggyback
PBS	phosphate buffered saline
PCR	polymerase chain reaction
PDZ	postsynaptic density protein, drosophila disc large tumor suppressor, and zonula occludens-1 protein
PEG	polyethylene glycol
PFA	paraformaldehyde
PhTx	philanthotoxin
PICK	protein interacting with C Kinase
PIP2	phospholipid phosphatidylinositol 4,5-bisphosphate
PIX	AKAP PxlXIT motif
PKA	protein kinase A or cyclic AMP-dependent protein kinase
PKC	protein kinase C
PKG	cyclic GMP-dependent protein kinase
PLA	proximity ligation assay
PM	plasma membrane
poly-Q	poly-glutamine
PP1	protein phosphatase 1
PPR	paired-pulse ratio
PPT	protein palmitoylthioesterase
pS	picosiemens
PSD	post-synaptic density
PSD-93	post-synaptic density protein 93, also known as Disc Large Homolog 2 (DLG2)
PSD-95	post-synaptic density protein 95, also known as Disc Large Homolog 4 (DLG4)
PTM	post-translational modification
PVDF	polyvinylidene fluoride or difluoride
Q	glutamine
Q/R	glutamine to arginine
QX-314	N-Ethylidocaine
R	arginine
RE	recycling endosome
RNAi	RNA interference
RT	room temperature
S2	non-synaptosomal soluble fraction
S818	serine 818 of GluA1 AMPAR subunit
S831	serine 831 of GluA1 AMPAR subunit
S831/845A	dual serine to alanine mutation at GluA1 amino acids 831 and 845
S831A	serine to alanine mutation at GluA1 amino acid 831

S845	serine 845 of GluA1 AMPAR subunit
S845A	serine to alanine mutation at GluA1 amino acid 845
SAP102	synapse-associated protein 102, also known as Disc Large Homolog 3 (DLG3)
SAP97	synapse-associated protein 97, also known as Disc Large Homolog 1 (DLG1)
SC	Schaffer collaterals
SDS	sodium dodecyl sulfate
SEM	standard error of the mean
SEP	super-ecliptic pHluorin
sEPSC	spontaneous excitatory post-synaptic current
SILAC	stable isotope labeling with amino acids in cell culture
SIM	structured illumination microscopy
SRC	proto-oncogene tyrosine-protein kinase Src (short for sarcoma)
sTBS	spaced theta burst stimulation
STDP	spike timing-dependent plasticity
STED	Stimulated emission depletion
STORM	Stochastic optical reconstruction microscopy
TARP	transmembrane AMPAR regulatory protein
TBOA	<i>threo</i> - β -Benzyloxyaspartic acid
TBS	theta burst stimulation
TCEP	tris(2-carboxyethyl)phosphine
TF-488	Alexa-488 labeled transferrin
TfR	transferrin receptor
TMD	transmembrane domain
TRPV1	transient receptor potential cation channel subfamily V member 1, also known as capsaicin receptor or vanilloid receptor 1
TTX	tetrodotoxin
TxP	triton-insoluble pellet
TxS	triton-soluble fraction
VTA	ventral tegmental area
WE	whole extract
WT	wild-type
wTBS	weak theta burst stimulation
β 2-AR	beta-2 adrenergic receptor
Δ PIX	AKAP mutant lacking the PxlxIT binding motif
Δ PKA	AKAP mutant lacking the PKA binding site by deleting 30 base pairs within the alpha-helix that anchors PKA to AKAP but retaining the extreme C-terminus

CHAPTER I

INTRODUCTION

Hippocampus: circuitry and relevance in learning and memory

Decades of research have gone into the study of learning and memory but despite this extended focus, the cellular and molecular mechanisms by which learning and memory take place remain incompletely characterized. Much research has focused on the hippocampus, the distinctive limbic structure in the medial temporal lobe of the brain, as the epicenter of memory formation. At the circuit level in humans, focal hippocampal lesions result in recall and memory deficits². Further evidence supporting learning and memory function of the hippocampus in humans are the profound deficits in patients with developmental and neurodegenerative diseases. At the synaptic level, the plasticity of synapses within the hippocampus in response to activity is thought to underlie learning and memory processes^{3,4}.

The structure of the hippocampus in the rodent is classified as a tri-synaptic loop (Fig 1.1). The primary input to the hippocampus comes from neurons in the entorhinal cortex (EC) that synapse onto cells in the dentate gyrus (DG) which in turn send axons to pyramidal cells within the Cornu Ammonis (CA) area 3 (CA3). These CA3 neurons then form excitatory synapses onto pyramidal neurons within the CA1 area, called the Schaffer collaterals. The CA1 neurons pass information through the subiculum, which send projections back to the EC, other parts of the cortex, and within the hippocampus itself. Due to this simple and well-defined circuitry, the rodent hippocampus has become an indispensable tool for the study of synaptic transmission and synaptic plasticity.

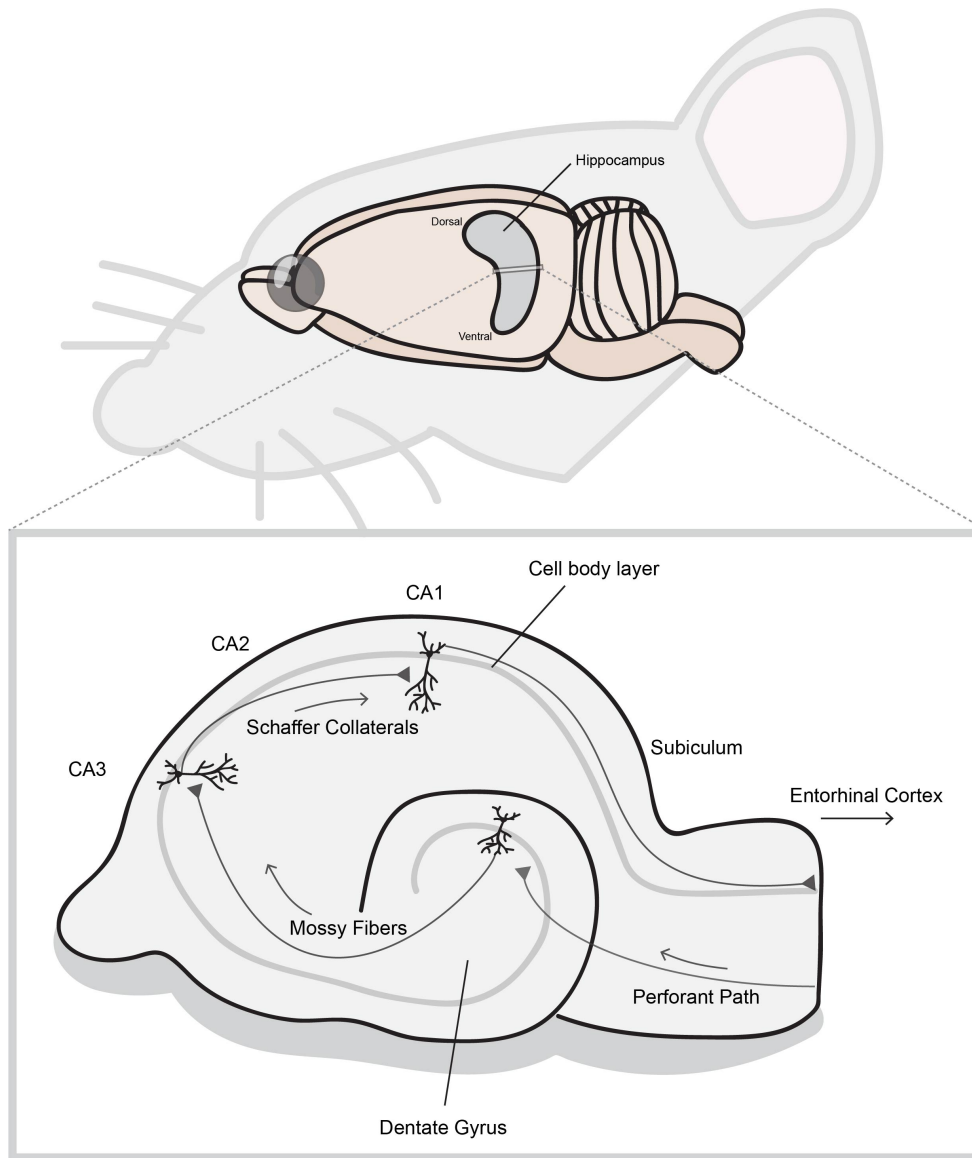


Figure 1.1: Structure of the rodent hippocampus.

The rodent hippocampus is organized into a tri-synaptic loop. The first part of the loop comes from the major input to the hippocampus, the entorhinal cortex, via the perforant path. Axons from the perforant path synapse onto granule cells in the dentate gyrus that then synapse via axons called mossy fibers onto CA3 pyramidal neurons forming the second synapse of the tri-synaptic loop. The final synapse within the loop originates from CA3 neuron axons called Schaffer collaterals forming connections with CA1 pyramidal neurons. This final synapse is one of the most studied synapses in all of neuroscience and has been found to be important for learning and memory. From here, CA1 neurons send output to subiculum back to the cortex.

Excitatory synapses

Pyramidal neurons, or principal neurons, within the hippocampus receive excitatory input in the form of an electrochemical signal (Fig 1.2). Pre-synaptic input converges on the dendrites of pyramidal neurons resulting in the modification of connectivity and activity. These dendrites reach out 100s of microns from the soma and are highly branched and complex. Dendrites are decorated with small, independent compartments forming protrusions on the shaft called dendritic spines (1-10 spines/micron of dendrite in primary neurons). Dendritic spines are the sites of excitatory synapses, formed when a post-synaptic spine forms contact with a pre-synaptic axon. Dendritic spines are quite heterogeneous structures, undergoing number, size and shape alterations throughout development and in response to activity. Axons can also form synapses onto the shaft of the dendrite, often the sites of inhibitory synapses. Synapses within the central nervous system are classified by the neurotransmitter and signaling action downstream. Here, excitatory synapses will refer to glutamatergic synapses and inhibitory synapses will refer to gamma-Aminobutyric acid (GABA)-ergic synapses. Inhibitory synapses help to balance neuronal activity by dampening neuronal firing. Inhibitory synapses form predominately on the dendritic shaft, as opposed to forming on dendritic spines like excitatory synapses. Their molecular organization and composition are distinguishable and distinct from excitatory synapses. During the experiments outlined in this thesis, inhibitory synapses were either not examined or pharmacologically inhibited to isolate excitatory contributions. Synapses will be used to indicate excitatory synapses for the remainder of this thesis.

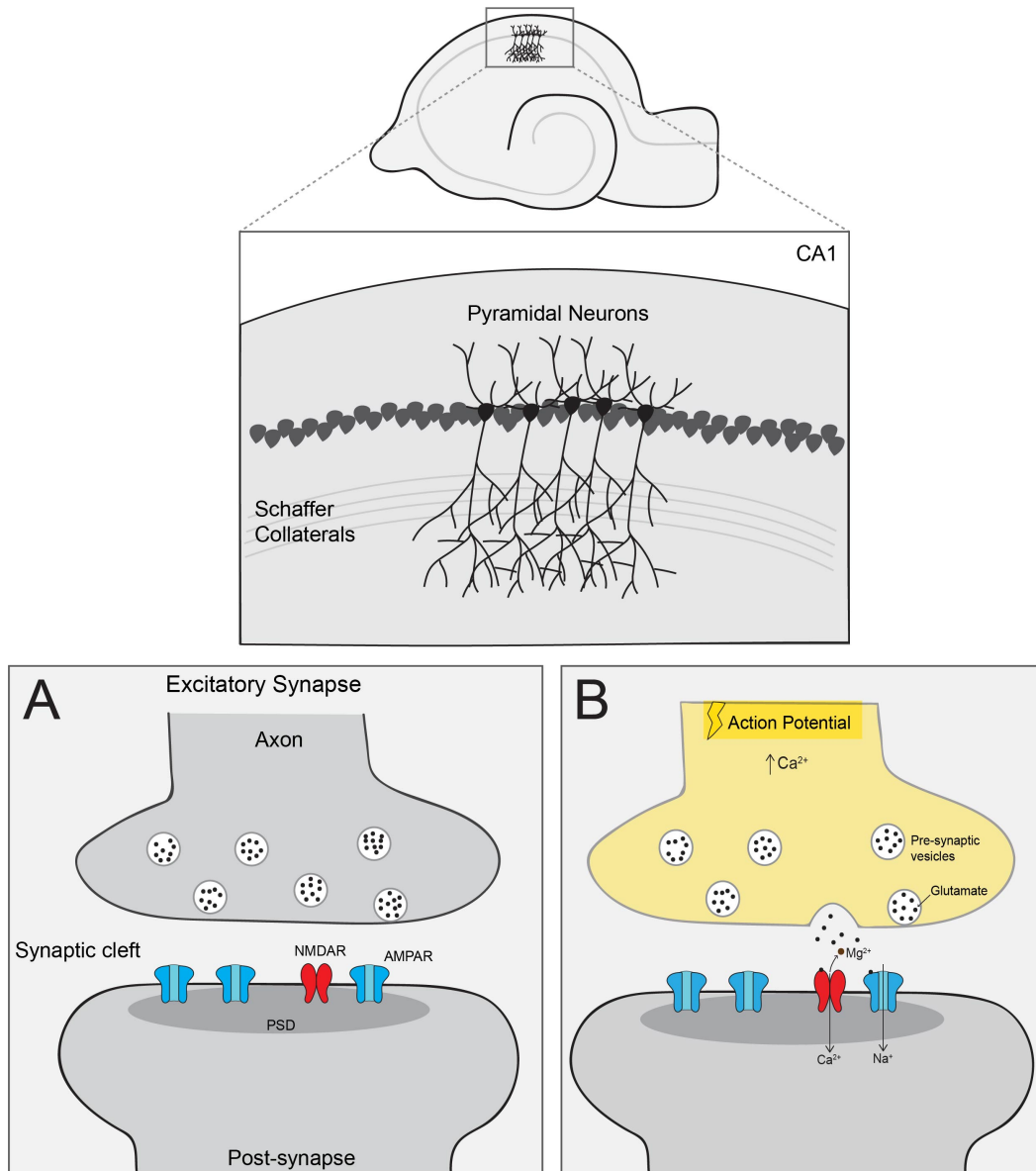


Figure 1.2: Excitatory synapses in CA1 of the hippocampus.

A closer look at neurons within the CA1 region of the hippocampus will reveal a clear laminar organization of the cell body layer containing mostly excitatory, pyramidal neurons. Schaffer Collaterals synapse onto dendrites of these CA1 neurons. A. A schematic showing a general and simplified excitatory synapse made up of an axon, synaptic cleft, and post-synapse. The post-synaptic density is shown in the post-synaptic dendritic spine containing glutamatergic ion channels. B. When the pre-synaptic neuron fires an action potential, the pre-synaptic bouton experiences an increased calcium concentration, causing vesicles containing the neurotransmitter glutamate to fuse with the membrane and glutamate to diffuse across the synaptic cleft. The glutamatergic ion channels bind the neurotransmitter and cause cations to flow into the post-synaptic neuron, initiating downstream signaling cascades.

Synapses are incredibly complex structures, but can be broken down into three essential components: the pre-synaptic terminal, the synaptic cleft and the post-synaptic compartment (Fig 1.2A).

Pre-synaptic terminal

The pre-synaptic axon terminal contains neurotransmitter vesicles that dock and fuse at the active zone to pass a chemical signal to the post-synaptic spine. The pre-synaptic terminal receives electrical information by way of an action potential (AP) and transmits the signal via neurotransmitter release. Ca^{2+} entry into the pre-synaptic terminal is mediated by depolarization caused by the conduction of the AP to the pre-synapse, which opens voltage-gated Ca^{2+} -channels and triggers Ca^{2+} -dependent exocytosis of neurotransmitter containing vesicles. Electron microscopy shows ~40 nm docked synaptic vesicles that defines the pre-synaptic specialization, the active zone (AZ). The AZ is directly apposed to the electron dense thickening of the post-synaptic membrane, at the interface between the pre-synaptic terminal and the synaptic cleft. Vesicle fusion takes place within less than 1 ms after AP-mediated pre-synaptic depolarization; thus, vesicles need to be close to release sites and the machinery required for fusion must be spatially and temporally regulated. Exocytosis of synaptic vesicles is limited to small membrane domains containing the molecular machinery and lipid composition to facilitate exocytosis where pre-docked vesicles (termed the “readily recruitable” pool of vesicles) fuse. There can be one or multiple exocytic sites per pre-synaptic terminal. Fusion sites tend to be situated near the AZ⁵ however individual exocytic events are not confined to a single release site⁶⁻⁸. Among the molecular machinery at fusion sites are proteins that trigger exocytosis by the binding of Ca^{2+} .

Generally, it is thought that the pre-synaptic AZ is organized by a handful of protein families^{9,10} including: RIM proteins, RIM-BP, Munc 13s, ELKs, Bassoon and Piccolo. Each protein family plays a role in organizing the pre-synaptic AZ to target vesicle fusion to particular sites by scaffolding vesicles, tethering/targeting Ca²⁺ channels, attaching vesicles to the membrane. This exquisite control of pre-synaptic neurotransmitter release allows for synapses to encode many different types of information, such as different action potential firing patterns. While these pre-synaptic events are incredibly important and are intimately tied to post-synaptic responses, the majority of this thesis will explore post-synaptic alterations during plasticity.

Synaptic cleft

The AZ and post-synaptic density are separated by about 20-25 nm, classified as the synaptic cleft. The cleft is not just an empty space between pre- and post-synapse; instead, the cleft is enriched with proteins. There are many protein structures spanning the cleft, organized in an irregular array. In fact, at the cleft there are electron dense regions, including at the periphery, perhaps suggesting distinct functional microdomains. Among the proteins spanning the cleft are cell adhesion molecules that form trans-synaptic complexes. This participation of pre- and post-synaptic proteins in trans-synaptic interactions is thought to stabilize the synapse and could potentially contribute to the alignment of functional domains between release sites and receptors¹⁰. The cleft has been found to participate in spine formation, maturation and transmission.

Post-synaptic compartment

The post-synaptic component of the synapse is formed onto dendritic spines and contains a post-synaptic density (PSD) so named due to the densely packed proteins

contained there within. This protein assembly is most dense halfway between the pre- and post-synaptic membranes^{11,12}. Glutamatergic synapses in the central nervous system (CNS) have prominent PSDs and are thus termed asymmetric synapses, due to the disproportionate electron density between the pre- and post-synapse. The PSD can range in size ~200-800 nm (with an average of ~300-400 nm) in diameter and ~30-50 nm thick¹³. Though relatively small, PSDs are highly specialized areas of the membrane that are incredibly abundant (between 10,000 and 100,000/neuron)¹³. After the early observations of electron density at the post-synaptic membrane, many efforts were focused to elucidate the proteins that made up this interesting post-synaptic feature.

In the 1970's, the first PSD purification experiments were carried out and in the 1990's PSD components began to be identified. Owing largely to the development of mass spectrometry, many PSD proteins have been identified in the past few decades. The proteins that provide the electron density and namesake for the PSD (with the average PSD having a molecular mass of ~1 gigadalton¹⁴) include receptors, scaffolding proteins, channels, cell adhesion molecules, cytoskeletal elements and enzymes. A key scaffold and marker of excitatory PSDs is Post-synaptic density protein 95 (PSD-95). However, there are 100-1,000s of proteins that occupy and make up the PSD, especially when different brain regions and distinct cell types exhibiting different PSD compositions are considered.

Proteins are dynamic within the PSD, with proteins changing over seconds or hours, due to developmental regulation or activity-dependent rearrangement. While we now appreciate a whole host of the molecular players within the PSD, we still do not have a thorough understanding of the molecular organization of the PSD. We do know

that within the post-synapse exists distinct regions: synaptic, perisynaptic (within 100 nm of the PSD)¹³ and extrasynaptic. These distinct synaptic subregions are in dynamic flux and are functionally connected. Following with this segmentation of the synapse, proteins are not homogenously distributed throughout the PSD. Core synaptic regions contain glutamate receptors and signaling proteins directly opposed glutamate release, while extrasynaptic regions contain metabotropic receptors and endocytic proteins.

Continuing with the flow of information from pre-synapse to post-synapse, once an AP causes Ca^{2+} influx in the axon causing neurotransmitter release, glutamate diffuses across the synaptic cleft and binds to receptors within the post-synaptic membrane (Fig 1.2B). Therefore, a key component of the PSD is the glutamate receptors that receive the pre-synaptic chemical signal on the post-synaptic neuron. The predominant glutamate receptors are the ionotropic α -amino-3-hydroxy-5-methyl-4-isoxazolepropionic acid receptors (AMPA) and N-methyl-D-aspartate receptors (NMDARs). Initially, AMPARs are activated by glutamate binding and allow Na^+ into the post-synaptic spine, which causes the membrane potential to become more positive or depolarized. This depolarization results in the Mg^{2+} -ion that resides in the pore of the NMDAR at more hyperpolarized conditions to be displaced, allowing Ca^{2+} and other ions to enter the cell through the NMDAR. The influx of Na^+ and Ca^{2+} through post-synaptic AMPARs and NMDARs initiates a number of signaling cascades and also advances the electrical signal to the rest of the neuron via membrane depolarization, which can result in AP firing in the post-synaptic neuron to initiate synaptic transmission to downstream connected neurons.

Glutamate receptors

Ionotropic glutamate receptors are integral membrane proteins that form ion channels from 4 individual subunits coming together to form an ion pore¹⁵. Each subunit is composed of 4 domains: amino (N)-terminal domain (NTD), a highly conserved extracellular clamshell-like ligand binding domain (LBD), transmembrane domain (TMD) and the intracellular carboxy (C)-terminal domain (CTD) (Fig 1.3). These receptors form as tetramers, composed of four individual subunits of the same receptor type. There are 4 classes of glutamate receptors: AMPA receptors, kainate receptors, NMDA receptors, and δ -receptors. Glutamate receptors are activated first by ligand binding to the LBD. Agonists of glutamate receptors are: glycine, D-serine, aspartate and glutamate. Once agonist binds, the LBD changes conformation causing the ion channel domain to open. Post-synaptic currents (such as current carried by AMPARs and NMDARs) are determined by multiple factors including: receptor number, probability of agonist bound and receptor opening, driving force, and conductance of channels. This section will focus on AMPA and NMDA receptors, the two predominate ionotropic receptors of excitatory pyramidal neurons within the hippocampus that are known to be important in baseline neuronal function and during plasticity.

AMPA receptors

AMPA receptor properties and assembly

AMPARs are expressed in neurons throughout the CNS. Under normal conditions, AMPARs are the primary mediators of fast excitatory glutamatergic neurotransmission within the brain. Due to their rapid kinetics, opening and closing on the sub-millisecond timescale, AMPARs allow for fast depolarization of the post-

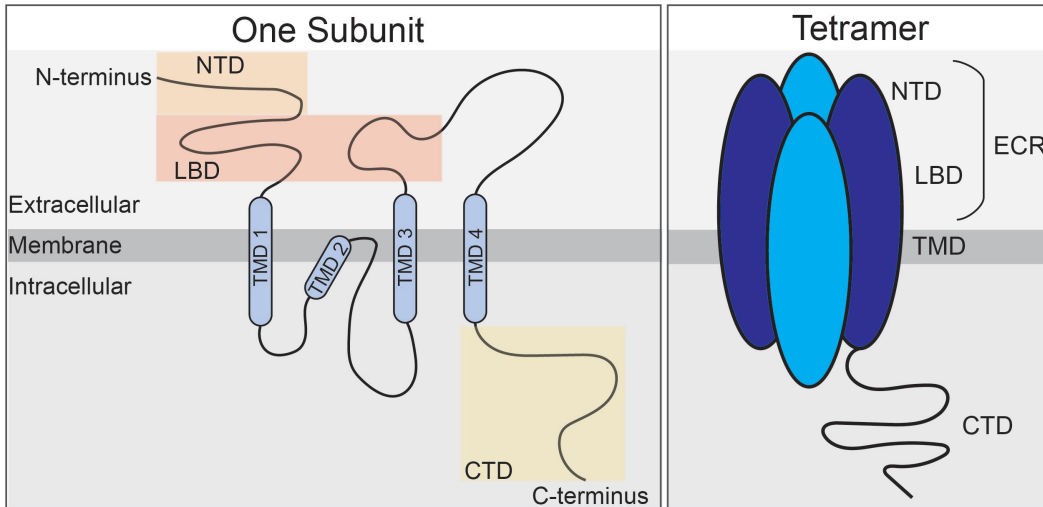


Figure 1.3: Ionotropic glutamate receptor structure.

Left, a single subunit of a general ionotropic glutamate receptor is shown. Right, ionotropic glutamate receptors form tetramers with their NTDs and LBDs protruding into the extracellular space, while the CTDs are exposed to the cytoplasm.

synaptic membrane and thus a high-fidelity propagation of signaling between pre- and post-synaptic neurons. AMPARs form tetramers of homo- and heterodimers composed of GluA1-4 subunits (genes *Gria1-4*), and are thus called dimers of dimers^{15,16}. Channel opening depends on glutamate binding to all subunits of the tetramer¹⁷. Each subunit contributes differently to receptor properties like channel kinetics, ion selectivity and trafficking. Accompanying subunit specific properties, heterodimerization, mRNA processing, auxiliary proteins and phosphorylation can add additional complexity to subunit control of receptor properties. AMPARs have four distinct domains (as mentioned generally above): ECR (extracellular region) that makes up the majority of the receptor (~85% of its mass, protruding 130 Angstroms into the synaptic cleft)^{18,19} containing the NTD that drives dimerization, TMD and then a CTD that varies in length and is highly modified^{15,20,21} (Fig 1.3).

AMPARs synaptic number varies widely from synapse to synapse and cell to cell¹³. With >10,000 synapses on each neuron, each synapse must independently and dynamically regulate synaptic AMPAR content²². Therefore, the logistics of delivery, retention and removal of individual receptors with particular subunit composition and channel characteristics is highly complex and requires a considerable amount of regulation. AMPARs are highly mobile and their synaptic abundance is highly regulated developmentally, basally and in an activity-dependent manner. Much work has gone into understanding AMPAR trafficking and how subunit composition can influence properties of AMPARs.

AMPARs can be edited at the RNA level, which precedes mRNA splicing and protein synthesis. This splicing occurs at an Arginine/Glycine site within GluA2-4 LBD

and Glutamine/Arginine/Asparagine site in the membrane re-entrant pore loop of GluA2 (Fig 1.4A). Editing at this 607 position in the pore loop results in Glutamine to Arginine (Q/R) that controls Ca^{2+} -permeability and conductance through the pore and as well as affecting receptor assembly to favor heterodimerization over homodimerization and may have increased endoplasmic reticulum (ER) residency¹⁵. Q/R editing has also been shown to be necessary for organism survival²³. Further, alternative splicing of AMPAR subunits can result in two isoforms; splice variants of the AMPARs have changes within the LBD and are called flip and flop and differ in desensitization, deactivation and sensitivity to allosteric inhibitors. AMPARs pass cations, such as Na^+ , K^+ and Ca^{2+} , which are gated by the GluA2 subunit. Most GluA2 subunits are Q/R edited resulting in low Ca^{2+} -permeability (or Ca^{2+} -impermeable AMPARs, CI-AMPARs) and insensitivity to block by polyamine blockade. Unedited GluA2 containing receptors (the minority of GluA2 subunits) are highly Ca^{2+} -permeable and insensitive to polyamine blockade. Alternatively, GluA2-lacking and GluA1-containing receptors (or Ca^{2+} -permeable AMPARs, CP-AMPARs) are highly Ca^{2+} -permeable (though less than NMDARs^{15,24}) and sensitive to channel block by polyamines and polyamine (philanthotoxin (PhTx), joro spider toxin, argiotoxin, IEM-1460, 1-naphthylacetyl-spermine (NASPM))²⁵⁻³². These polyamine-derivatives can extracellularly block CP-AMPARs and are useful to probe receptor subunit composition^{28,33-36}. AMPARs have a reversal potential at 0 mV and at more depolarized membrane potentials, endogenous polyamines block the pore of the GluA1-containing AMPARs in a voltage-dependent manner preventing outward flux of K^+ -ions. This phenomenon of passing less outward current than inward

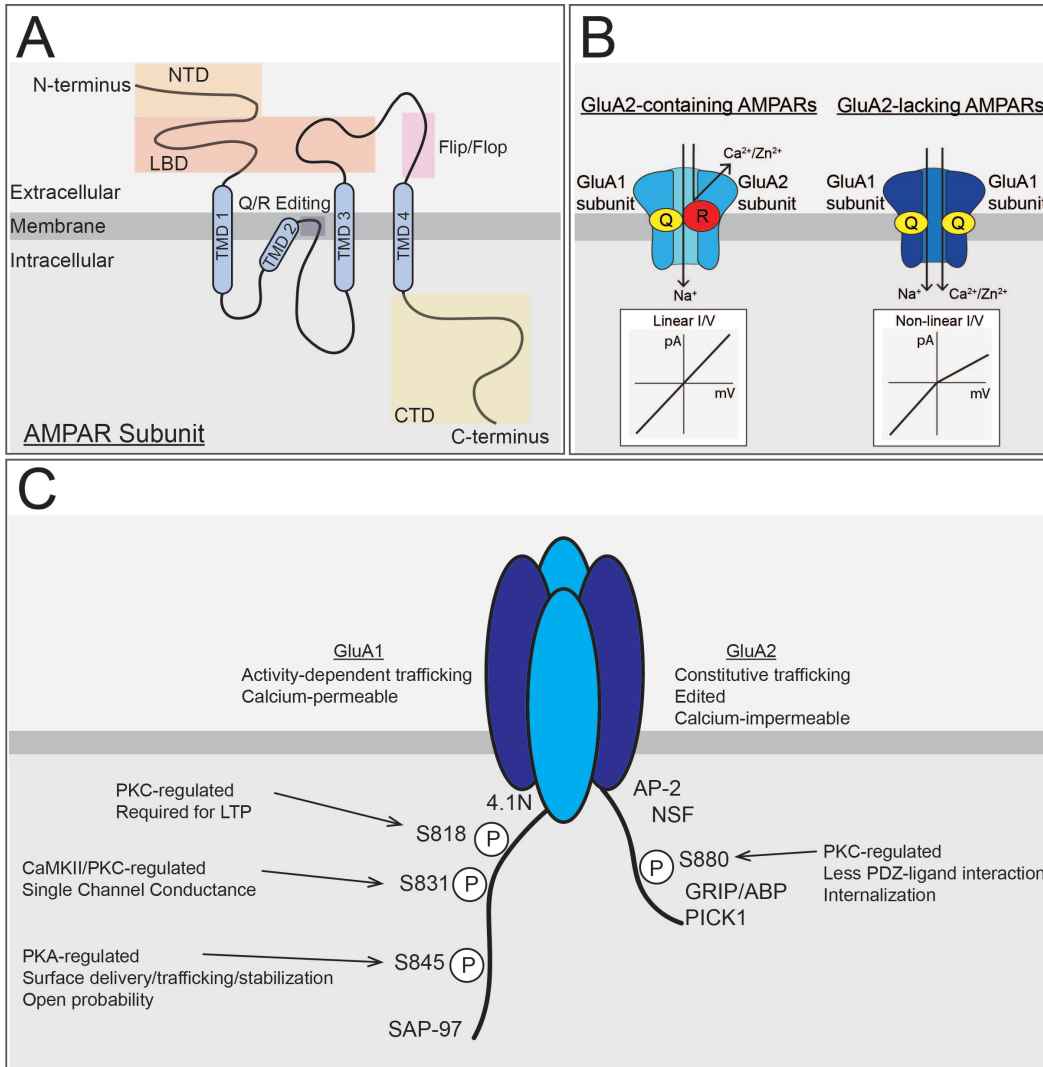


Figure 1.4: AMPAR structure and characteristics. **A.** AMPAR specific subunit structural domains. **B.** AMPARs containing the GluA2-subunit are unable to pass calcium due to the positive charge of the arginine residue within the pore, causing a linear current-voltage relationship. AMPARs lacking the GluA2-subunit can pass calcium and have a non-linear current-voltage relationship. **C.** Schematic of the CTDs of GluA1 and GluA2 with numerous phosphorylation sites and protein-protein interaction domains.

current is called inward rectification (Fig 1.4B). Subunit composition can regulate single channel currents with GluA1 homomers conducting an average of ~12 pS and GluA1/2 heteromers passing much less at ~3 pS²¹. It appears the majority of AMPARs are heteromeric GluA2-containing receptors with low Ca²⁺-permeability and low single-channel conductance. However a small number of Ca²⁺-permeable, GluA2-lacking receptors with high single-channel conductance form a significant minority and play a critical role in signaling, plasticity and disease³⁷⁻³⁹. GluA4 containing subunits are developmentally regulated and sparsely expressed at glutamatergic synapses, but are important in AMPAR-mediated transmission in interneurons⁴⁰.

AMPAR protein turnover is between 10 hours and 2 days depending on the neuron type and developmental age²². Though the basic machinery for the production of transmembrane proteins is highly conserved in eukaryotic cells, including neurons, the unique structure and function of neurons renders the secretory pathway to be more complex⁴¹. The precise mechanisms governing AMPAR subunit assembly still are not well understood. But we do know that AMPAR subunit assembly occurs in the ER, as with other transmembrane proteins. It is assumed that the AMPAR receptor subunits initially form homodimers that can eventually rearrange into heterodimers. The NTD of the AMPAR subunit drives initial dimerization, with the NTD of different subunits having varied affinities for assembling with other subunits¹⁵. For example, in hippocampal pyramidal neurons GluA1 has much higher affinity for GluA2 than other GluA1 partners, which is thought to bias receptor composition toward GluA1/2 heteromer assembly and result in more GluA2 containing receptors¹⁶ and low levels of GluA2-lacking receptors⁴². Further, all domains participate or have a role in driving subunit tetramerization. Usually

receptors have either no GluA2 subunits or two GluA2 subunits⁴³⁻⁴⁵. Flexibility in the NTD dimer interface allows for the formation of GluA2-lacking receptors⁴⁶. Because GluA2 subunits must undergo editing, these subunits are retained in the ER for longer than GluA1 homomers that do not undergo editing and thus can be exported rapidly to the plasma membrane (PM)⁴⁷. The edited GluA2 is mostly unassembled and retained in the ER allowing more dwell time and increased chance of interaction with GluA1 to also promote heterodimerization with GluA1 to facilitate ER export^{44,48,49}. In other cell types with less ER retained GluA2, there are fewer GluA2 containing receptors²⁴. There also exist ER chaperones that control AMPAR subunit ER retention such as BiP and calnexin⁴⁷.

From the ER, AMPARs are trafficked to the Golgi where receptors can be further modified. Because neurons are large highly polarized cells, membrane proteins must navigate long distances to get to the PM. It still remains unclear where AMPARs are first inserted once at the membrane. Membrane insertion is subunit dependent with GluA2-containing receptors rapidly and constitutively inserted^{50,51} and GluA2-lacking receptors added to the synapse in an activity-dependent, regulated manner. GluA1 subunit rules seem to dominate when GluA1 is part of a complex with GluA2. This activity-dependent trafficking will be described later in the following plasticity section.

AMPA variable CTD contributes to subunit regulation

Because AMPAR subunits are homologous, the highly variable C-terminal tail is thought to be a site of distinct regulation between the subunits conferring receptor regulation, including membrane targeting, stabilization, and degradation. AMPAR subunits CTDs contain a number of sites for post-translational modifications as well as

domains that facilitate protein-protein interactions⁵² (Fig 1.4C). AMPARs (and NMDARs, as well) can interact with a number of post-synaptic proteins, such as scaffolds, cytoskeletal elements, adaptors, anchors, and enzymes. GluA1 and GluA4 have long C-terminal tails and GluA2 and 3 have short tails. Initially, NMDARs were identified as binding to PSD-95⁵³ through their CTD and AMPAR GluA1 subunits showed interactions with Synapse-associated protein 97 (SAP97)⁵⁴. PSD-95 was the founding member of synaptic proteins containing PDZ domains, modular protein-protein motifs, which serve as scaffolds at the synapse^{55,56}. These PDZ domains bind to the C-termini of ion channels, such as NMDARs and AMPARs. A large family of highly homologous PDZ-containing proteins has been identified at the synapse called Membrane-associated guanylate kinase (MAGUK) proteins. The MAGUKs include PSD-95, Post-synaptic density protein 93 (PSD-93), Synapse-associated protein 102 (SAP102) and SAP97. The functions of MAGUKs have some overlap^{56,57} and their expression is important for AMPAR targeting to the synapse. For example, if PSD-95 is overexpressed, synapse formation is increased along with increases in AMPAR levels at the synapse^{58,59}. AMPAR GluA1 CTD can also directly interact with transmembrane AMPAR regulatory proteins (TARPs), to influence receptor dynamics (discussed more below).

CTD phosphorylation of different AMPAR subunits can differentially regulate their channel properties and localization. GluA1-4 subunits are phosphorylated at over 20 serine, threonine, and tyrosine residues by many kinases, such as Calcium/calmodulin-dependent protein kinase II (CaMKII), Protein Kinase A (PKA), Protein Kinase C (PKC), Protein Kinase G (PKG), proto-oncogene tyrosine-protein kinase Fyn (Fyn) and c-Jun

N-terminal kinase (JNK)^{20,60}. GluA1 CTD phosphorylation has been extensively studied with three sites prominently featured (Fig 1.4C): Serine 818 (S818), Serine 831 (S831), and Serine 845 (S845). S818 is phosphorylated by PKC and is important for GluA1 synaptic incorporation during plasticity⁶¹. CaMKII and PKC phosphorylate S831, which is thought to increase single channel conductance and could affect receptor surface delivery⁶¹. S845 is phosphorylated by PKA and is involved in both regulation of open probability⁶² and receptor trafficking¹⁵. It has been determined that ~15% of receptors are phosphorylated at S831 and S845 at rest⁶³. As detailed below, these phosphorylation events appear to play a critical role in controlling receptor function, particularly during synaptic plasticity.

The GluA2 subunit CTD can also be modulated by phosphorylation at Tyrosine 876 by Src and Serine 880 by PKC, which regulates protein-protein (Glutamate Receptor Interacting Protein [GRIP1]/AMPA Binding Protein [ABP]) interactions. GluA2 can be further regulated by protein-protein interactions in the CTD. In the 1990's, yeast two-hybrid screens identified a number of AMPAR interacting proteins, including the PDZ interaction between GluA2 and 3 and GRIP 1 and 2 and Protein Interacting with C Kinase (PICK1)⁶⁴⁻⁶⁹. N-ethylamine-Sensitive Factor (NSF) is an ATPase that is required for membrane fusion interacts with the C-terminus of GluA2. In that same region AP2, a protein required for clathrin-dependent endocytosis, interacts with GluA2. This GluA2-NSF interaction is important in maintaining AMPAR content at the synapse⁶⁹⁻⁷⁵. PKC phosphorylation of GluA2 within the PDZ domain disrupts the binding of GluA2 and GRIP1/2 to increase PICK1 binding^{76,77}.

AMPA synaptic organization

With the advent of super resolution techniques (such as Photoactivated light microscopy (PALM)/Stochastic optical reconstruction microscopy (STORM) and Stimulated emission depletion (STED) microscopy) and proteomics, there have been profound discoveries about the organization and identification of new proteins within synapses. AMPARs are concentrated at the synapse directly opposite of pre-synaptic terminals such that pre-synaptic glutamate release is tightly coupled to receptor activation¹⁰. AMPARs are only a few fold more enriched in the PSD than the periphery. But within the synapse, receptors organize into high-density “hotspots”, termed nanodomains or nanoclusters, the clustering of which depends on a number of protein-protein interactions⁷⁸⁻⁸⁰. There are ~1-3 nanodomains per PSD, averaging 80-100 nm in diameter and tend to be at the periphery but can be localized anywhere within the synapse. It is thought that there are 10s of receptors per ~100 nm radius nanodomains spaced ~20 nm from center-to-center^{10,53,81}. Larger synapses with more than one central PSD domain tend to have more AMPAR nanodomains^{7,78,79}. PSD-95 itself can form nanodomains, but not as well defined as receptor clusters. These PSD-95 nanodomains are ~80 nm and an average of 1-3 exist in a synapse⁷⁸. Studies have determined that PSD-95 patterning can influence AMPAR distribution^{7,78,79,82}. A number of factors can affect PSD-95 (and MAGUK family) nanoclustering and this clustering can influence the localization and distribution of a number of proteins due to the extensive protein-protein interactions between these synaptic scaffolds and other important synaptic proteins. PSD molecule clusters are highly variable between neurons and even neighboring synapses⁸³. This modular structure of the synapse suggests that the

synapse is composed of multiple independent trans-synaptic modules that form individual AMPAR transmission units. The AMPAR nanodomain hypothesis claims that activation of receptors within these hotspots can beat desensitization of the channel and therefore generate a quantal current. Super-resolution imaging^{78,79,83} supports the idea of the alignment of “nanocolumns”⁷ or trans-synaptic modules⁸⁴.

AMPARs are on average highly mobile so it stands to reason that there are proteins at the synapse that must act to retain receptors and restrict their mobility to organize and position the receptors within the PSD. In support of this idea, AMPAR mobility is restricted within PSD nanodomains but more mobile in between the nanodomains^{79,85}. These receptors stay immobile for long periods of time within the PSD nanodomains⁸⁶⁻⁸⁸. In this way, synaptic scaffolds (like PSD-95) could serve as a building block of synapses by assembling receptors (like AMPARs) at the sites of neurotransmitter release¹⁰. This could be orchestrated by direct PSD-95 binding⁸⁹ or due to physical diffusion barrier⁹⁰. It seems rational that macromolecular crowding is at play as it could explain why proteins with no PSD-95 binding have lower mobility in crowded portions of the PSD⁹¹. Further, the NTD of AMPARs can participate in a number of protein-protein interactions once the AMPAR is at the synapse, including interacting with cell adhesion molecules (CAMs) that are pre- and post-synaptic transmembrane proteins like neuexins or cadherins that could also aid in stabilizing AMPARs at the synapse.

Auxiliary proteins

AMPARs participate in protein-protein interactions with a number of proteins within the PSD, one of which are the AMPAR auxiliary proteins. AMPAR auxiliary

subunits can determine receptor gating, channel conductance, sensitivity to pharmacological agents and expression at the synapse⁹². Multiple auxiliary protein families exist including transmembrane AMPAR regulatory protein family (TARPs) and cornichons. AMPARs assemble with auxiliary subunits early on in receptor biogenesis. The collection of AMPARs and associated auxiliary proteins is thought to number >30 different proteins within an AMPAR complex⁹². The classic TARP family of AMPAR auxiliary proteins can interact with all four GluA subunits at a number of interfaces, extracellular, intracellular and at the TMD of both types of proteins. AMPARs can interact with 1-4 TARPs, which can control desensitization of the receptor⁹³. The receptors themselves do not directly interact with PSD-95 but do so indirectly via TARPs as well as direct binding to the other synaptic MAGUK, SAP97. And in this way, TARPs can also influence accumulation of AMPARs at the synapse via this MAGUK interaction. TARPs themselves can be modified and are differentially expressed across different brain regions and cell types and different types of TARPs can interact with different receptor assemblies. Further, TARPs can be regulated by CaMKII and PKC phosphorylation on multiple sites on the cytoplasmic C-terminal tail of TARPs, which can control both constitutive and activity-dependent AMPAR trafficking^{94,95}.

Outstanding questions

While decades of research have gone into understanding AMPAR biogenesis, trafficking and regulation, many outstanding questions still exist. Though many studies have provided seminal and foundational knowledge about AMPARs, there needs to be a re-examination of AMPAR regulation using manipulations that do not perturb endogenous AMPAR function and using endogenous AMPARs as a readout. It is still

unknown how the subunit composition of AMPARs is regulated rapidly and independently at the single synapse level. And it is still not understood if there are specific receptor reserves that can be tapped into under different conditions, such as during extremely high activity states. Further, how the subunit composition of locally synthesized receptors is controlled and how those locally synthesized receptors are incorporated into the synapse still remains a pressing and exciting avenue of exploration. Ultimately, because information can be stored in the brain for years, yet AMPARs are highly dynamic with a half-life of only a few days, how can AMPARs be so essential in determining synaptic strength that is maintained over days, months and years?

NMDA receptors

N-methyl-D-aspartate receptors, or NMDARs, are also ligand-gated ion channels that are expressed throughout the brain in a spatially and temporally controlled fashion. NMDARs play key roles in development and into adulthood in plasticity-related processes. NMDARs form the functional core of the synapse with ~20 NMDARs per PSD¹³. Unlike AMPARs that are highly variable in number from spine to spine, the number of NMDARs is fairly consistent across synapses and is very stable over time¹³. The NMDAR is named for (glutamate site partial) agonist N-methyl-D-aspartate, which selectively binds to NMDARs and not other glutamate receptors. NMDARs are heterotetramers, formed with two GluN1 subunits and two variable subunits, either GluN2 or GluN3^{15,96}. NMDAR subunits are subject to alternative splicing and result in multiple variants; *Grin1* encodes for 8 variants of the GluN1 subunit and individual genes *Grin2A*, *Grin2B*, *Grin2C*, and *Grin2D* encode the GluN2A-D subunits. NMDARs

must be co-activated by glutamate at the GluN2 subunits and glycine at the GluN1 or 3 subunits simultaneously¹⁵. GluN1 subunits are expressed throughout the brain in various cell types. GluN2 subunits are more regulated in expression patterns; individual GluN2 subunits are differentially expressed across brain regions and contribute to differences in NMDAR channel properties. GluN2A and GluN2B subunits are expressed in the hippocampus and have different temporal expression patterns. For example, GluN2B expression is high early development and decreases over the first few weeks postnatally while GluN2A levels begin to increase at this time. The particular subunit composition of the channel determines the biophysical properties of the NMDAR, including desensitization and Ca^{2+} -conductance¹⁵.

Each GluN2 subunit has a variable CTD that interact with different intracellular effectors, much as described above for AMPAR subunit CTDs. AMPARs are purely ion gated but can act as “gatekeepers” or aid in coincidence detection of NMDARs by allowing passage of cations into the cell. NMDARs are not only ion-gated like AMPARs, but are also voltage-gated by virtue of the depolarization requirement (as carried out by entry of cations through the AMPARs) in order to expel the Mg^{2+} -ion block and open the channel. As a result of this Mg^{2+} pore block, NMDARs are not responsible for much of the current at the resting membrane potential of -70 mV. Once the channel is activated, nonselective passage of cations is allowed, mostly Na^+ , a small amount of Ca^{2+} in and K^+ flow out. While NMDAR Ca^{2+} -current makes up only a small percentage of the current passed through the channel, it is essential for neuronal signaling and plasticity.

Synaptic plasticity

There are 100 billion neurons in the brain forming thousands of synapses each. One key feature of synapses is their remarkable ability to change strength and structure in response to activity. Experience can modify these connections *in vivo*, strengthening some synapses while weakening others. The capacity for hippocampal synapses to change their properties post-synaptically is largely due to protein dynamics in and out of the PSD. It is this ability to alter synaptic strength that is thought to underlie the ability to learn and remember. The faculty to change structure and function of synapses has been termed synaptic plasticity. Therefore, identifying the molecular basis of synaptic plasticity could provide the foundation to understanding learning and memory.

Long-Term Potentiation (LTP)

History of LTP in the hippocampus

In the late 1800's Santiago Ramon y Cajal hypothesized that learning could result from modulations in synaptic connectivity. Hebb's famous and recited theory stating neurons that wire together fire together was proposed in 1949, again positing that connectivity and activity of neurons provides a neural mechanism of memory storage⁹⁷. Synaptic plasticity as we know it was not demonstrated until almost twenty years after Hebb's theory and over a century after Ramon y Cajal⁹⁸. Synaptic plasticity within the hippocampus was first established⁹⁸ by delivering electrical stimulation to the perforant path, which contains axons that synapse onto dentate granule cells. Bliss and Lømo observed a sustained increase in the evoked response within the cells of the DG that persisted for days. This increased, or potentiated, response due to an enhancement in the synaptic strength or coupling between pre-synaptic input and post-

synaptic response was termed long-term potentiation (LTP). After these seminal studies, it has become widely accepted that LTP is the primary mechanism for synaptic plasticity and is the cellular correlate of learning and memory.

Through extensive study, it was determined that LTP occurs at excitatory synapses across many different brain regions. However, the classic LTP circuit most commonly studied is from the Schaffer collaterals (SC) to CA1 region in the hippocampus (Fig 1.1). It was determined that this Hebbian LTP had important facets including synapse specificity, cooperativity and associativity³. LTP is only induced at synapses that are stimulated with nearby synapses not potentiated, leading to synapse specificity. LTP can only be induced with converging inputs to create a depolarization in the cell large enough to produce potentiation, causing LTP to be cooperative. And LTP is associative because inputs that were too weak to produce potentiation alone can be paired with strong inputs to induce potentiation³.

There is strong evidence to support changes in the post-synaptic cell as conferring LTP⁹⁹, despite early debate as to whether LTP was a pre- or post-synaptic phenomenon. LTP results from activation of post-synaptic receptors by pre-synaptic glutamate leading to strong post-synaptic depolarization. During LTP induction, AMPARs are activated and relieve NMDAR pore blockade by Mg^{2+} to permit Ca^{2+} entry into the post-synaptic cell, increasing post-synaptic Ca^{2+} concentrations and initiating changes in synaptic strengthening^{99,100}. The post-synaptic mechanisms of LTP require downstream signaling cascades initiated by NMDAR Ca^{2+} , such as kinase signaling of CaMKII, PKA, and PKC. For example, CaMKII is necessary and sufficient for LTP induction and expression⁴. One common result of initiating these signaling cascades is

complex changes in AMPARs, such as change in number (via endo- and exocytosis or lateral diffusion), subunit composition, protein-protein interactions and/or phosphorylation state to influence channel localization and biophysical properties^{20,99,101,102}. Each of these processes is governed by a number of proteins that alter AMPAR trafficking and scaffolding at the synapse. The result of enhanced post-synaptic response to glutamate is increased AMPAR-mediated transmission and long-lasting potentiation.

Calcium-permeable AMPARs and LTP

It has long been appreciated that NMDARs are required for induction of LTP (the NMDAR competitive antagonist AP5/V blocks induction of LTP in hippocampal slices) and that the Ca^{2+} they provide is an important signal for LTP, but more recent studies^{36,103,104} have implicated another Ca^{2+} source, the CP-AMPA. Though pyramidal cells in the mature hippocampus highly express GluA2-containing AMPARs and basally NMDARs are likely the major source of Ca^{2+} in dendritic spines, these cells can still recruit or express GluA2-lacking receptors under certain conditions^{36,105-108}. Early evidence suggested no requirement for AMPARs during LTP induction^{109,110}, however considerable research has been dedicated to AMPAR involvement in LTP since these early studies.

The earliest CP-AMPA literature studied synaptic transmission onto local circuit cortical GABAergic interneurons important for precise timing of the excitatory pyramidal cell AP firing and coordinating large populations of pyramidal cells. This excitatory transmission onto interneurons was classified as having rapid rise and decay times¹¹¹⁻¹¹³ and mossy fiber synapses were found to have almost exclusively GluA1-containing

receptors¹¹⁴ that are blocked by polyamines and have high single-channel conductance¹¹⁵. A novel form of short-term plasticity was identified in interneurons involving short-term facilitation by activation of GluA2-containing receptors¹¹⁶⁻¹¹⁸ that relieves the endogenous polyamine block on GluA1-containing receptors^{26,119,120}, which causes a use-dependent increase in current. CP-AMPA receptors were first implicated in long-term forms of plasticity at excitatory synapses onto interneurons within the amygdala¹²¹; it was found that LTD at this synapse was NMDAR-dependent but also requires CP-AMPA receptors.

CP-AMPA receptors, classified by their increased inward rectification and sensitivity to polyamine-derived drugs (such as NASPM, IEM, and PhTx¹⁵) are recruited to synapses in the hippocampus resulting in an increase in inward rectification after LTP^{36,104}. These receptors are incorporated into the synapse and then subsequently removed within ~15 min of LTP induction³⁶. Blocking CP-AMPA receptors at early time points after LTP induction will prevent LTP, but not after LTP is already established around 30 minutes after induction^{29,36,122,123}; this indicates CP-AMPA receptors are important in a short window following induction and that early Ca²⁺ entry through these receptors is important for establishing the expression of LTP but not in maintaining LTP expression once established. As mentioned previously, GluA1/2 heteromers have much smaller single channel conductance than GluA1 homomers and it has been revealed that >80% of synaptic receptors in the hippocampus are GluA1/2 heteromers¹⁶ and most GluA1 homomer expression is limited to immature synapses (>P7) (but see¹²⁴, 8-10%). GluA2/3 receptors are not thought to be involved in plasticity^{16,125} (but see¹²⁶). Because there are so few CP-AMPA receptors basally (>10%), their transient introduction could

reasonably result a significant change in post-synaptic current with only ~5% CP-AMPAR receptor content needed to account for the increased conductance seen during LTP^{21,127,128}, hence the attractive and experimentally supported hypothesis that CP-AMPARs help to increase post-synaptic currents for a short yet critical period after LTP induction.

Controversy surrounding CP-AMPAR involvement in LTP

Though multiple lines of investigation suggest that CP-AMPARs are recruited during LTP, significant controversy still exists due to other studies showing there is no GluA1 homomer involvement^{125,129}. It has become clear over time and with more experimental evidence that a number of variables could be contributing to the inconsistency of CP-AMPAR involvement in plasticity, including age of animal, and induction protocol (Table 1.1). One crucial variable that appears to contribute to the CP-AMPAR participation in LTP is age of the animals used in the study. The Dell'Acqua laboratory and others^{36,103,104} have shown that at approximately 2 weeks of age there is robust recruitment of CP-AMPARs during LTP induction, which disappears between P14 and P17 and then reappears >P42. This corresponds with AMPAR subunit expression during development where CP-AMPARs are expressed early and then exchanged for CI-AMPARs after ~2 weeks¹³⁰. The baseline expression of receptors matters a great deal to the output basally as well as the susceptibility to potentiating stimuli, therefore age will highly influence the underlying mechanisms of plasticity by determining the AMPAR milieu at the synapse and altering the plasticity of plasticity itself, or so-called meta-plastic state. Another variable contributing to receptor involvement in LTP is the type of plasticity studied. Not only has it emerged that there

exist many types of plasticity *in vivo*⁸¹, but also within the literature there exist many diverse protocols to induce LTP *ex vivo* in slices whether using extracellular field recordings or whole-cell voltage and current clamp recording. The inconsistency in induction protocol plays a pivotal role in the signaling pathways initiated and then probed for, including the mechanisms that recruit CP-AMPARs. A further conundrum exists whereby studies in the past (and even ongoing studies) have tried to understand AMPAR involvement in plasticity by manipulating the receptor. But there are clear problems with the “receptor-centric” approach to understanding AMPAR subunit contributions. Often AMPARs are used to measure synaptic transmission, however, when manipulations are made to the receptor itself it can complicate interpretations as the manipulation could affect receptor function and therefore the experimental readout. Whole receptor or subunit knockouts are further complicated due to compensation by other receptors or subunits, potentially forming non-physiological receptors and conditions. Therefore, while there is strong evidence to suggest the involvement of CP-AMPARs in some types of plasticity, there still remains controversy and questions about the precise forms of plasticity and signaling mechanisms.

LTP mechanisms: AMPAR recruitment hypotheses

AMPAR insertion models: trafficking and lateral diffusion

Despite the controversy of the involvement of CP-AMPARs in plasticity, it is widely accepted that AMPARs are recruited to the synapse in order to increase synaptic strength. A number of non-mutually exclusive hypotheses exist to explain how AMPARs get retained or recruited to the PSD in an activity-dependent manner. One model is the

Table 1.1 CP-AMPA plasticity studies

Paper	Age/Species	LTP Induction Protocol	CP-AMPA?
Gray <i>et al.</i> 2007 ¹³¹	2-3, 8-12 weeks (15-17 days, 21-23 days) Mouse	Fields: 2 x 100 Hz, 10 s interval; Whole-cell: 2 Hz, 100 pulses paired - 10 mV holding; current clamp recordings	All were insensitive to 100-200 μ M IEM1460
Adesnik and Nicoll 2007 ¹²⁹	2-3 weeks Mouse and Rat	Fields: 4 x 100 Hz, 20 s interval; Whole-cell: 2 Hz, 60 s paired between -10 – 0mV	All insensitive to 10 μ M PhTx-433
Granger <i>et al.</i> 2013 ¹²⁵	P17-20 mouse	Whole-cell: 2 Hz, 90 sec at 0 mV	<i>Gria1-3^{fl/fl}</i> ; rescued with mutant receptors (all were Ca ²⁺ permeable). No AMPAR subunit important for LTP.
Plant <i>et al.</i> 2006 ³⁶	2-3 weeks Mouse	Whole-cell: 0.5 – 2 Hz, 50 – 100 pulses paired to 0 or -10 mV	Rectification changes for ~15 min post-induction; sensitive to 10 μ M PhTx-433
Guire <i>et al.</i> 2008 ¹²⁸	4-6 weeks Rat	Fields: TBS (4 x 100 Hz, 5 trains at 5 Hz) or HFS (3 x 100 Hz, 20 s interval)	TBS stim (not HFS) sensitive to 30 μ M IEM1460 immediately after induction (not 20 min later)
Lu <i>et al.</i> 2007 ¹⁰³	2,3,4,8 weeks (P12-14) (P20-22) Mouse	Fields: 2 x 100 Hz, 20 s interval	2 week old sensitive to 2.5 μ M PhTx and 20 μ M NASPM 3,4,8 week old insensitive
Yang <i>et al.</i> 2010 ¹²²	P13-18 Rat	Fields: TBS (3 bursts of 5 Hz, 5 pulses 100 Hz 2x, 20 s interval)	Incomplete expression of LTP with 10 μ M PhTx-433, Ca ²⁺ entry from CP-AMPA required for LTP
Sanderson <i>et al.</i> 2016 ¹⁰⁴	2,3 weeks Mouse	Fields: 1 x 100 Hz, 1 s	2 week old 70 μ M IEM1460 sensitive, 3 week old insensitive
Park <i>et al.</i> 2016 ¹³²	3-12 weeks Rat	Fields: cTBS 3 TBS episodes, 10 s interval, sTBS 3 TBS episodes, 2 min-1 hr interval wTBS 1 TBS episode	wTBS,cTBS insensitive to 30 μ M IEM1460 sTBS sensitive to 30 μ M IEM1460
Zhou <i>et al.</i> 2018 ¹³³	3-4 weeks Mouse	Whole-cell: LTP 1x100 Hz, 4x100 Hz; Fields: 100 Hz, 1 s 1 or 4 times with inter-train interval of 10 s or 5 min	LTP depends on GluA1 C-terminal tail; did not address CP-AMPA but based on GluA1 requirement and conductance change

AMPA insertion model, which includes AMPAR trafficking and lateral diffusion^{41,51,87,134}. Dogma at the neuromuscular junction (NMJ) suggested that post-synaptic acetylcholine receptors were quite stable and minimally regulated¹³⁵. However, it was observed that synapses in the CNS vary in AMPAR content¹³⁶⁻¹³⁹ and it was found later that AMPAR trafficking is dynamic and can be modified by neuronal activity. One proposed mechanism for AMPARs delivery to the synapse is through exocytosis from internal stores. A seminal contribution to elucidating plasticity related mechanisms was that dynamic membrane trafficking is required for expression of LTP and LTD^{69,140,141}.

Most models of LTP include a significant pool of surface receptors needed for LTP expression^{101,125,142}. An additional pool of receptors could reside in internal stores to be recruited or replenished during activity. One prominent pool of internal AMPARs is the recycling endosome (RE). REs have been observed in dendritic spines^{143,144} and bases of spines¹⁴⁵. To support the idea of receptor delivery from internal vesicle pools, the fusion machinery requisite for exocytosis is required for LTP expression¹⁴⁶⁻¹⁴⁹. NMDAR activity can influence RE pools¹⁴⁸, such as after LTP, which increases recycling and promotes RE translocation into spines^{148,149}. However, blocking post-synaptic exocytosis acutely does not affect basal transmission, although chronic blockade will eventually lead to run-down, hinting that there may be two pathways for AMPAR membrane delivery: constitutive (such as for the GluA2-containing receptors/heteromers) and activity-dependent (which could largely include GluA2-lacking receptors/GluA1 homomers). This model, implicating two AMPAR pathways, imparts that GluA2-containing (either GluA1/2 or GluA2/3) receptors are constitutively

trafficked to the cell surface. Multiple lines of evidence suggest that during activity GluA2-lacking receptors are recruited and then replaced with GluA2-containing receptors after activity to maintain AMPAR number and activity-state^{20,36,150,151}. PICK1 associates with GluA2 and seems to be involved in the regulated recycling/endocytosis of GluA2-containing receptors during LTP and promoting GluA1 insertion¹²³. GRIP1 anchors AMPARs at synapses⁶⁴ and NSF helps regulated the constitutive cycling of GluA2-containing AMPARs⁷². It has also been demonstrated that LTP relies on receptor recycling¹³⁴. These studies support the hypothesis that AMPARs need to be exchanged in and out of the synapse from internal stores both basally and during activity to maintain proper synaptic strength.

Another hypothesis of how AMPARs are dynamically regulated at the synapse is through AMPAR lateral diffusion. As previously mentioned, AMPARs are mobile within the PM^{89,101}, with extrasynaptic receptors exhibiting high mobility. The extrasynaptic receptor population can enter the synapse, which subsequently decreases their mobility¹⁵². Some believe that AMPARs are only recruited from a large surface pool of receptors during plasticity to account for the need of receptors to increase synaptic strength^{153,154}. It appears that this mechanism of receptor recruitment is not the only mechanism for receptor recruitment given the evidence above regarding AMPAR mobilization from internal stores, indicating cooperation between different mechanisms of receptor recruitment. In fact, in a recent paper¹⁵⁵, the Choquet laboratory showed that blocking lateral mobility of AMPARs blocks early LTP, but only when lateral mobility and exocytosis from internal stores is blocked will both induction and maintenance of LTP be fully prevented.

AMPA synaptic recruitment by means of phosphorylation

Whether AMPARs are recruited to the synapse from internal stores or through lateral diffusion, there still exists the fundamental question of what signal mobilizes them to the synapse? One hypothesis to explain receptor recruitment is AMPAR phosphorylation or modification. In the late 1980's, it was demonstrated that kinase activity was required for induction of LTP¹⁵⁶⁻¹⁵⁸. This led to a hypothesis that AMPAR subunits were phosphorylated during LTP leading to the regulation of the receptor and an increase in synaptic currents^{159,160}. Since then, studies of activity-dependent AMPAR phosphorylation have focused on modification of GluA1 and GluA2 subunits, as the sites on these subunits were shown to be regulated by neuronal activity^{20,60}. Strong evidence supporting the importance of phosphorylation control of AMPARs in plasticity was shown in the late 1990s, with increased phosphorylation correlated with LTP and decreased with LTD¹⁶¹⁻¹⁶⁴. GluA1 phosphorylation at S831 by CaMKII and/or PKC has been shown to increase channel conductance from 12 pS to 20 pS¹⁶⁵. PKA-dependent phosphorylation of S845 promotes insertion of the receptor, especially extrasynaptically^{122,166-169}, and is required for LTP¹⁷⁰.

To study the subunit specific requirements of LTP, many labs have used a knockout, knock-in or molecular replacement approach. It is not surprising that, as in much of the AMPAR literature, the significance of subunit specificity of plasticity is contentious. No C-terminal tail manipulation that blocks phosphorylation of the AMPAR CTD residues completely blocks LTP. LTP is still present in double mutant S831/845A¹⁷¹, with the single point mutants showing normal LTP¹⁷², and there is normal LTP when GluA1 knockout is rescued with a construct lacking the C-terminal tail¹²⁵.

GluA1 PDZ interactions are not required for LTP^{88,173}, but can act in a modulatory role¹⁷⁴. Nevertheless, a reproducible result is that knocking out GluA1 results in impaired AMPAR surface expression and LTP^{125,175}, but GluA2 and GluA3 knockouts have normal LTP¹⁷⁶. Interestingly, a recent study¹³³ examining the requirement of the C-terminal tails of GluA1 and GluA2, showed that loss of GluA1 C-terminal tail blocks LTP but it can be rescued by reintroducing only the GluA1 CTD and even by swapping the CTD of GluA2 with the CTD of GluA1. This study firmly established the GluA1 CTD as essential for AMPAR trafficking and LTP expression. These studies use varying protocols for inducing LTP and study subunit CTDs using non-physiological conditions, which could contribute to discrepancies in conclusions (Fig 1.4, Table 1.2). Nonetheless, AMPAR phosphorylation appears to play a crucial role in receptor function and localization and a complicated role in LTP.

AMPA organization within the synapse during LTP.

Once at the synapse, AMPARs are organized within and around the PSD^{78,79}. There are around 5 times more PSD-95 molecules than AMPAR molecules in the synapse¹³ so it appears unlikely that recruiting more PSD-95 itself could account for increased AMPAR retention during LTP. During LTP, hearkening back to the idea of modular synaptic composition, the addition of AMPARs to silent modules (i.e. synapses lacking AMPARs) is thought to underlie increased transmission instead of adding receptors to already functional AMPAR modules⁸¹. Early LTP seems to depend on an increase in quantal response and later LTP depends on increase in quantal content, which could result from an increased number of release sites and addition of new

Table 1.2 AMPAR studies in transgenic mice

Paper(s)	Mutation	Age	Result
Kim <i>et al.</i> 2005 ¹⁷⁷ (PDZ ligand)	K1 mutant mice lacking last 7 a.a. GluA1; MALE	3 weeks-7 months	Unaffected: Basal localization and transmission, LTP (fields: 1 TBS, whole-cell pairing: 2 Hz, 200 pulses at 0 mV) and LTD (Fields: 1 Hz, 900 pulses, whole-cell pairing: 0.5 – 1 Hz, 200 – 300 pulses at -40 mV)
Granger <i>et al.</i> 2013, 2014 ^{125,178}	<i>Gria1-3^{tm1}</i> ; replaced with different mutant receptors	P17-20	No single portion of the GluA1 C-terminal tail is required for LTP (2 Hz, 90 sec at 0 mV), GluA2, GluA2(Q) or GluK1 replacement sufficient to rescue LTP GluA1 and GluA2 conditional knockouts have normal LTD (1 Hz, 15 min), GluK1 replacement in GluA1-3 conditional knockout sufficient to rescue LTD
Zamanillo <i>et al.</i> 1999 ¹⁷⁵ Jensen <i>et al.</i> 2003 ¹⁷⁹ Hoffman <i>et al.</i> 2002 ¹⁸⁰ Reisel <i>et al.</i> 2002 ¹⁸¹	GluA1 knockout	3 months P14-42 P41-56 Adult	LTP (Fields: 1x100 Hz, 1 s): impaired; normal spatial learning (Morris Water Maze) LTP: (Fields 1x100 Hz, 1 s/Whole-cell 0.67 Hz, 3 min at 0 mV)- modest/normal amount of LTP at P14 disappears by P42 LTP: TBS- decreased initially but normalizes to WT after 25 min Normal spatial memory; spatial working memory deficits
Jia <i>et al.</i> 1996 ¹⁸² Gerlai <i>et al.</i> 1998 ¹⁸³ Meng <i>et al.</i> 2003 ¹⁷⁶	GluA2 knockout	P16-30 5-8 weeks 2-3 weeks 2-3 months	LTP: (Fields 5 x 100 Hz, 200 ms pulses) enhanced growth retardation and motor deficits, normal brain anatomy, increased excitability, alterations in a number of behaviors across multiple brain areas Normal LTD Fields (1 Hz, 15 min); normal Depotentiation (HFS 100 Hz 1 sec followed by LFS 1 Hz, 15 min); impaired depotentiation but enhanced LTP (100 Hz, 1 sec) in adults
Meng <i>et al.</i> 2003 ¹⁷⁶	GluA3 knockout	2-3 weeks 2-3 months	Normal basal transmission and pre-synaptic function Normal LTD (1 Hz, 15 min) 12-16 days Normal depotentiation 2-3 weeks Enhanced LTP (100 Hz, 1 sec) adults and enhanced level of LTP saturation (6 trains of 100Hz, 1 sec with 5 min interval) in adults

Table 1.2 cont'd

Paper(s)	Mutation	Age	Result
Lee et al. 2003 ¹⁷¹	GluA1 S831/845A knock-in	Young (P21-P28) and old (3 months or older)	<p>Normal basal transmission</p> <p>LTP: old (TBS fields) mostly blocked, young (TBS fields) normal</p> <p>LTD: (Fields PP 1 Hz, 15 min) blocked; young animals lack LTD as well (1 Hz 15 min); lack receptor internalization</p> <p>MWM: learning normal, impaired retention of spatial memory (delayed sessions)</p>
Lee et al. (2010) ¹⁷²	GluA1 S831A knock-in	Young (3 weeks) and old (3 months+)	<p>Young-</p> <p>Normal basal transmission</p> <p>LTP: 4xTBS fields normal</p> <p>LTD: 1Hz fields slight decrease but not statistically significant</p> <p>Old-</p> <p>Normal basal transmission</p> <p>LTP: 4xTBS and 1xTBS fields normal</p> <p>LTD: PP-1 Hz fields normal</p> <p>Normal de-potentialization and de-depression</p>
Lee et al. (2010) ¹⁷²	GluA1 S845A knock-in	Young (3 weeks) and old (3 months+)	<p>Young-</p> <p>Normal basal transmission</p> <p>LTP: 4xTBS fields normal</p> <p>LTD: 1Hz fields virtually absent</p> <p>Old-</p> <p>Normal basal transmission</p> <p>LTP: 4xTBS and 1xTBS fields normal</p> <p>LTD: PP-1 Hz fields mostly blocked</p> <p>Normal de-potentialization</p>
Zhou et al. (2018) ¹³³	GluA1 and GluA2 C-terminal tail swap knock-ins	3-4 weeks old mice for LTP; 13-15 days for LTD	<p>Both show normal basal transmission</p> <p>GluA1-C2KI has normal NMDAR LTD, impaired LTP (1x100 Hz, 4x100 Hz)</p> <p>GluA2-C1KI has normal mGluR LTD (100 μM (RS)-3,5-DHPG for 10 min), not NMDAR LTD (900 pulses at 1 Hz), enhanced LTP (4x100 Hz)</p> <p>Double replacement: normal everything</p> <p>Behavior: GluA1-C2KI impaired spatial learning and memory, GluA2-C1KI contextual fear memory impaired</p>

AMPARs modules. It follows then that receptor number alone does not determine strength of post-synaptic transmission and still concentration of glutamate also matters for receptor activation. Recent work recruiting AMPARs to the synapse from the Kennedy laboratory showed that only synapses opposed to a release site could be strengthened by recruited receptors¹⁸⁴, indicating the necessity for specificity and activity-dependence for plasticity-relevant receptor recruitment.

Another way to explain how AMPARs are recruited to particular synapses is through the PSD slots hypothesis^{154,185-190}. In the PSD slot model, CaMKII acts on PSD to create receptor slots, which can trap the highly mobile AMPARs in the synapse (due to diffusional trapping during plasticity^{89,173} or increasing AMPAR retention in the synapse during LTP by increasing the affinity of AMPARs for the underlying synaptic architecture^{191,192}). Incorporated into this idea of slots is that structural rearrangement must occur within the PSD to accommodate for additional receptors during potentiation. Another iteration of this theory is that slots exist in the PSD but cannot themselves trap receptors. This model suggests that receptors are targeted to the PSD through phosphorylation (CTD would play a mandatory role) and then those receptors are captured once already at the PSD (PSD interacting proteins would be essential as well).

None of these hypotheses as stated in this section can account for all the observations of AMPAR recruitment during LTP. However, the recurrent themes from these hypotheses are that AMPARs of specific subunit composition must be available to be mobilized to the synapse during LTP and must be retained there for some amount of time to confer synapse strengthening or removal for weakening.

Other LTP phenomena: structural plasticity and LTP in vivo

Structural plasticity

In order to accommodate or support the new proteins delivered or stabilized at the synapse, it has been observed that physical spine size increases after LTP. This occurrence detected in the later stages of LTP is called structural plasticity. This includes delivery of membrane, increased adhesion molecule involvement and cytoskeletal remodeling or reinforcement. The resulting change is an enlargement of existing spines that lasts for hours¹⁹³. This thesis will focus more on the molecular changes and signaling processes that occur during plasticity; however, these structural changes are also occurring but will not be explicitly studied here.

LTP correlates to learning and memory in vivo

Potentiation has historically been studied using exogenous stimulation by electrodes that activate many axons outside the realm of physiological, naturally occurring input. Further, whole-cell pairing protocols often match this pre-synaptic stimulation with post-synaptic depolarization. It is no wonder that NMDAR-dependent plasticity mechanisms studied in acute slice preparations with less than physiological stimuli have been difficult to fully recapitulate or discover in natural behaviors in animals. However, *in vivo* learning and memory mechanisms appear to at least overlap with the mechanisms identified *ex vivo*, providing relevant and important information about learning and memory. Through early behavioral experiments, it was found that hippocampal-dependent spatial memory has a parallel requirement for NMDAR activation as in LTP in acute slices; NMDAR antagonists applied before a learning task blocked memory acquisition¹⁹⁴. However, NMDARs have actions independent from

LTP, such as involvement in baseline neuronal transmission. Confusingly, genetic manipulations that disrupt hippocampal LTP can still have intact hippocampal-dependent learning and memory (such as in ¹⁷⁵) and manipulations that keep LTP intact can impair spatial learning (for example, ¹⁹⁵). Work in the perforant pathway to DG in rats demonstrated that saturating LTP as applied by bipolar electrode stimulation could occlude memory formation as tested by Morris Water Maze (MWM) performance¹⁹⁶. Similarly, LTP induced inhibitory avoidance learning in animals can occlude subsequent LTP compared to untrained animals¹⁹⁷. This study demonstrated not only that LTP is likely occurring during behavior but also that it likely acts in the same way as HFS-induced LTP. There have been similar findings in other brain areas (such as in the amygdala with fear conditioning¹⁹⁸). Recent work out of the Malinow laboratory¹⁹⁹ revealed the interplay between LTP and LTD *in vivo*, using optogenetics to either elicit LTD-stimuli to inactivate or LTP to reactivate fear memories.

As for the direct involvement of AMPAR-mediated mechanisms of LTP *in vivo*, Takemoto *et al.* showed that inactivation of synaptic AMPARs through chromophore-assisted light inactivation (CALI) erased fear memories²⁰⁰. Of note, CP-AMPA trafficking has been identified as important in whisker response in the neocortex¹⁰⁵. Fear conditioning requires phosphorylation of S845 and promotes synaptic recruitment of CP-AMPA in the amygdala while fear extinction requires CP-AMPA removal^{201,202}. Within the addiction and drug use literature, cocaine has been found to increase CP-AMPA insertion in the Ventral tegmental area (VTA)²⁰³⁻²⁰⁵. Though most of this work is highly correlative, taken together, these studies suggest strong physiological relevance of LTP mechanisms elucidated *ex vivo* or *in vitro* and behavior *in vivo*.

Long Term Depression (LTD)

Twenty years after the discovery of LTP in the hippocampus⁹⁸ and ten years after the finding that LTP initiation requires NMDAR activation²⁰⁶, LTD within the circuit was discovered²⁰⁷. In contrast to LTP induced by brief, high frequency stimulation, LTD induction results in a smaller response to the same test stimulus after low frequency stimulation for longer periods of time (minutes rather than seconds in LTP). There are many different forms of LTD including homosynaptic, heterosynaptic, *de novo*, or depotentiation following LTP²⁰⁸. In addition, there are multiple protocols for experimentally inducing LTD, like low frequency stimulation (LFS), spike timing dependent plasticity (STDP) and chemical LTD (cLTD). Apart from NMDAR-dependent LTD, another mechanism for LTD induction is through an mGluR-dependent pathway. This mGluR-LTD is usually induced with similar activation patterns as NMDAR-LTD, however mGluR-LTD can be induced using paired-pulse LFS²⁰⁹ and the group I mGluR agonist dihydroxyphenylglycine (DHPG)²¹⁰. This mGluR-dependent form of LTD will not be further discussed in this thesis, and any use of LTD hereafter will be referring to NMDAR-dependent LTD.

NMDAR-dependent LTD requires post-synaptic Ca^{2+} influx and phosphatase activity supported by evidence that LTD expression is blocked by BAPTA (Ca^{2+} chelation)²¹¹ and calcineurin (CaN) inhibition²¹². Depotentiation and *de novo* LTD rely on NMDAR activation and downstream signaling²⁰⁷. This is paradoxical because LTP also requires NMDAR activation. Like LTP, NMDAR-LTD alters post-synaptic receptor content, but unlike LTP, LTD results in a decreased response to pre-synaptic glutamate release by removing AMPARs from the synapse and/or changing receptor

conductance²¹³. One way to explain different outcomes from the same Ca²⁺ source could be that higher Ca²⁺ is needed to activate low-affinity kinases, but lower Ca²⁺ activates higher-affinity phosphatases. In fact, low-level Ca²⁺ from NMDARs initiates phosphatase signaling through protein phosphatase 1 (PP1) and CaN²¹⁴⁻²¹⁶.

Among the targets of phosphatases, AMPARs are dephosphorylated at S845 during LTD by CaN and PP1, which promotes receptor endocytosis and is required for LTD^{104,163,171,172}. Endocytic zones have been discovered at the periphery of excitatory synapses²¹⁷ and these zones are the sites of clathrin-coated pit formation²¹⁸ and AMPAR internalization²¹⁹. Using a cLTD treatment¹⁶², it was discovered that there is rapid AMPAR endocytosis²²⁰⁻²²³, and then AMPARs are sorted in endosomes for either recycling or degradation. It was also observed that there is decreased synaptic AMPAR content with *in vivo* LTD induction²²⁴. For NMDAR-dependent AMPAR internalization (like LTD) Ca²⁺ influx and activation of CaN is needed^{220,223,225}. Interestingly, our laboratory recently identified the transient incorporation of CP-AMPARs during LTD induction and then subsequent removal within 5 minutes of induction¹⁰⁴. This is similar to LTP in young animals however the time-scale is different (removal within ~15 min of LTP induction) and provides an additional link of the CP-AMPAR to plasticity mechanisms.

Though it is widely accepted that AMPARs are removed during LTD, there is no coherent model of the removal of AMPARs during LTD. The CTD of GluA2 is a phosphorylated at Serine 880, disrupting scaffolding interactions with its PDZ ligands to block LTD^{226,227}. To support this idea of receptor phosphorylation occurring in LTD, kinase activity appears to be important for LTD; PKA, CaMKII, Cyclic Dependent Kinase

5 (CDK5), p38 Mitogen-Activated Kinase (MAPK), and Glycogen Synthase Kinase (GSK3) have all been implicated in LTD²⁰⁸. Additionally, studies show that the GRIP/ABP-GluA2/3 interaction is required for LTD²²⁸ and the PICK-GluA2 interaction during LTD is regulated by Serine 880 phosphorylation. However, both GluA2 and GluA2/3 double knockout retain LTD¹⁷⁶. But, LTD is deficient in S845 to Alanine (S845A) GluA1 mutant¹⁷², but LTD is normal in mice lacking GluA1 subunit²²⁹. Therefore the mechanisms of AMPAR removal during LTD are still a bit ambiguous in the hippocampus.

Additional LTD happenings: structural plasticity and LTD *in vivo*

Structural LTD, as mentioned above concerning LTP, also occurs in hippocampal neurons resulting in spine shrinkage or elimination and actin remodeling. Also as mentioned above, this will not be the focus of the research explained further in this thesis.

De novo NMDAR-dependent LTD is easily expressed early in development but becomes more difficult to induce in adult brains^{230,231} or *in vivo*²³²⁻²³⁴. LTP and synaptic potentiation have been shown to be involved in learning and memory *in vivo*, however the role of LTD *in vivo* has yet to be firmly established due to the inability to specifically block LTD with pharmacology or protein disruption because of the overlap in mechanism with LTP. There is mixed and varied evidence for LTD *in vivo* but limited examples include: in the hippocampus correlating with learning and memory such as behavioral flexibility and novelty, the amygdala with fear extinction, and other brain areas (amygdala, perirhinal cortex, VTA, and nucleus accumbens)²⁰⁸. The best evidence for physiological states that involve Hebbian LTD lies in sensory deprivation

experiments, such as during monocular deprivation, demonstrating that LTD is important in the developing visual system²⁰⁸. Monocular deprivation can induce LTD at thalamo-cortical inputs in visual cortex to decrease visual responsiveness to the deprived eye^{235,236}. But this LTD is developmentally regulated and is more difficult to induce in adults, as mentioned previously²³⁶. Some compelling evidence that LTD (and LTP) are involved in behavior was in the amygdala using optogenetic stimulation; fear conditioning could either be inactivated by LTD stimulation or reactivated by LTP stimulation¹⁹⁹. Intriguingly, if the memory was inactivated by LTD, it could be reactivated by LTP stimulation of the pathway. By mimicking HFS stimulation using optogenetics, this study shows a clear relationship between LTP- and LTD-like stimuli and behavioral output. Despite having less robust experimental evidence than LTP, LTD appears to play an important role in a number of processes and behaviors *in vivo*.

Plasticity and learning and memory in disease

Plasticity has long been studied to gain a better understanding of learning and memory with the ultimate goal of identifying the fundamental and basic processes underlying human cognitive function. Beyond this goal of understanding how a typical brain orchestrates these essential functions, there is a great need to understand what happens to these processes during abnormal brain states or diseases. Pathological synapse development and/or function has been implicated in neuropsychiatric disorders (schizophrenia, autism, intellectual disability (ID)), neurodegeneration (Alzheimer's Disease (AD)) and following stroke¹³. Some of the molecules implicated in plasticity could be involved in neuropsychiatric and neurodegenerative disorders^{237,238}. As an example, because AMPAR expression is so important to normal physiology, problems

with AMPAR regulation have been linked to multiple nervous system diseases (AD, ischemia, epilepsy, traumatic brain injury, Amyotrophic lateral sclerosis, among others)²³⁹. Consequently, understanding synaptic function and plasticity at the molecular and cellular level is fundamentally important and has clear clinical implications.

A-kinase anchoring proteins

It is ever so intriguing that the vast number of signaling molecules within the immense, convoluted volume of a neuron can signal in a specific or activity-dependent manner. What has become appreciated through years of study is that a number of signaling molecules are not just randomly drifting through the cytoplasm, but can instead be scaffolded near their sites of action. One such scaffolding molecule that plays an essential role in neuronal activity-coupled signaling is A-kinase anchoring protein (AKAP) 79/150. AKAPs are defined by their ability to bind the cAMP-dependent protein kinase A (PKA); all AKAPs have a canonical amphipathic α -helix, which acts as a docking site for the regulatory subunit of PKA. Regulatory subunit composition determines sensitivity to cAMP (Regulatory subunit I > Regulatory subunit II) and selectivity of AKAP interactions (some AKAPs preferring RII over RI and vice versa).

PKA is a Serine/Threonine kinase that forms a heterotetrameric holoenzyme composed of two catalytic (C α or C β) and two regulatory (RI α , RI β , RII α or RII β) subunits. A flexible linker between AKAP anchoring and the cAMP binding C-subunit of PKA allows for PKA to adopt a number of conformations, allowing for cAMP-independent PKA activity under basal conditions^{240,241}. Recent work showed that the activity range of anchored PKA could be restricted to 150-250 Å of the PKA-AKAP complex^{241,242}. Despite the shared PKA binding that provides the moniker for the AKAP

family of proteins, it is a large family with differential expression across multiple cell types and tissues and participation in varied cellular processes. In fact, a number of the AKAP family members are also multivalent scaffolds, anchoring additional signaling enzymes and effector proteins throughout assorted subcellular compartments (such as AKAP79/150 anchoring both PKA and CaN on the same AKAP molecule²⁴³. This thesis will hone in on AKAP79/150 (also called AKAP5).

AKAP79/150

AKAP79 (human)/150 (rodent) encoded by the *AKAP5* gene is highly enriched in brain, found within the hippocampus at the excitatory post-synapse^{103,244-246}, recycling endosomes^{247,248}, and in dendrites²⁴⁹. It has also been found in superior cervical ganglion^{250,251}, dorsal root ganglion at the somatic PM²⁵², the nucleus accumbens in medium spiny neurons at the excitatory post-synapse²⁵³, and in the ventral tegmental area within dopamine neurons at the inhibitory post-synapse²⁵⁴. AKAP79/150 is known to bind the kinase PKA^{244,255} at the distal C-terminus of the scaffold using the aforementioned canonical amphipathic α -helix. It also can bind the Ca^{2+} -CaM-dependent phosphatase CaN^{243,246,256-258} through the CaN-A subunit binding to a PxIxIT motif located just N-terminal to the PKA binding site (Fig 1.5A). This is particularly important when considering the synaptic signaling that requires bidirectional PKA and CaN signaling, like controlling the phosphorylation state of AMPARs during plasticity. AKAP79/150 also can anchor PKC^{259,260}, which is activated by Ca^{2+} and diacylglycerol (DAG), at the N-terminus of AKAP with a pseudo-substrate like motif and competes with binding of Ca^{2+} -Calmodulin that is by nature tightly coupled to changes in intracellular Ca^{2+} ²⁶¹.

The N-terminus of the AKAP79/150 protein participates in many different cellular activities^{245,249,259,262,263}, including interacting with the PM. Immunocytochemistry for AKAP150 protein in hippocampal neurons shows a clear association with the somato-dendritic plasma membrane but notably enrichment in dendritic spines. Which begs the question: how is AKAP79/150 itself targeted? Previous studies showed that within the N-terminus exist three membrane targeting polybasic domains (A, B, and C), two of which also contain conserved palmitoylation sites^{247,248,264,265}. AKAP79/150 can interact with the membrane through electrostatic interactions of the three polybasic domains with the acidic phospholipid phosphatidylinositol 4,5-bisphosphate (PIP₂). AKAP79/150 can also bind N-cadherin (a neuronal CAM), and the actin cytoskeleton (F-actin) via these domains^{245,256,262}. AKAP79/150 can be further targeted to post-synaptic glutamate receptor signaling complexes through its internal MAGUK binding domain²⁶⁶⁻²⁶⁸. The MAGUK family of proteins, specifically PSD-95 and SAP97^{267,269}, can interact with AKAP79/150 by way of their C-terminal SH3 and GK domains and these interactions allow assembly of large signaling complexes by bringing the AKAP near scaffolded substrates such as the AMPAR and NMDAR²⁶⁷. Of note, but not to be focused on further, AKAP79/150 can also associate with adenylyl cyclase (AC)^{270,271}, the L-type Ca²⁺ channel (LTCC) through a modified leucine zipper (LZ) at the extreme C-terminus²⁵⁷, TRPV1^{252,272}, potassium channels K_v7.2/3²⁵⁰ and K_v4.2²⁷³, and the β₂-adrenergic receptor (β₂-AR)²⁷⁴.

It has been estimated that there are ~20 AKAP79/150 molecules per synapse⁵³ positioned near and acting on AMPARs. This emphasizes the connection during synaptic plasticity, the expression of which is heavily influenced by number of receptors

and biophysical properties of receptors, controlled by kinase and phosphatase mediated phosphorylation and dephosphorylation. Accordingly, AKAP-anchored PKA and CaN are important in regulating synaptic AMPAR content^{104,269,275}. The first evidence of AKAP-anchored PKA influencing AMPAR-mediated transmission came from pharmacological studies utilizing a peptide Ht31 that interferes with AKAP-PKA binding²⁵⁵, revealing that blocking this interaction resulted in decreased AMPAR currents²⁷⁶. Later studies found that AKAP79/150 is the primary AKAP targeting PKA to post-synaptic spines^{256,277,278}. AKAP79/150 interacts indirectly with AMPARs via SAP97^{266,267,277} to couple synaptic activity with PKA-dependent phosphorylation of S845 on GluA1^{166,170,279}. Other studies have found that AMPARs can be further regulated by AKAP-anchored PKC through phosphorylation of S831²⁶³. During LTP and LTD, AKAP can help facilitate AMPAR addition and/or removal via its complex with AMPA/PKA/CaN^{104,275}. Further, it has been demonstrated that AKAP-anchored CaN is required for LTD²⁸⁰ and AMPAR endocytosis²⁶⁶. In line with their clear importance in controlling neuronal functions, AKAP79/150 and other AKAPs have been implicated in diseases such as seizures, addiction, pain, and neurodegeneration like AD and Parkinson's disease²⁵³.

AKAP79/150 mutation studies

To understand AKAP79/150 function, our laboratory and others have taken to transgenic mouse models to study the effects of manipulating AKAP anchoring at the synapse. As explained below, the AKAP150 total knockout showed surprisingly mild phenotypes given the deletion of such an important signaling hub. It is a notable caveat that compensation can occur especially when knocking out a protein from birth in a

transgenic animal. Further, it can be complicated figuring out what particular component of the scaffold is responsible for what phenotypic expression due to the multivalent capacity of the protein. So to circumvent these issues, the Dell'Acqua laboratory and others have studied the importance of AKAP79/150 specific enzyme anchoring in hippocampal neurons using overexpression, knockdown/replacement and knock-in mutations altering the different enzyme anchoring sites. A summary of the published data is listed in (Table 1.3, Fig 1.5B) and detailed below.

AKAP150 knockout (KO)

Two separate knockout mouse lines of AKAP150 have been generated^{281,282}. The first mutant described²⁸¹ exhibited a lack of PKA localization to dendritic spines. This was accompanied by decreases in GluA1 S845 phosphorylation and AMPA agonist-induced current, impaired LTD, and decreased spatial memory retention in the MWM hippocampal-dependent behavioral task. These first AKAP150 KO mice also showed impairments in various cerebellum-dependent behavioral tasks, as AKAP150 is highly expressed in cerebellar neurons. Finally, this knockout showed a decreased susceptibility to pilocarpine-induced seizures.

The second mutant²⁸² had normal LTP and LTD with normal performance in the MWM, reversal learning, novel object recognition task and open field test. Similar to the first report, PKA is lost from spines and increases association with the dominant dendritic PKA scaffold, MAP2. However, the phenotypes in this mutant are for the most part mild and largely no different than WT controls. These KO models hint that disrupting a multivalent scaffold can have offsetting results, such as by perturbing both the kinase PKA and phosphatase CaN.

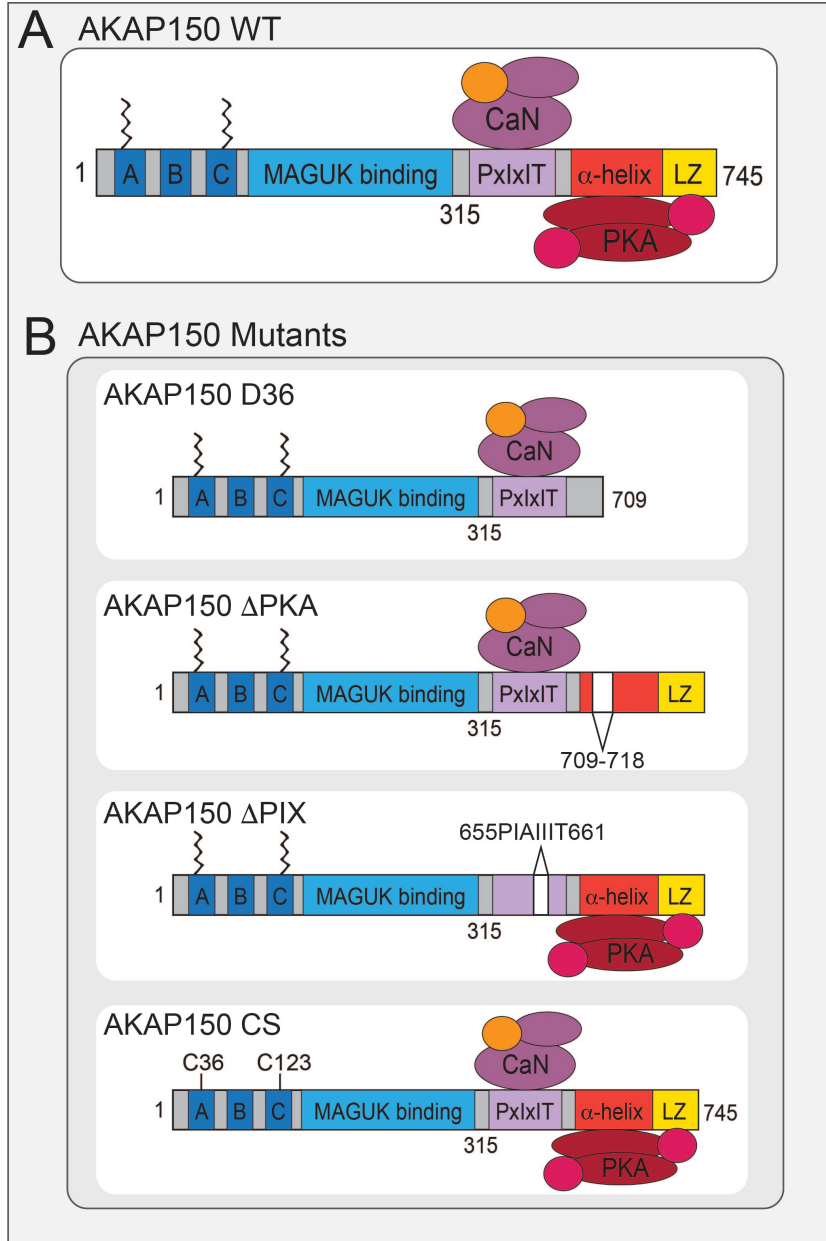


Figure 1.5: AKAP150 WT and binding-deficient mutants.

A. WT AKAP150 interacts with and anchors a number of proteins at the post-synapse. Namely, AKAP localizes to the membrane through interactions within the polybasic domains at the N-terminus of the protein. AKAP anchors the phosphatase CaN and kinase PKA to provide bidirectional signaling. **B.** AKAP mutants.

AKAP150-PKA binding deficient mutants Δ PKA and D36

To specifically study AKAP150-PKA uncoupling, specific mutations that perturb AKAP-PKA binding through mutating the amphipathic α -helix that PKA binds to on the AKAP were generated through a knock-in transgenic mouse model. The D36 AKAP150 PKA-binding mutant was developed first by truncating the last 36 amino acids of the C-terminal domain of AKAP. D36 mice were found to have normal basal transmission (in 2, 4-5 and 7-12 week old animals) and normal basal S845 phosphorylation (at 1, 4 and 8 weeks) but impaired activity-induced phosphorylation of S845 at 4 weeks^{103,283}. LTP is normal in 4-5 week old animals, but impaired at 8 weeks¹⁰³. LTD is impaired in 2 week old animals however depotentiation is normal. These mice also exhibit impairment in the reversal-learning phase in an operant conditioning task²⁸².

The D36 model has a few complications due to the nature of the truncation; the mutant removes the C-terminal portion of AKAP resulting in the removal of an important interaction domain for the LTCC. To circumvent any issues with deleting the additional LZ domain that binds the LTCC¹⁰⁴, our laboratory developed the AKAP150-PKA binding deficient mutant Δ PKA that just removes 10 amino acids (709-718) from the N-terminal portion of the amphipathic α -helix PKA RII binding site. Overall, phenotypes for the D36 and Δ PKA animals are very similar. Δ PKA animals have normal basal transmission (excitatory and inhibitory transmission at 2-3 weeks) but decreased GluA1 S845 phosphorylation basally. Δ PKA mice show a slight increase in dendritic spine number. Similar to D36, Δ PKA animals retain only ~10% of LTD expression. LTP expression is normal but insensitive to CP-AMPA antagonism with IEM1460, unlike WT that is sensitive to IEM1460 antagonism at this age. Overall, Δ PKA mouse studies indicate that

AKAP-anchored PKA promotes GluA1 phosphorylation and CP-AMPA recruitment both during LTP and LTD.

AKAP150-CaN binding deficient mutant Δ PIX

Similar to D36 and Δ PKA animals, to study decoupling of AKAP150 and CaN, our lab generated a mutant mouse model that deletes the 7 amino acids (655-661) containing the PIAIIT PxlIT domain, which we call Δ PIX. Δ PIX mice have normal spine density and basal transmission with enhanced basal GluA1 S845 phosphorylation²⁷⁵. Mice with this mutation exhibit impaired NMDAR-dependent LTD and enhanced 100 Hz LTP. The mechanism for this appears to be a lack of removal of AMPARs and AKAP150 from the PSD following LTD. Further, Δ PIX animals show enhanced CP-AMPA basally that act to inhibit LTD and facilitate enhanced LTP. AKAP-anchored CaN appears to be important for restricting synaptic incorporation of CP-AMPA, by opposing PKA-mediated phosphorylation of S845, basally and in the removal of transiently recruited CP-AMPA both during LTP and LTD^{104,275}.

Protein palmitoylation

Palmitoylation, the dynamic post-translational lipidation

As mentioned above, AKAP79/150 is targeted to the membrane through a number of interactions within the N-terminal domain. In addition to this targeting, AKAP79/150 is also post-translationally modified by fatty acids at two sites in the targeting domain to facilitate membrane interactions. Besides scaffolding proteins, cells have adapted numerous methods to facilitate the precise trafficking and distribution of proteins to various specialized compartments. Some of these methods are post-translational modifications (PTMs), including phosphorylation, ubiquitination, and

Table 1.3 AKAP150 transgenic mouse model studies

AKAP150 mutation	Phenotype	References
Knockout (2 different lines)	<p>Basal 2 weeks normal or slightly enhanced 8 weeks normal</p> <p>LTP (100 Hz, 1 sec) 8 weeks normal</p> <p>LTD (1 Hz, 15 min) 2 weeks normal 8-16 weeks impaired (?)</p> <p>Behavior Modest deficits spatial memory Normal reversal learning Impaired cerebellar behaviors Reduced pilocarpine seizures</p>	<p>Tunquist <i>et al.</i> 2008²⁸¹ Weisenhaus <i>et al.</i> 2010²⁸²</p>
D36	<p>Basal Normal</p> <p>LTP (100 Hz, 1 sec) 4-5 weeks normal 8 weeks impaired</p> <p>LTD (1 Hz, 15 min) 2 weeks impaired (retain ~10%)</p> <p>Depotentialation (100 Hz, 1 sec and 5 min later 1 Hz, 15 min) Normal</p> <p>Behavior Impaired reversal learning Normal spatial learning, working memory, and open field behaviors</p>	<p>Lu <i>et al.</i> 2007¹⁰³ Lu <i>et al.</i> 2008²⁸³ Weisenhaus <i>et al.</i> 2010²⁸²</p>
Δ PKA	<p>Basal Normal</p> <p>LTP (100 Hz, 1 sec) 2 weeks normal magnitude (but not CP-AMPA dependent)</p> <p>LTD (1 Hz, 15 min) 2 weeks impaired (retain ~10%)</p>	<p>Sanderson <i>et al.</i> 2016¹⁰⁴</p>
Δ PIX	<p>Basal Normal but increased CP-AMPA</p> <p>LTP (100 Hz, 1 sec) 2 weeks enhanced, but 50 Hz, 2 sec normal</p> <p>Depotentialation (100 Hz, 1 sec and 30 min later 1 Hz, 15 min) Impaired: depotentiates to a similar amount but does not reach WT baseline levels</p> <p>LTD (1 Hz, 15 min) 2 weeks impaired (1 Hz PP 900 pulses 50 ms interval LTD and 10 Hz transient depression also impaired)</p>	<p>Sanderson <i>et al.</i> 2012²⁷⁵ Sanderson <i>et al.</i> 2016¹⁰⁴</p>

glycosylation. These modifications allow for activity-dependent changes beyond genetic control to facilitate protein trafficking, function, interactions and/or stability. In particular, fatty acid modifications increase hydrophobicity of proteins and subsequent insertion into intracellular membranes and the PM. It was first discovered that proteins could contain covalently bound fatty acids in the late 1970's²⁸⁴. In the years since, it was found that many types of lipidations commonly occur in cells to help maintain ordered protein distribution; common lipid modifications include myristoylation, prenylation, and palmitoylation. A broad range of lipidations can be added to cysteines and this general fatty acid linkage to cysteines is called acylation. Acylation appears to be an abundant modification as it is estimated that ~10% of the human genome encodes proteins that are modified by acylation²⁸⁵. One particular type of acylation is palmitoylation. Specifically, S-palmitoylation is the addition of 16-carbon saturated fatty acid to cysteine residues via labile thioester linkage to both soluble and integral membrane proteins. This attachment makes S-palmitoylation unique among lipidations because it is reversible, allowing for dynamic regulation. S-palmitoylation was first shown to be reversible less than a decade after the discovery of acylation²⁸⁶. N-palmitoylation is irreversible due to the addition of a stable amide bond. For the purpose of this thesis, "palmitoylation" will refer to the reversible S-palmitoylation.

Many different types of proteins are modified by palmitoylation. As such, palmitoylation can control different protein properties not just simply trafficking to the PM, and has also been shown to target proteins to precise microdomains such as lipid rafts (membrane specializations containing sphingolipids and cholesterol)²⁸⁷ or localization to or trafficking through particular endomembranes (such as endosomes

and Golgi), affecting their subcellular location²⁸⁸. Though there is no real consensus sequence for determining palmitoylation sites, some information has been gleaned about palmitoylation sites on different types of proteins like cytosolic and integral membrane proteins. Cytosolic proteins are usually palmitoylated at cysteines found near the N- or C-terminus and near basic residues, which facilitate membrane interactions with acidic lipid head groups. This is not always the case because there are also instances of cytosolic proteins modified by palmitoylation at internal sites or sites near other hydrophobic lipid modifications. One classic, well-studied example of cytosolic protein palmitoylation is H-Ras, palmitoylation cycling of which results in membrane and cytosol shuttling²⁸⁹. Integral membrane protein palmitoylation usually occurs at residues proximal to the TMD to potentially cooperate with other membrane targeting motifs. Still, very little is known about why and where palmitoylation events occur on particular cysteines in a given protein. At the very least, it seems like palmitoylation occurs at cysteines neighboring membranes largely due to the requirement of proximity to the membrane-localized palmitoyl acyltransferases (PATs), discussed in the next section.

Enzymes governing palmitoylation

DHHCs

Palmitate is transferred from palmitoyl-CoA via a cysteine rich domain to cysteine residues on the acceptor protein. In the early days of palmitoylation research, it was contested whether palmitoylation required a palmitate transferase to catalyze the deposition of the palmitate group onto the acceptor protein. This was largely because it was shown that palmitoyl linkage could occur spontaneously *in vitro* in the presence of palmitoyl-CoA and with a neutral pH²⁹⁰. However, PATs, enzymes that can catalyze

palmitoylation, were discovered in yeast^{291,292}. And in fact, this yeast research demonstrated that the majority of palmitoylation was catalyzed by a particular family of PATs, the DHHC proteins²⁹³. DHHC proteins²⁹⁴ are an integral membrane protein family composed of 23 members in mammals and 7 proteins in yeast. DHHC proteins have four or more TMDs and a conserved cysteine rich domain (CRD) within a cytosolic loop between TMDs. The CRD is a ~50 amino acid stretch containing a D-H-H-C (Aspartate –Histidine –Histidine – Cysteine) motif that has been found to be required for PAT activity²⁹⁵ (Fig 1.6A). A two-step mechanism has been proposed for DHHC driven palmitoylation; first, DHHC is autopalmitoylated through the addition of a palmitoyl moiety to the Cysteine in the DHHC motif by way of palmitoyl-CoA and second, the substrate is palmitoylated by transfer of the moiety from the DHHC motif^{296,297} (Fig 1.6B). The first step involves autopalmitoylation, the palmitoylation of the DHHC family members themselves, which appears to be an important intermediate before the transfer of the palmitoyl moiety to the substrate. Autopalmitoylation could also act as a method to regulate the DHHC enzymatic function or localization to direct it toward substrate and confer palmitoylation reaction competency. Due to the large number of members in the DHHC family, PATs exert wide-ranging palmitoylation control and specificity for substrates and subcellular localization, and thus have the potential for diverse and divergent roles in the cell. Adding another layer of complexity, some substrates can be palmitoylated by more than one PAT, while others require palmitoylation by a single PAT, hinting at functional redundancy between DHHC family members. Recently, the first PAT crystal structures have been reported and yield insight

into the function of the DHHC proteins and molecular mechanism underlying palmitoylation^{298,299}.

Early work determined that much of the palmitoylation in cells is occurring through DHHC PAT activity²⁹³, but identifying PAT-substrate pairs has proven difficult. The substrate specificity of the palmitoylation moiety transfer by the DHHC family of proteins could be conferred by the localization of the PAT within the cell. DHHCs are found throughout the entire endomembrane system of cells, indicating proteins can be modified by palmitoylation at varied cellular localizations throughout their lifetimes³⁰⁰. There appears to be substrate redundancy or overlapping specificities between different DHHC proteins; accordingly one palmitoylation site on a protein could be the substrate for multiple DHHCs throughout the cell. DHHC proteins are mostly ubiquitously expressed across multiple cell types but appear to localize to specific compartments within cells. It is unknown how the individual DHHC isoforms are targeted within the cell; however, we have come to know that the DHHC proteins are often localized to specific subcellular compartments, such as DHHC3 in the Golgi, DHHC2 in the synapse and within recycling endosomes, and DHHC5/8 at the PM at the PSD. The Golgi appears to be particularly saturated with DHHC proteins (12 of 23 DHHC proteins localize to the Golgi³⁰¹), indicating that it is a hub for palmitoylation. However, subcellular targeting of DHHC proteins might depend on cell type³⁰². Apart from the highly conserved DHHC-CRD, the remainder of the DHHC protein sequence is quite divergent. The NTD and CTD of DHHCs could confer some localization specification. For example, DHHC3, 5 and 8 all contain PDZ-binding motifs, which is important for substrate recruitment and other protein-protein interactions²⁸⁵. However, there needs to be more research to

determine if the NTDs or CTDs confer substrate specificity³⁰³. Overall, the different subcellular localizations of PATs allows for an additional level of dynamic control of protein palmitoylation to ensure proper coupling of activity/extracellular signaling to PAT function.

The large size of the DHHC family has also contributed to the difficulty in identifying specific PAT-substrate pairings. Nonetheless, using candidate based approaches and coexpression studies, a number of pairs have been identified³⁰³. For example, PSD-95 is palmitoylated by both DHHC2 and DHHC3; DHHC2 palmitoylation is more important during synaptic activity for the dynamic recruitment of PSD-95 to the synapse while DHHC3 constitutively palmitoylates PSD-95 in the Golgi³⁰⁴. As more pairs are identified, it will be easier to pull out DHHC-specific consensus sequences. Contributing to this difficulty, there is no current method to visualizing palmitoylated proteins in cells (apart from a PSD-95 specific intrabody that identifies palmitoylated PSD-95), which is much different than other modifications such as phosphorylation. DHHC knockout mice have helped determine some function and substrate information^{303,305}. These mouse models will be discussed in more detail below.

PPTs

Palmitoylation is removed by protein palmitoylthioesterases (PPTs), which are far less studied than the PATs. PPTs, in contrast to PATs, hydrolyze S-acylated cysteines to remove palmitoylation. They belong to the serine hydrolase superfamily that constitutes ~115 genes in the human genome³⁰⁶. Only a handful of PPTs have been identified. This woefully small list so far contains PPT1, APT1, and several ABHD proteins³⁰⁷. It is known that PPT1 is a lysosomal protein and mutations in the gene

encoding for PPT1 have been implicated in neurological disorders. PPTs were thought to be localized only to the lysosome where evidence showed they aided in lysosomal degradation of fatty-acid modified proteins. However, it was demonstrated that protein palmitoylthioesterase-1 (PPT1) is distributed throughout neurons, in the soma and neurites³⁰⁸. PPT1 expression is regulated developmentally and spatially and correlates with synapse development³⁰⁹, with preferential targeting to axons over dendrites in mature neurons. Acylprotein thioesterase-1 (APT1) is thought to remove palmitoylation from the cytosolic surface of membranes. It is unknown how PPTs are regulated, though APTs are thought to act ubiquitously due to the need for tight control of palmitoylation. Several ABHD proteins have also been shown to have PPT activity³⁰⁶. Work looking at inhibition of serine hydrolases using the drug hexadecylfluorophosphonate (HDFP) showed that depalmitoylation of a number of proteins was blocked in the presence of the drug. The majority of the HDFP-sensitive serine hydrolases contain an alpha/beta-hydrolase fold domain (ABHD) and act as PPTs³¹⁰. ABHD17³¹¹ depalmitoylates N-Ras and PSD-95 and it is proposed that ABHDs might be more specific in substrates than other PPTs. While some proteins are palmitoylated just after translation and remain palmitoylated for the lifetime of the protein, other proteins go through palmitoylation and depalmitoylation cycles. Palmitoylation and depalmitoylation cycles can be dynamically or constitutively regulated by cellular processes or signaling to allow for exchange of proteins between different cellular compartments. Palmitoylation appears to be important for protein stability because depalmitoylation is essential for protein degradation³¹² and palmitoylation protects proteins from degradation²⁹⁵. It is clear that the opposing

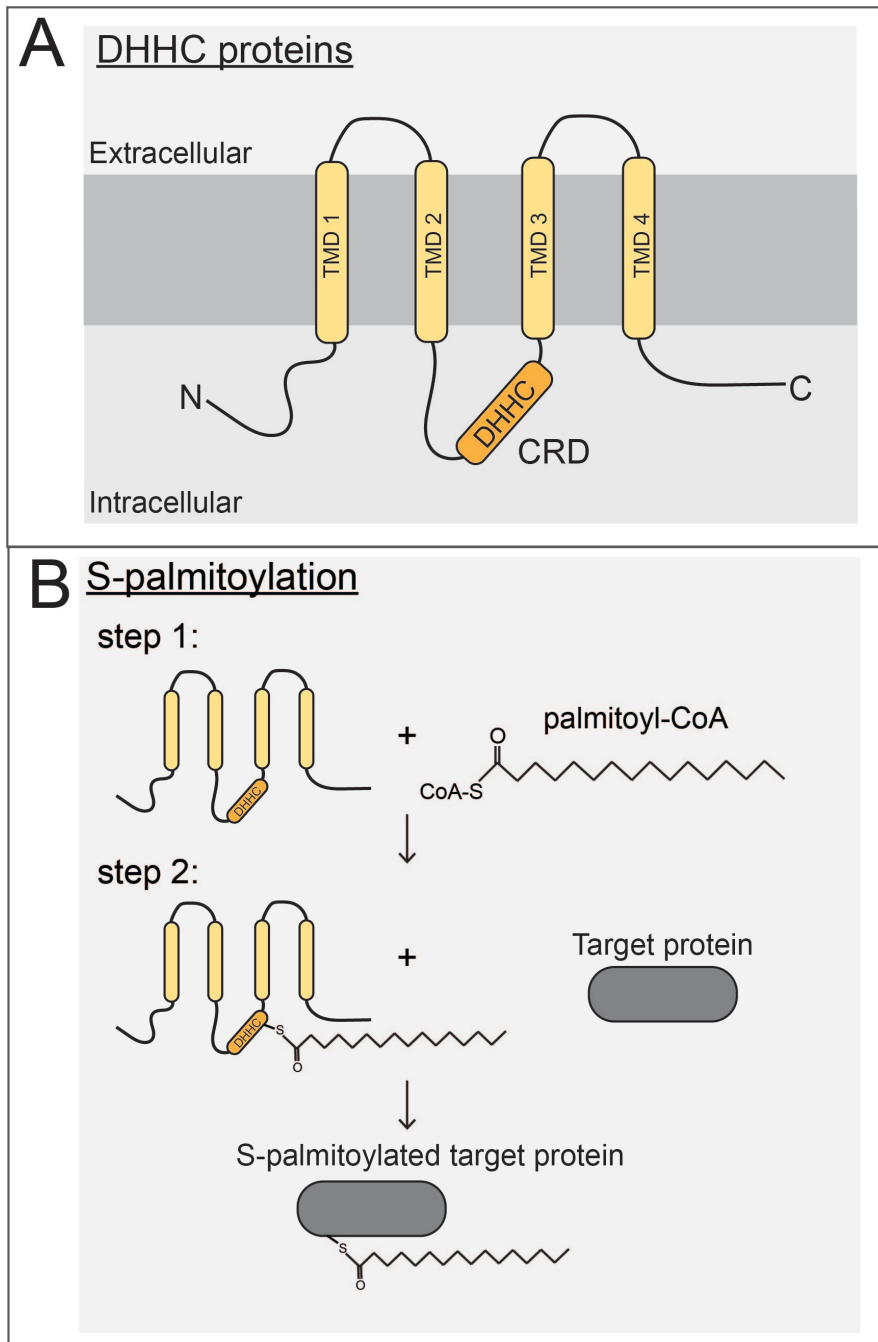


Figure 1.6: The DHHC proteins and palmitoylation mechanism.

A. Schematic of the general structure of the DHHC family of proteins, containing four transmembrane domains and a cysteine rich domain containing the DHHC motif important for catalyzing the transfer of palmitoyl moieties onto target proteins. **B.** The two-step method of S-palmitoylation.

reaction to palmitoylation, depalmitoylation is also incredibly important for normal cellular function.

Detecting palmitoylation in cells

Historically it was quite difficult to assess palmitoylation state due to the previously mentioned lack of consensus sites paired with lack of detection methods. Unlike phosphorylation, there are virtually no antibodies for detecting palmitoylation modifications on proteins. However, over the past twenty years progress in palmitoylation research has been exponential due to the advancement in detection methods, most of which are biochemical. These methods have varying levels of quantitation, sensitivity and amenity to different cells systems. Methods to detect palmitoylation can be broadly grouped into two categories, metabolic labeling and biochemistry/biotin exchange³¹³ (Fig 1.7).

Metabolic labeling

Metabolic labeling (Fig 1.7A), the most commonly used technique to detect palmitoylation, utilizes synthetic analogues of fatty acids with biorthogonal tags that get incorporated onto cysteines of modified proteins. The oldest method for detecting palmitoylation is radioactive labeling²⁸⁴, where cells are fed tritiated palmitate that is incorporated into proteins and visualized using autoradiography^{314,315}. One shortcoming of this technique is that it depends on the palmitoylation turnover of a protein of interest, because the radiolabeled palmitate must have time to be incorporated into the endogenous protein. In this way, radiolabeled palmitate can be used in pulse-chase style experiments to measure the half-life of protein palmitoylation. As with any radioactivity assay, these assays have issues because of the hazardous nature of the

method. Further, this approach is only able to monitor palmitoylation of a single protein. It cannot be directly used to identify palmitoylation sites and requires mutations of predicted palmitoylation sites and good antibodies to the target areas of the protein to attempt palmitoylation site discovery. Finally, there are some concerns about the specificity of the labeling due to nonspecific labeling of other non-palmitoylation fatty acylation. Needless to say, radiolabeling proved useful early on but has since been replaced by more tenable methodologies.

To combat the problems with radioactivity, click chemistry using biorthogonally labeled analogs of palmitic acid (either alkyne or azide tagged) was combined with metabolic labeling³¹⁶. This method has also been used successfully paired with mass spectrometry (MS)^{316,317}, stable isotope labeling with amino acids in cell culture (SILAC)²⁹⁴ and pulse-chase experiments³¹⁸⁻³²⁰. Click chemistry has been successfully paired with proximity ligation assays (PLA); this method must use fixed cells but can be used to image palmitoylated protein localization using subcellular compartment markers³²¹. Pairing PLA with click chemistry is the only current method for visualizing palmitoylation *in situ*. A similar issue with click chemistry plus metabolic labeling and radiolabeling is that there is no way to standardize palmitoylated protein levels to the unpalmitoylated protein levels. This approach is useful in cell culture systems but has dubious *in vivo* applications owing to the potent inhibitory effect of the most common fatty acid analogues used in click chemistry methods on cytochrome P450 hydroxylase, which is important for fatty acid synthesis³¹³.

Biochemical approaches to palmitoylation detection

Biochemical methods (Fig 1.7B) for detecting palmitoylation take advantage of protection of free thiol groups with N-ethylmaleimide (NEM) followed by hydroxylamine cleavage of palmitoyl groups. This method was first described³²² paired with radioactive alkylation reagents read out by autoradiography and proved to be more sensitive than metabolic labeling and can be used in cells and tissues³¹³. Further iterations of this technique, lacking radiolabeling have been developed. Three main methods of detection using biochemical techniques are: acyl-biotin exchange, acyl-RAC, APEGs. The first development was acyl-biotin exchange (ABE); ABE utilizes protection of free thiol groups with NEM, cleavage of palmitoylation moieties with hydroxylamine (HAM), however the final step is to label the newly freed thiols with biotin. This method can be used with the downstream readout of western blotting or MS. Due largely to a lack of consensus sequence, the palmitoylproteome was studied early on in yeast through proteomics and ABE chemistry³²² by labeling all palmitoylated proteins to pull them down and affinity-purify with streptavidin for processing with tandem MS-based proteomics²⁹³. This technique was also used to study synaptosomes from rat brains³²³ and probe specifically for the proteins that are palmitoylated at neuronal synapses. A further extension of this method has also been successfully employed using western blotting to analyze the palmitoylation state of specific proteins of interest^{324,325}. The ABE method has a few caveats, largely coming from the sample preparation methods. Like the metabolic labeling approaches, the ABE method also does not provide information about the exact site of palmitoylation. In order to isolate the palmitoylated proteins, a number of protein extractions must be carried out that can result in loss of sample.

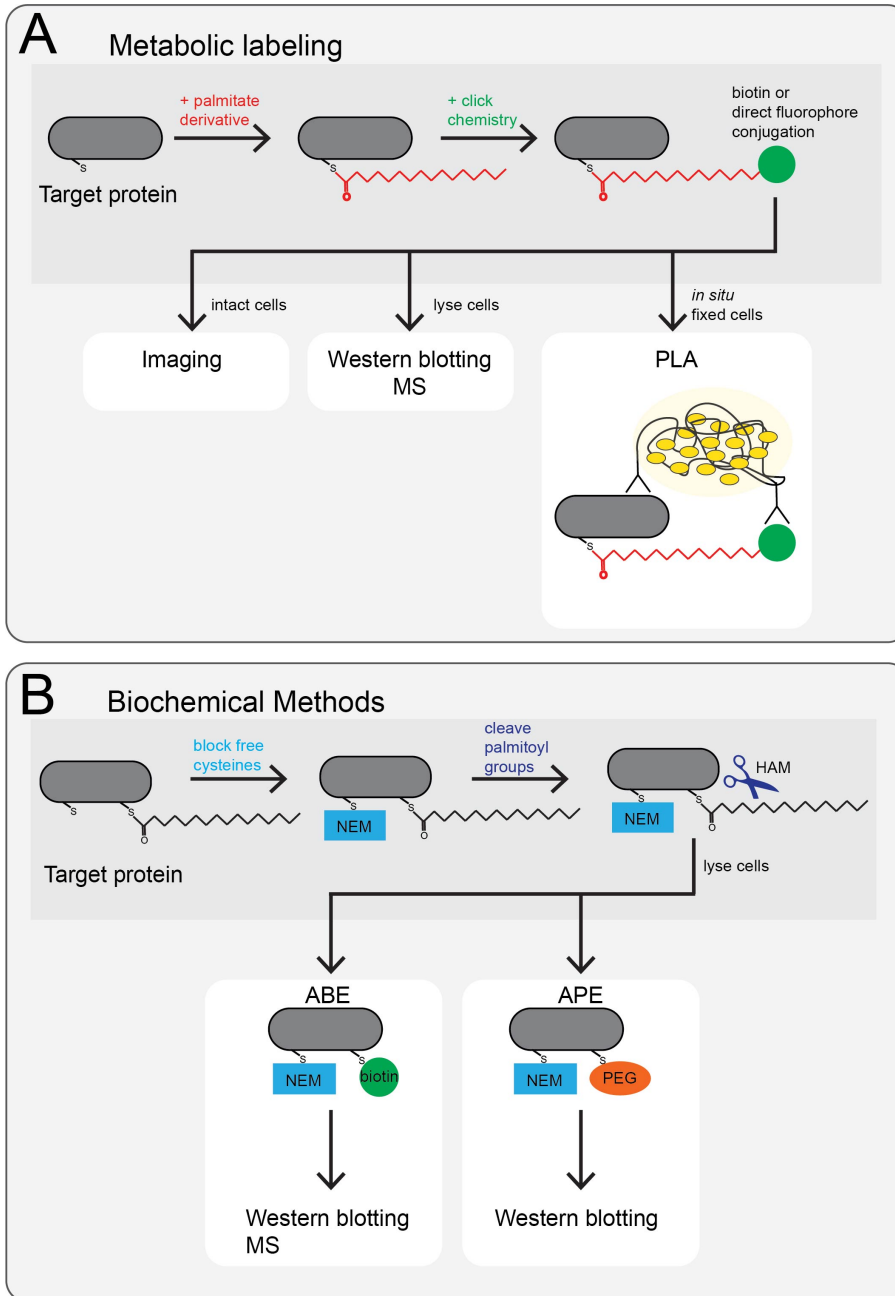


Figure 1.7: Palmitoylation detection techniques.

A. Metabolic labeling techniques; historically metabolic labeling was used to detect palmitoylation of a targeting protein using either radioactivity or biotin/fluorescence. **B.** More recently, more user friendly and sensitive biochemical techniques have been developed for use in combination with western blotting and mass spectrometry with the potential to read out palmitoylation of a large number of proteins.

Another consideration is that all free cysteines must be blocked in order to assure there are no false positives; similarly, incomplete thioester hydrolysis and/or biotin labeling can cause false negatives. The ABE method allows for quantitative analysis and the ability to enrich samples for palmitoylated proteins increasing signal to noise. As an alternative approach to ABE, researchers have used resin-assisted capture (Acyl-RAC), which replaces the biotin pulldown steps with a direct conjugation to a resin containing groups that are reactive with thiols^{326,327}. Acyl-RAC can be paired with MS and has similar limitations as the ABE method.

The most recent development in biochemical palmitoylation detection methods is Acyl-PEG exchange (APE). APE uses NEM protection and HAM to cleave thioesters like the previous biochemical methods but directly labels the individual groups with maleimide-conjugated polyethylene glycol polymers. This causes a molecular weight shift in the labeled protein when resolved with western blotting, Acyl-PEG exchange gel-shift (APEGs)^{306,328}. APE shares the same shortcomings as the above mentioned biochemical assays, but has the distinct advantage of being internally controlled and able to separate distinct palmitoylation states within the same sample (i.e. if a protein is modified by multiple palmitoyl-moieties, the ratio of unpalmitoylated to mono-palmitoylation to dual-palmitoylation etc. can be compared).

Overall, protein palmitoylation has been demonstrated to be a complex and dynamic way to alter protein function and localization; palmitoylation of a single cysteine includes a complicated cascade of events from the identification of the site, the palmitoylation event by a particular PAT, depalmitoylation by a specific PPT, and the subcellular compartmentalization of the palmitoylation and depalmitoylation events, all

of which can contribute to the effect that palmitoylation has on properties of the palmitoylated protein. However, there is much to understand about the process of palmitoylation cycling and how it influences many different cellular processes both physiologically and under nonphysiological conditions.

Synaptic protein palmitoylation

Considering the complex architecture of the neuron, with long ranging projections like axons and extensive processes like dendrites, it is not surprising that neurons require precise protein trafficking and localization to ensure proper functioning. Neuronal proteins are lipidated most frequently through palmitoylation²⁹⁴, which have emerged as a useful means within neurons to ensure for proper protein distribution. It has long been appreciated that neuronal proteins can be modified by palmitoylation³²³ and palmitoylation is quite common among neuronal proteins; it is thought that upward of ~40% of synaptic proteins are palmitoylated³²⁹, including cytoplasmic and integral membrane proteins, such as enzymes, receptors³³⁰, and scaffolds³³¹. Palmitoylation is important in a number of synaptic processes including: axon guidance, synaptic vesicle fusion, protein sorting and trafficking, receptor clustering, and protein scaffolding at the synapse³³². Importantly, half of all DHHC proteins are expressed in the brain³³³ with different levels of expression across different brain areas and with particular family members localizing to synaptic sites. Indeed, DHHCs1, 2, 5, 8 and 12 have been found in dendrites and DHHCs 2, 5 and 8 are expressed at the neuronal PM and found within subsynaptic compartments³³³. DHHC protein targeting within the cell is still a problem yet to be solved and it is still unknown how DHHC proteins acquire information about activity state of the neuron and if and how that in turn regulates their activity²⁹⁴.

One classic example of a neuronal protein undergoing dynamic protein palmitoylation cycling is the important synaptic scaffold PSD-95, one of the first synaptic palmitoylation substrates to be studied. PSD-95 is the predominate organizer of the post-synaptic density and has been found, using super-resolution fluorescence imaging techniques, to organize into heterogeneous and dynamic nanoclusters^{78,79,334}. PSD-95 palmitoylation is necessary for localization to the synapse^{331,335} and localization to the membrane³⁰²; a palmitoylation-deficient mutant of PSD-95 is completely cytosolic³³⁶. Palmitoylation of PSD-95 also limits its lateral movement within the plasma membrane once the protein is at the synapse³³⁴. PSD-95 palmitoylation is dynamic with palmitate half-life around two hours, which is controlled in a activity-dependent manner³³². PSD-95 palmitoylation cycles can happen within a single dendritic spine and individual PSD-95 nanodomains can undergo rapid and continuous palmitoylation and depalmitoylation^{302,334}. Palmitoylation of PSD-95 has been found to also regulate downstream processes and associated proteins. AMPAR localization to synapse is correlated with PSD-95 palmitoylation, with a decrease in AMPAR synaptic occupancy with decreased PSD-95 palmitoylation³³⁷. It was later discovered that PSD-95 could be palmitoylated by both DHHC3 and DHHC2³⁰⁴ and recent work out of the Fukata laboratory identified the ABHD17 family as PPTs that depalmitoylate PSD-95³⁰⁶.

Palmitoylation in neuronal pathology

Not surprisingly, due to the extensive list of proteins modified by palmitoylation and dependent on this modification for proper protein function, multiple components of palmitoylation cycling have been identified as altered in diseases. This is especially

true in neurological disorders³¹³, such as in neurodegenerative disorders like Alzheimer's disease, Huntington's disease and infantile neuronal ceroid lipofuscinosis.

Alzheimer's disease (AD) is a progressive neurodegenerative disorder, characterized by large protein aggregates in the brain causing neuronal dysfunction resulting in memory loss and cognitive decline. The hallmark pathological feature of AD is amyloid plaques caused by aggregation of the protein beta-amyloid (A β). A β is derived from amyloid precursor protein (APP) through proteolytic cleavage by β -secretase (BACE1) and γ -secretase. APP is normally processed by α -secretase resulting in non-amyloidogenic species; amyloidogenic species of A β are created by APP cleavage by BACE1 then γ -secretase, sequentially. This pathogenic form of A β can go on to form the plaques characteristic in AD patient brains. A number of genetic mutations have been identified that predispose individuals for early-onset familial AD, such as in APP and presenilin, a protein important for amyloidogenic cleavage of APP in the γ -secretase complex³³⁸. Palmitoylation has been found to be an important regulator of a number of important proteins in AD, including APP and BACE1³³⁸. APP is palmitoylated and this palmitoylation has been implicated in amyloidogenic processing of APP. Palmitoylated APP associates with lipid rafts and promotes cleavage by BACE1 rather than α -secretase³³⁹. BACE1 is also palmitoylated, though it is controversial what role this modification plays in amyloidogenesis and AD. There is evidence both that BACE1 palmitoylation enhances A β production and also that it has no effect at all³³⁸. A recent study targeted BACE1 palmitoylation specifically using a knock-in mouse model mutating the four cysteine residues that are palmitoylated to unpalmitoylatable residues³⁴⁰. The authors saw no effect of this mutation on APP processing, but did find

a significant decrease in amyloid burden and resistance to cognitive decline when crossing the BACE1 mutant with a mouse model of AD³⁴⁰. While there are hints that palmitoylation of key AD players could influence cognitive function, much more needs to be understood about AD pathology and palmitoylation in AD pathogenesis.

Huntington's disease (HD) is a neurological disorder caused by a poly-glutamine (poly-Q) expansion in the huntingtin protein. A hallmark of this disease is protein aggregation within cells that is thought to arise from protein misfolding due to the polyQ-repeats. Huntingtin-interacting-protein-14 (HIP14) was discovered to have PAT activity, also known as DHHC17³⁴¹. Huntingtin is a strong candidate to be a substrate for HIP14 palmitoylation and mutant huntingtin appears to be less palmitoylated than wild type (WT). Further, less palmitoylation of mutant huntingtin was associated with more aggregation and more toxicity to cells³⁴². A mouse model exhibiting less than 10% WT protein levels of HIP14/DHHC17 has decreased striatal volume, loss of medium spiny neurons, decreased excitatory synapses, impaired hippocampal LTP and memory, and deficits in motor behaviors³⁰². Interestingly, a more similar phenotype to HD mouse models is observed in DHHC13 KO mice³⁰². However, it is unclear how these two PATs converge in humans and how they may contribute to human HD has yet to be determined.

Infantile neuronal ceroid lipofuscinosis (INCL) is a neurodegenerative disorder in children caused by a variety of mutations in the PPT1 gene³⁴³. The disease results from a nearly total loss of cortical neurons as well as causing vision loss due to retinal cell loss. This initial loss of neurons is followed by massive glial proliferation, resulting in gliosis. The proposed mechanism of neuron loss is through lysosomal storage

dysfunction and aberrant depalmitoylation³⁴³. PPT1 knockout mice recapitulate the human disease, with progressive cortical neuron loss and seizures, resulting in early death^{344,345}.

Evidence that palmitoylation is implicated in cognitive function was found by creating transgenic mice altering various DHHC family members. DHHC8 KO homozygotes have axonal growth and branching abnormalities, while heterozygotes have impaired working memory³⁴⁶. DHHC8 mutants exhibit sex-specific behavioral deficits with pre-pulse inhibition and locomotor activity due to increased fear in female mice. Related to these schizophrenia-associated phenotypes, regions of the DHHC8 gene in humans have been connected to schizophrenia susceptibility^{347,348} and microdeletions in this gene region show cognitive deficits and ~30% develop schizophrenia³⁴⁶. The phenotypes observed between DHHC5 and DHHC8 mutants are overlapping, not surprisingly due to their homology. Studies with a DHHC5 hypomorph, which only display ~7% of the protein expression of WT, is born at half the rate expected and has a significant deficit in contextual fear conditioning and hippocampal learning³⁴⁹. DHHC5 is known to palmitoylate GRIP1³²⁵ and δ -catenin³⁵⁰ among other synaptic proteins. Additionally, DHHC9 mutations have been implicated in X-linked intellectual disability³⁵¹. As a final example, DHHC2 is a tumor suppressor that is lost in a number of metastatic cancers³⁰² and was found to be important in control of cell morphology.

Thus, emerging evidence suggests that palmitoylation and the enzymes that catalyze the reaction, PATs and PPTs, may be associated with human disorders,

including neurodevelopmental and neuropsychiatric conditions, further highlighting the importance of studying these complex but essential mechanisms.

AKAP79/150 palmitoylation

Proteomics experiments from rat synaptic membranes identified AKAP79/150 as a palmitoylated protein³²³. Our laboratory subsequently identified the sites of AKAP79/150 palmitoylation on two conserved Cys residues within the N-terminal membrane-targeting domain²⁴⁷. Palmitoylation of AKAP is not a requirement for membrane targeting, unlike cytosolic proteins, because a mutant AKAP79 that cannot be palmitoylated (achieved by mutating the two Cys to Ser) is still targeted to the PM. However, palmitoylation appears to target AKAP79/150 to specific membranes, namely the RE and lipid rafts in the PSD^{247,264}. Glycine chemical LTP (cLTP) stimulation and kainate-induced seizures increase AKAP79/150 palmitoylation while NMDA cLTD decreases AKAP79/150 palmitoylation^{247,265}. Interestingly, AKAP79/150 palmitoylation state correlates with its occupancy in dendritic spines, with more palmitoylation correlating with more spine occupancy. If a palmitoylation-deficient AKAP79 (AKAP79 CS) is acutely overexpressed in cultured rat hippocampal neurons, AKAP79 shows a decreased colocalization with endosomal markers (transferrin receptor [TfR], early endosome antigen 1 [EEA1]) and is less strongly associated with the PSD, as demonstrated by easier removal from spines with detergent extraction and NMDA treatment²⁴⁷. This palmitoylation-deficient AKAP CS mutant resulted in enhanced basal transmission by whole-cell voltage clamp experiments recording mini excitatory post-synaptic currents (mEPSCs) and impaired cLTP response with no increase in AMPAR-mediated transmission and no increase in already elevated super-ecliptic pHluorin

(SEP)-TfR imaged exocytosis from REs. Further work by our laboratory identified DHHC2 as the PAT responsible for AKAP79/150 palmitoylation²⁴⁸. Micro-RNA interference (RNAi)-mediated knockdown of DHHC2 largely phenocopied AKAP79 CS overexpression with enhanced RE exocytosis and increased basal AMPAR-mediated transmission. Thus, AKAP79/150 palmitoylation appears to regulate a number of important synaptic properties important for both basal and activity-induced transmission. It follows that, AKAP79/150 palmitoylation could be important for organizing synapses and controlling signaling during synaptic plasticity in the hippocampus.

CHAPTER II

THESIS STATEMENT

Rationale

AKAP79/150 provides a focal point for the intersection of two prominent intracellular signaling pathways: phosphorylation and palmitoylation. In particular, AKAP-anchored CaN and PKA afford phospho-regulation of AMPARs but for this signaling complex to exert its control on the receptor it must be in close proximity to the receptors in the membrane, which can be directed by palmitoylation. Given the previous research on AKAP79 CS overexpression in rat hippocampal cultures, AKAP palmitoylation appears to be important in synaptic transmission and plasticity. However, being unable to test a number of plasticity relevant measures and chronic effects of AKAP palmitoylation ablation, we turned to a knock-in transgenic mouse approach. We developed an AKAP CS mouse, which has Cys36 and 123 mutated to Serines to prevent AKAP150 palmitoylation. Chapter III is composed of a published manuscript detailing the characterization of this AKAP CS mouse in mice aged 2-3 weeks. Chapter IV details future directions and unpublished data from AKAP CS cultures and acute slices from young mice exploring more mechanisms of AMPAR function. Chapter V concludes with discussion and future directions.

Research question

How does palmitoylation of AKAP150 control subcellular targeting within neurons and how does this, in turn, regulate synaptic function and plasticity?

Specific aims

1. Understand how AKAP150 palmitoylation influences sub-synaptic protein localization
2. Characterize the involvement of AKAP150 palmitoylation in synaptic transmission and plasticity

Hypotheses

I hypothesize that AKAP150 palmitoylation controls the localization of AKAP to key nanodomains within spines and dendrites, such as the core PSD and REs, which are essential to synaptic function. Further, due to the enzyme anchoring of CaN and PKA, palmitoylation of AKAP ensures proper downstream signaling, including the phospho-regulation of the AMPAR. I expect that AKAP palmitoylation will be required for maintaining proper synaptic function basally and during various forms of synaptic plasticity that are known to involve phospho-regulation of the AMPAR.

CHAPTER III

AKAP150 PALMITOYLATION REGULATES SYNAPTIC INCORPORATION OF CA²⁺-PERMEABLE AMPARS BASALLY AND DURING LTP²

Introduction

AMPARs are the primary mediators of fast excitatory neurotransmission in the central nervous system and regulation of the number and activity of post-synaptic AMPARs is crucial for forms of synaptic plasticity that support learning and memory, including NMDA receptor (NMDAR)-dependent LTP and LTD⁹⁹. AMPARs are tetramers assembled from GluA1-4 subunits, with incorporation of GluA2 subunits decreasing channel conductance and inhibiting Ca²⁺ influx. After the early postnatal period, the majority of AMPARs at hippocampal CA1 synapses under basal conditions are Ca²⁺-impermeable GluA1/2 or GluA2/3 heterotetramers^{16,124,127}. However, Ca²⁺-permeable GluA1 homomeric receptors (CP-AMPARs) can be recruited to hippocampal synapses from extrasynaptic and/or intracellular stores to regulate synaptic strength during LTP, LTD, and homeostatic plasticity^{36,103,104,107,108,167,275,352-354}, but see^{129,131}. These recruited CP-AMPARs, due to both greater single channel conductance and Ca²⁺-permeability, can in turn not only influence the level of plasticity expression but also alter the capacity of synapses to undergo subsequent plasticity, so called meta-plasticity. Importantly, CP-AMPAR-mediated meta-plasticity in the nucleus accumbens and amygdala are, respectively, linked to reward learning relevant for drug addiction and fear memory extinction relevant for post-traumatic stress disorder^{201,355}. However, the roles of CP-

² Portions of this chapter were previously published in *Cell Reports* and are included with the permission of the copyright holder.¹

AMPA receptors in regulating LTP/LTD and meta-plasticity at hippocampal synapses relevant for spatial and contextual learning and memory are less clear and remain controversial.

We know that phosphorylation and dephosphorylation of S845 in the GluA1 C-terminal domain by the cAMP-dependent protein kinase PKA and the Ca²⁺-calmodulin-dependent protein phosphatase 2B/calcineurin (CaN) regulates CP-AMPA receptor synaptic insertion and removal, respectively^{166-169,356-359}. However, we still do not understand how post-synaptic PKA and CaN signaling are coordinated to control CP-AMPA receptor trafficking between intracellular compartments, such as REs, the extrasynaptic membrane, and the PSD. An increasing body of evidence indicates that the scaffold protein AKAP79/150 (human79/rodent150; Akap5 gene) targets both PKA and CaN to AMPA receptors to regulate GluA1 phosphorylation and trafficking to control LTP/LTD balance and homeostatic potentiation^{103,104,275,280,281,354,360,361}. Thus, a key question is how is the post-synaptic localization of AKAP79/150 itself regulated.

AKAP79/150 is targeted to the post-synaptic PM primarily by an N-terminal polybasic domain that binds to PIP2, cortical F-actin, and cadherin adhesion molecules and secondarily by an internal domain that binds PSD-95, a major structural scaffold of the PSD^{245,249,262,267,269}. More recently we discovered that AKAP79/150 is S-palmitoylated on two conserved Cys residues (C36 and C129 human/123 mouse) within the N-terminal targeting domain by the RE-localized palmitoyl acyltransferase DHHC2^{247,248}. AKAP palmitoylation is not required for its general targeting to the PM or its binding to F-actin²⁴⁵ but is required for its specific localization to dendritic REs and association with cholesterol-rich, detergent-resistant membrane lipid rafts^{247,264}. Of note, the PSD is biochemically defined by its detergent-insolubility and, accordingly, many PSD proteins

are palmitoylated and lipid-raft associated, including PSD-95^{247,287,294,304,332-334}.

However, it is not known if AKAP79/150 palmitoylation also controls its association with the PSD.

In contrast to other protein lipidations like myristoylation and prenylation, palmitoylation is reversible, with palmitate removal being catalyzed by protein palmitoyl thioesterases³⁰⁶. Importantly, palmitoylation of PSD-95, AKAP150 and other PSD scaffolds is affected by seizures and anticonvulsants *in vivo* and has been implicated in regulating AMPAR trafficking and synaptic strength in cultured neurons *in vitro*^{247,248,323,325,332,350,361,362}. In particular, AKAP79/150 palmitoylation and dendritic spine targeting are bidirectionally regulated by neuronal activity in cultured neurons to coordinately control a number of cellular correlates of LTP/LTD, including RE exocytosis, spine morphology, GluA1 surface expression, and AMPAR synaptic activity^{247,248,265}. However, we do not know whether palmitoylation controls AKAP79/150 post-synaptic localization or AMPAR regulation during synaptic plasticity in the intact circuitry of the hippocampus *in vivo*. In addition, despite the prominence of palmitoylation modifying PSD proteins, no *in vivo* models have been developed to specifically disrupt palmitoylation of a specific post-synaptic protein and then determine the impacts on synaptic function. Importantly, here we developed a palmitoylation-deficient AKAP150 C36, 123S (AKAP CS) knock-in mutant mouse line to characterize the role of AKAP palmitoylation in regulating its targeting to the PSD and in controlling CP-AMPA incorporation both basally and during LTP at CA1 synapses.

Aims

- Determine the effect of AKAP150 palmitoylation on sub-synaptic protein localization
- Characterize the regulation of synaptic transmission and plasticity by AKAP150 palmitoylation

Materials and methods

Generation of AKAP150 CS knock-in mice

The Transgenic and Gene Targeting Core at the University of Colorado Anschutz Medical Campus constructed the Akap5CS targeting vector. The Akap5CS mutation introduced mutations of AKAP150 cysteines 36 and 123 to serines in the single coding exon of an Akap5 genomic DNA fragment via piggyBac (PB) transposon based method from a C57BL/6 BAC clone. In this targeting vector, the AKAP150 CS mutation was introduced by piggyBac method with a neomycin resistance cassette flanked by the 3' and 5' long-terminal repeat (LTR) of PB inserted within the Akap5 exon. The targeting construct was electroporated into a hybrid C57BL/6 129 embryonic stem (ES) cell line EC7.1 and G418-resistant clones were screened for homologous recombinants by PCR-based genotyping. The neomycin resistance cassette was then removed from the targeted locus by remobilizing the PB with transient expression of PB transposase. One positive clone was expanded, injected into blastocysts, and implanted into surrogate mothers. Chimeric F0 founders were born and bred to C57BL/6J to establish germ-line transmission. F1 mice heterozygous for the CS mutation were identified and then bred to yield F2 CS homozygous offspring. For PCR genotyping, DNA was extracted from tail snips using REExtract-N-Amp Tissue PCR kit (Sigma-Aldrich) following

manufacturer's protocol. PCR with forward (5'- GGAGACCAGCGTTTCTGAGATT-3') and reverse (5'- ATCTCCAAATCGTCTGCCTCTC-3') primers amplified the mutated region of the coding sequence, giving a 461 bp fragment for both the WT allele and the CS allele. After PCR amplification, the samples were digested with HindIII for 90 minutes and then resolved on a DNA gel. For the WT allele, no fragment will result from cutting (461 bp fragment) while the CS allele results in two fragments (100, 360 bp). AKAP150 CS mice were backcrossed to C57BL several generations but then maintained on a mixed C57BL/6J 129 background. Both male and female mice between the ages of P12-21 were used for experiments and analyzed together. Mixed litters of male and female neonatal day 1-3 mouse pups were used for cultures. All animal procedures were conducted in accordance with National Institutes of Health (NIH)–United States Public Health Service guidelines and with the approval of the University of Colorado, Denver, Institutional Animal Care and Use Committee.

Primary mouse hippocampal neuron culture

Mouse hippocampal neurons were cultured from postnatal day 1–3 mixed sex mice as previously described^{275,354}. Briefly, the hippocampus was dissected from postnatal day 1–3 AKAP150 WT or CS mice and dissociated in papain. Neurons were seeded at a density of 150,000-200,000 cells/well in 12 well dishes on 18 mm glass coverslips coated with poly-D-lysine and Laminin or 400,000-500,000 cells/well in 6 well dishes on 25 mm glass coverslips coated with poly-D-lysine and laminin (BD Biosciences). Cells were maintained at 37°C, 5% CO₂ in Neurobasal-A medium supplemented with B27, Glutamax, and Pen/Strep for 14–16 days before processing.

Fractionation and immunoblotting of brain tissue

Subcellular fractionation and immunoblotting of WT and CS hippocampal or forebrain (cortex and hippocampus) lysates were performed as in^{104,275,363,364}. For immunoblotting, 15 µg of whole extract (WE), 10 µg of P2, 20 µg of S2, 5 µg of TxP, and 15 µg of TxS were resolved on Tris-SDS gels and transferred in 20% methanol to PVDF membranes. Membranes were incubated with primary antibodies for 2 hours as follows: rabbit anti-AKAP150 (1:1000)³⁶⁵, mouse anti-PKA-RIIβ (1:1000; BD Biosciences Transduction Laboratories), mouse anti-PSD-95 (1:1000; Millipore), rabbit anti-GluA1 (1:1000; Millipore), and rabbit anti-GluA1-S845 (1:1000; Millipore). Signal detection was performed using Horse Radish Peroxidase (HRP)-coupled secondary antibodies (Bio-Rad; 1:10,000) followed by ECL (West Pico or West Dura Chemiluminescent Substrate; Pierce). Chemiluminescence was imaged using an Alpha Innotech Fluorchem gel documentation system, and band intensities were analyzed using ImageJ (NIH). Band intensities were normalized to WT WE from the same blot.

APEGS palmitoylation assay

AKAP150 palmitoylation state was assessed using the APEGS (Acyl-PEG Exchange Gel-Shift) assay as previously described^{265,306}. Forebrain whole extracts or subcellular fractions from above were tumbled in PBS buffer containing 4% SDS and 5 mM EDTA with 20 mM TCEP for 1 h at room temperature in the presence of protease inhibitors. Next, free thiols were blocked by incubation with 50 mM N-ethylmaleimide (NEM) overnight at room temperature. Following a chloroform-methanol precipitation (CMP), pellets were resuspended in 4% SDS PBS buffer and thioester bonds were cleaved with 1M Hydroxylamine (HAM, Sigma) for 1 h at room temperature with end

over end rotation. After another CMP, free thiols were labeled with 10 kD polyethylene glycol moieties (SUNBRIGHT maleimide PEG, NOF America) for 1 h at RT with rotation. Following a final CMP, samples were re-suspended and boiled in sample buffer with 50 mM dithiothreitol and resolved via SDS-PAGE and western blotting with AKAP150 antibody.

Extracellular fEPSP recordings

For slice preparation, animals (P12-P21) were decapitated under anesthesia with isofluorane. The brain was removed into 4°C cutting solution (in mM: 3 KCl, 1.25 NaH₂PO₄, 12 MgSO₄, 26 NaHCO₃, 0.2 CaCl₂, 220 sucrose, 10 glucose; all chemicals were purchased from Sigma-Aldrich.). Hippocampi were removed from the brain, and 400- μ m-thick slices were made using a McIlwain tissue chopper. Slices were recovered at 29-31 °C for >90 min in artificial cerebrospinal fluid (ACSF)/cutting solution mixture (ACSF in mM: 126 NaCl, 5 KCl, 2 CaCl₂, 1.25 NaH₂PO₄, 1 MgSO₄, 26 NaHCO₃, 10 glucose, 2 N-acetyl cysteine). Following recovery, slices were transferred to a recording chamber and maintained at 29-31°C in ACSF as described above (without N-acetyl cysteine). A bipolar tungsten stimulating electrode was placed in the Schaffer collateral pathway to evoke field excitatory post-synaptic potentials (fEPSPs) recorded in CA1 stratum radiatum using a glass micropipette filled with ACSF. Input/Output (I/O) curves were measured by evoking fEPSPs at various intensities until maximal response was determined by plotting initial fEPSP slope against stimulus intensity. For studies of LTP, LTD, and de-depression, the test stimulus intensity was set to evoke 40–60% of the maximum slope. Both data acquisition and analysis was done using WinLTP.

Whole-cell electrophysiology

For whole-cell voltage-clamp electrophysiological recordings, 300 μm horizontal hippocampal slices were prepared as above (cutting solution in mM: 85 NaCl, 75 sucrose, 2.5 KCl, 1.3 NaH₂PO₄ monobasic, 24 NaHCO₃, 0.5 CaCl₂, 4 MgCl₂, 25 D-Glucose) using a Vibratome. After 30 minutes at 31.5 °C, slices were recovered at room temperature for >60 minutes in ACSF/cutting solution mixture (ACSF in mM: 126 NaCl, 2.5 KCl, 1 NaH₂PO₄ monobasic, 26.2 NaHCO₃, 2.5 CaCl₂, 1.3 MgSO₄-7H₂O, 11 D-Glucose at ~290 mOsm). Slices were transferred to a recording chamber and maintained at 29.5 °C and visualized using infrared–differential interference contrast microscopy. Pipettes had a resistance between 2 and 5 M Ω . CA1 pyramidal neurons were held at -70 mV and recorded from using an intracellular solution containing the following (in mM): 115 Cs-Methanesulfonate, 15 CsCl, 8 NaCl, 10 Tetraethylammonium-Cl, 0.2 EGTA, 2 Mg-ATP, 0.3 Na-GTP, 10 HEPES, 10 Na²- phosphocreatine, 1 MgCl₂, pH 7.3 with CsOH at ~300 mOsm. AMPAR sEPSCs were isolated using 50 μm picrotoxin (Tocris) and mEPSCs were isolated with the addition of 0.5 μm tetrodotoxin (TTX, Tocris) extracellularly. For hippocampal cultures, coverslips were transferred to ACSF containing 0.5 μm TTX and 50 μm picrotoxin or 0.5 μm TTX, 50 μm picrotoxin and 70 μM IEM1460 and then recorded from as above.

For Evoked EPSCs, a bipolar tungsten stimulating electrode was placed as in the field experiments and CA1 pyramidal cells were recorded from using an internal solution containing 5 mM N-Ethylidocaine (QX-314) to prevent action potential firing. Baseline responses were established in whole-cell mode and then currents were evoked at holding potentials of -70 mV to assess inward AMPAR current and then +40 mV to

assess outward AMPAR and NMDAR current. Traces (≥ 5) were averaged across recordings from a single neuron at each respective holding potential to calculate AMPA/NMDA ratios. AMPA currents were measured at the peak amplitude of the EPSC at both +40mV and -70mV divided by NMDA current at 50 ms after the onset of the EPSC at +40 mV. For NASPM sensitivity, ACSF containing 20 μ M NASPM was washed on after establishing a baseline evoked response and the change in response was calculated as EPSC amplitude after NASPM /EPSC amplitude before NASPM.

For Evoked I/O curves, responses were established at various stimulus intensities and fixed multiplier setting. For PPR, baseline responses were established in whole-cell mode and then paired-pulses at various intervals were recorded at -70 mV to assess paired-pulse facilitation as a read out of pre-synaptic function.

For AMPA rectification measurements, AMPAR currents were isolated using 100 μ M DL-APV (Tocris) and 50 μ M Picrotoxin in extracellular solution and with 10 μ M spermine and 5 mM QX-314 (Tocris) in the internal solution. Baseline responses were established in whole-cell mode and the currents were evoked at different holding potentials (-70, -40, -20, 0, +20, +40 mV). Rectification index was calculated by taking the -70 mV amplitude/+40 mV amplitude, resulting in a larger number for more rectifying channels/CP-AMPARs. For NMDA I/O measurements, NMDAR currents were isolated using 10 μ M NBQX and 50 μ M Picrotoxin. +40 mV responses were established at various stimulus intensities and fixed multiplier settings. For LTP experiments, slices were stimulated for 10-15 min at moderate stimulus intensity before going into whole-cell mode. Once a cell was patched, baseline was established within 5 min of breaking in. After a 3 min baseline measurement, cells were depolarized to 0 mV and then

tetanized. Cells were then stepped back down to -70 mV and recorded for 50-60 min post-tetanus. Cells were monitored for membrane resistance and seal quality throughout. In NASPM LTP experiments, 20 μ M NASPM was included in ACSF throughout. Whole-cell data was collected using a Digidata 1440 with Multiclamp 700B amplifier (Molecular Devices). Evoked experiments were conducted using a Model 2100 Isolated Pulse Stimulator (A-M Systems). All data was acquired with pCLAMP software and analyzed in Clampfit.

TF-488 feeding to label REs

DIV 14 neurons were transferred into Neurobasal with no additives and supplemented 0.1% BSA for 30 min at 37°C. Cells were incubated with Alexa 488 labeled transferrin (TF-488) (Invitrogen) for 30 min at 37°C and then processed for fixation and immunocytochemistry (rabbit anti-AKAP150 1:1000, followed by goat anti-rabbit-Alexa 568 1:1000). TF-488 (final concentration of 5 μ g/well) was microcentrifuged at max speed for 1 min prior to application and only the supernatant was added to cells to prevent aggregation. Imaging was carried out on an Axio Observer microscope (Zeiss) with a 63 \times Plan Apo/1.4 NA objective using 488 and 561 nm laser excitation and a CSU-XI spinning-disk confocal scan head (Yokogawa) coupled to an Evolve 512 EM-CCD camera (Photometrics) driven by SlideBook 6.0 (Intelligent Imaging Innovations). Z-stacks of 13 optical sections (0.33 μ m each) were acquired. Data was analyzed with SlideBook 6.0 using single optical sections of in-focus TF-488 signal. Masks were drawn over in-focus dendritic segments and only single-plane masks were analyzed using Pearson's correlation for AKAP and TF-488 signals.

SEP-TfR imaging

Imaging of super-ecliptic pHluorin-tagged transferrin receptor was conducted essentially as previously described^{247,248}. DIV 11-14 hippocampal neurons from WT and AKAP150 CS mouse cultures were transfected (Lipofectamine 2000) with plasmids encoding SEP-TfR and mCherry (as a cell fill) and imaged 3 days later. Imaging was conducted on the spinning-disk confocal microscope detailed above. Prior to imaging, neurons were incubated in ACSF plus 1 mM MgCl₂ for 30 min and were maintained during imaging at 33–35°C in a perfusion chamber (Warner Instruments). Baseline rates of SEP-TfR exocytic events (events defined as 2.5-fold above the median intensity of the dendrite) were determined by acquiring z-stacks of 10 optical sections (1.0 μm spacing) every 6 s for 5 min.

Immunocytochemistry on mouse primary hippocampal neuron cultures for dendritic spine analysis

For dendritic spine counting in cultured hippocampal neurons, DIV12-14 neurons were transfected with a plasmid encoding GFP using Lipofectamine 2000 (Invitrogen) and fixed after two days of expression on DIV14-16. Neurons were washed with ACSF (in mM: 130 NaCl, 5 KCl, 2 CaCl₂, 1 MgCl₂, 10 HEPES, 20 Glucose) x 2, then fixed in 4% paraformaldehyde (PFA), permeabilized in 0.1% Triton X-100 in PBS, and blocked overnight in a 5% BSA/PBS solution. Primary anti- GFP antibodies were incubated for 2h at room temperature in 5% BSA/PBS. Cells were then washed in PBS and incubated in secondary antibody conjugated to Alexa 488 for 1h at room temperature. Coverslips were washed in PBS and mounted onto glass slides with Pro-Long Gold (Invitrogen). Images were obtained on a Zeiss Axiovert 200M microscope equipped with a 175W

xenon lamp (Sutter), 63xPlan- Apo/1.4 NA objective, FITC/Alexa 488, Cy3/Texas Red and Cy5/Alexa 647 filter sets (Chroma), Coolsnap CCD camera, and Slidebook 5.0 software. Three-dimensional z-stacks with 0.33 μm steps were collected. Spines were counted from 50-100 μm segments of secondary or higher-order dendrites in Slidebook 6.0 (3 individual neuron preps, 2-3 coverslips per prep per genotype).

Dendritic spine analysis by Dil labeling

Slices were prepared as for whole-cell electrophysiology (300 μm on a Vibratome). Slices were fixed in 4% PFA overnight at 4°C, washed in PBS 3 x 15 min. After washing, sonicated Dil powder was collected on the tip of a needle and gently placed on the CA1 region of the hippocampus³⁶⁶. Dil was allowed to incorporate overnight at room temperature. Slices were washed in PBS 3x15 min and then mounted onto glass slides using Vectashield (Vector Laboratories). Slices were imaged via spinning-disk confocal microscopy as detailed above. Spines were counted from for 50-100 μm segments of secondary or higher-order dendrites in ImageJ (NIH) (< 3 neurons per slice were counted, 2-3 slices/animal, 3 animals per genotype).

Surface GluA1 antibody labeling

DIV 14-16 neurons plated on #1.5 glass coverslips were transferred to ACSF with 1 mM Mg^{2+} for 30 min. Cells were transferred to ACSF for 30 min then rabbit anti-GluA1 antibody (Millipore 1:250) was live-fed for 15 min at 37°C before being washed in ice-cold ACSF 2x and fixed in 4% PFA. Cells were then processed for STED imaging by labeling with mouse anti-PSD-95 primary antibodies and fluorescent secondary antibody conjugates as described below.

Super-resolution stimulated emission depletion (STED) nanoscopy

Neurons plated on #1.5 glass coverslips were washed 2x ACSF then fixed with 4% PFA for 10 min. Coverslips were washed 3x5 min with PBS with rotation and then permeabilized with 0.1% Triton. Neurons were next washed 3x5 min with PBS and then blocked overnight with filter-sterilized 5% BSA/PBS. Neurons were incubated with primary antibody in 5% BSA/PBS at room temperature (rabbit anti-AKAP150 1:1000, mouse anti-PSD-95 1:500), then washed 3x5 min PBS and incubated at room temperature for 1 h with secondary antibodies (goat anti-rabbit-Atto 647N 1:500 and goat anti-mouse-Atto 594 1:500; Rockland). Images were acquired on a custom built STED microscope³⁶⁷. Custom ordered 40 nm beads (Life Technologies) labeled with red and far-red dyes (proprietary) were used for resolution measurement and system alignment.

STED image analysis

The methodology of image segmentation and geometric analysis applied to STED images here will be described in more detail elsewhere along with its application to 3D-structured illumination microscopy (SIM) images³⁶⁸. Briefly, a Split-Bregman image segmentation algorithm first described in³⁶⁹ and subsequently incorporated into the MOSAIC image processing suite for ImageJ/FIJI (<http://mosaic.mpi-cbg.de/>)³⁷⁰ was utilized to delineate object boundaries from background-corrected STED images (using a histogram-based background estimator, also implemented as part of the MOSAIC suite). Binary masks generated in this process were then imported into MATLAB (Mathworks) where the geometric properties of the defined objects were calculated. Output metrics were then imported into Prism (GraphPad) for further analysis.

Table 3.1: Key resources table

REAGENT or RESOURCE	SOURCE	IDENTIFIER
Antibodies		
Polyclonal rabbit anti-AKAP 150	Brandao et al., 2012	RRID: AB_2532138
Monoclonal mouse anti-PKA-RII β	BD Transduction Laboratories	Cat# 610625, RRID: AB_397957
Monoclonal mouse anti-PSD95	Millipore	Cat# MAB1596; RRID: AB_2092365
Polyclonal rabbit anti-GluR1	Millipore	Cat# ABN241; RRID: AB_2721164
Polyclonal rabbit anti-GluR1, phosphoSer845	Millipore	Cat# AB5849; RRID: AB_92079
Anti-Rabbit IgG (H&L) Antibody (Goat) ATTO 647N Conjugated	Rockland	Cat# 611-156-122; RRID: AB_10893043
Anti-Rabbit IgG (H&L) Antibody (Goat) ATTO 594 Conjugated	Rockland	Cat# 611-155-122; RRID: AB_10894686
Anti-Mouse IgG (H&L) Antibody (Goat) ATTO 647N Conjugated	Rockland	Cat# 610-156-121; RRID: AB_10894200
Anti-Mouse IgG (H&L) Antibody (Goat) ATTO 594 Conjugated	Rockland	Cat# 610-155-121; RRID: AB_10893162
Chemicals, Peptides, and Recombinant Proteins		
SUNBRIGHT Maleimide PEG	NOF America	Cat#Me-100MA10kD
Tetrodotoxin (TTX)	Tocris Bioscience	Cat# 1078
Picrotoxin	Tocris Bioscience	Cat# 1128
QX-314 bromide	Tocris Bioscience	Cat# 1014
NASPM trihydrochloride	Tocris Bioscience	Cat# 2766
IEM 1460	Tocris Bioscience	Cat# 1636
DL-APV (AP5)	Tocris Bioscience	Cat# 0105
NBQX disodium salt	Tocris Bioscience	Cat#1044
Spermine tetrachloride	Tocris Bioscience	Cat# 0958
Experimental Models: Organisms/Strains		
AKAP5CS mice (allele symbol: Akap5<tm3.1Mdaq>; Allele synonyms: Akap5CS AKAP5CS, AKAP150CS)	This paper	RRID: MGI_6198520
C57BL/6J mice	Jackson Laboratories	RRID: IMSR_JAX:000664
Software and Algorithms		
ImageJ	NIH	https://imagej.nih.gov/ij/
Slidebook	3i- Intelligent Imaging Solutions	https://www.intelligentimaging.com/slidebook
Prism	GraphPad	https://www.graphpad.com/scientific-software/prism/
pClamp/Clampfit	Molecular Devices	www.moldev.com
WinLTP	WinLTP Ltd. and The Univ of Bristol	http://www.winltp.com
Mosaic Suite (FIJI/ImageJ plugin)	Mosaic Group	http://mosaic.mpi-cbg.de/?q=downloads/imageJ
MatLab	Mathworks	http://www.mathworks.com

Quantification and statistical analysis

Data compilation and statistical analysis were performed in Prism (GraphPad) with significance value as $\alpha=0.05$. All data are reported as mean \pm SEM. Prism provides exact p-values unless $p < 0.0001$. The statistical tests used, p-values and replicates with definition of n for all experiments can be found in the figure legends. No tests were used to estimate sample size. All experiments, except the initial APEGS assay in Fig. 1B, were performed at least 3 separate times (or on at least 3 separate animals) to ensure rigor and reproducibility. Both male and female mice were used for electrophysiology experiments, and we observed no differences between sexes, therefore data from both sexes were pooled for all experiments.

Results

AKAP CS palmitoylation-deficient knock-in mice exhibit reduced AKAP150 levels in PSD-enriched fractions.

To study the impacts of loss of AKAP150 palmitoylation, we generated a palmitoylation-deficient AKAP150 mouse (AKAP CS) (Fig 3.1A) using a piggyBac transposon-based ES cell targeting vector strategy to introduce mutations into the mouse *Akap5* gene locus (Fig 3.2A). The resulting *Akap5*CS mutant allele replaces Cys at positions 36 and 123 with Ser (Figs 3.1A&3.2A), while simultaneously introducing a HindIII site to facilitate genotyping (Fig 3.2B). AKAP CS mice are viable and are visibly indistinguishable from their WT littermates, with no apparent physical deficits or changes in overall brain anatomy (not shown). In addition, we observed no changes in dendritic spine numbers or morphology in CA1 stratum radiatum of *ex vivo* brain slices

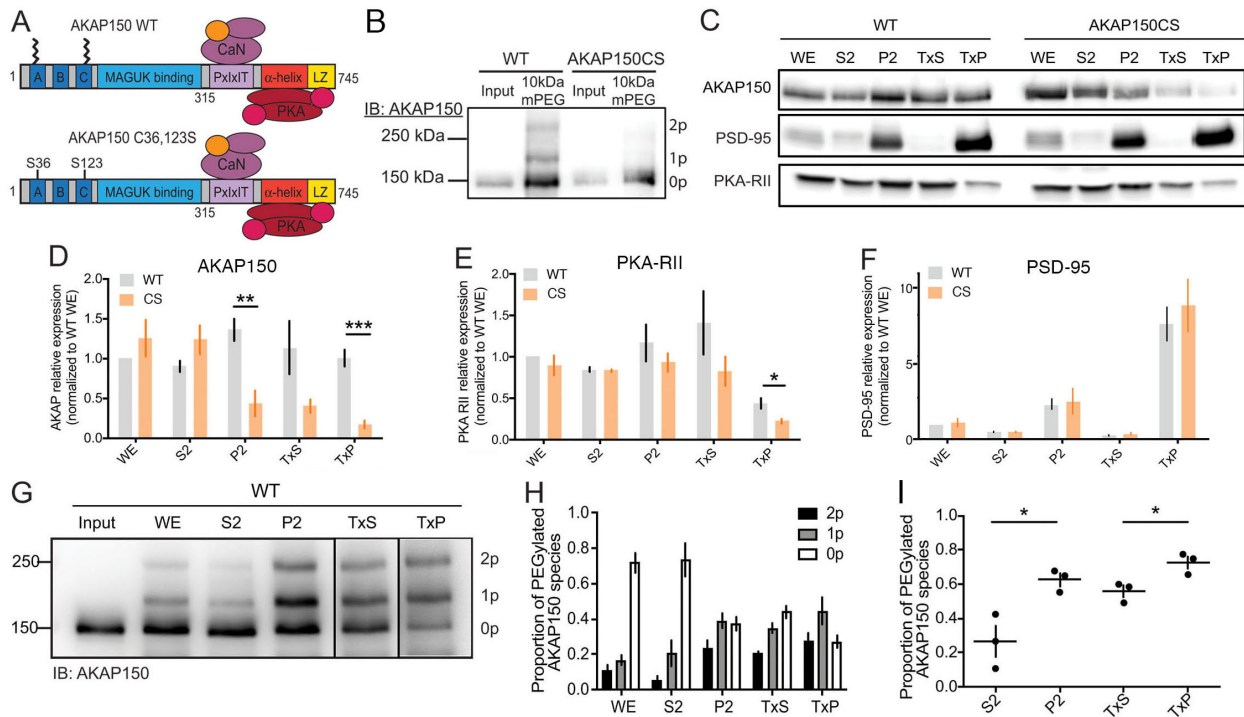


Figure 3.1: AKAP150 and PKA-RII levels are reduced in PSD-enriched fractions from AKAP CS palmitoylation-deficient mice.

(A) Schematic of AKAP150 highlighting binding partners and functional domains. AKAP150 is palmitoylated at Cys 36 and 123, and these residues are mutated to Ser to create the AKAP CS palmitoylation-deficient mutant mouse. (B) APEGS assay showing that AKAP150 WT, but not CS, is palmitoylated in lysates from mouse brain. (C) Subcellular fractionation and western blotting from WT and CS P21 mouse hippocampus for AKAP150, PSD-95, and PKA-RII β . P2, crude synaptosomes; S2, cytosol and light membranes; TxP, triton-insoluble sub-fraction of P2 = PSD-enriched fraction; TxS, triton-soluble sub-fraction of P2; WE, whole extract. (D–F) Quantification of subcellular fractionation from (C) normalized to WT WE levels showing (D) decreased AKAP150 protein levels in P2 and TxP fractions from CS mice (P2: WT 1.36 ± 0.14 , CS 0.44 ± 0.16 , unpaired t test $**p = 0.0033$; TxP: WT 1.00 ± 0.10 , CS 0.17 ± 0.05 , unpaired t test $***p = 0.00028$; WT $n = 5$, CS $n = 4$), (E) decreased PKA-RII β protein levels in TxP fractions from CS mice (WT 0.44 ± 0.063 , CS 0.22 ± 0.029 , unpaired t test $*p = 0.036$; $n = 3$), but (F) no change in fractionation of PSD-95 in CS versus WT mice. (G) AKAP150 APEGS assay of subcellular fractions from WT mouse forebrain. (H) Quantification of the proportion of AKAP150 in the unpalmitoylated lower MW band and the mono- and di-palmitoylated higher MW bands across the subcellular fractions in (G). (I) Quantification of the total proportion of palmitoylated AKAP150 (mono- plus di-) revealing significantly more palmitoylated AKAP150 in P2 versus S2 and TxP versus TxS (S2 0.26 ± 0.16 , P2 0.63 ± 0.065 , unpaired t test $*p = 0.022$; TxS 0.56 ± 0.059 , TxP 0.73 ± 0.062 , unpaired t test $*p = 0.028$; $n = 3$). $*p < 0.05$, $**p < 0.01$, and $***p < 0.001$ by unpaired t test. Data are reported as mean \pm SEM; $n =$ number of animals.

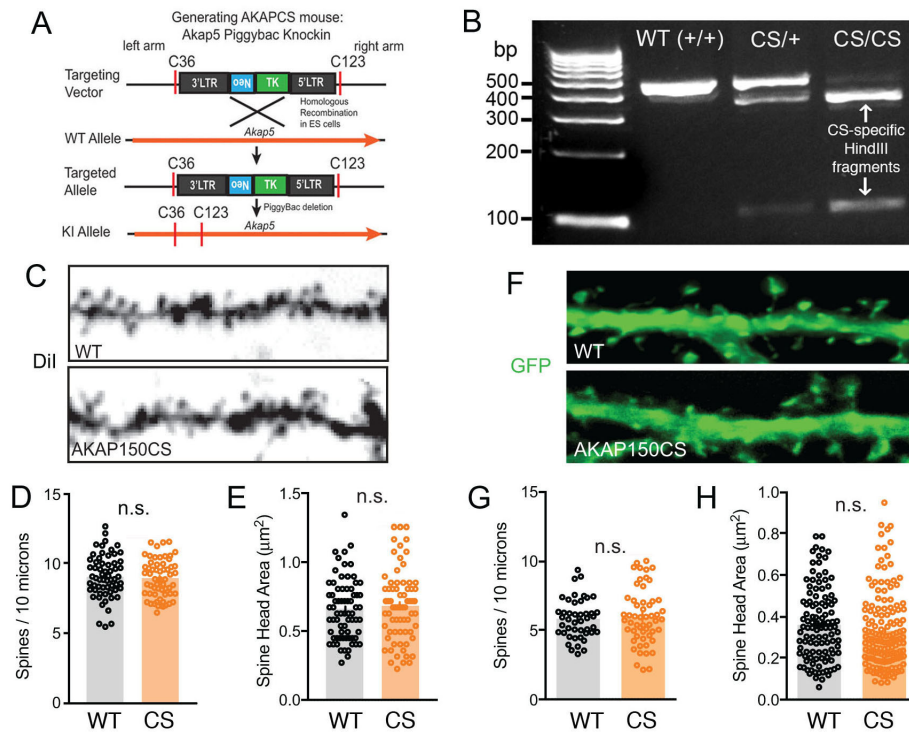


Figure 3.2: Additional characterization of AKAP CS mice and cultured neurons. (A) Generation of AKAP CS mice using the Piggybac method, introducing two point mutations and a HindIII site. (B) Genotyping by PCR and restriction digestion of AKAP150 WT and AKAP150 CS heterozygous and homozygotes; HindIII digestion results in AKAP150 CS specific fragments. (C) Dendritic segments from neurons in region CA1 of the hippocampus from WT or AKAP CS Dil stained slices, showing no significant difference in (D) spine number or (E) spine head area. (F) DIV14-16 hippocampal cultures transfected with GFP, show no significant difference in (G) spine number or (H) spine head area.

(Fig 3.2C-E) or in cultured hippocampal neurons prepared from CS compared to WT mice (Fig 3.2F-H). To confirm loss of AKAP150 palmitoylation in CS mice, we employed an APEGS (Acyl-PEGyl Exchange Gel-Shift) assay of palmitoylation that exchanges palmitates for polyethylene glycol polymers to produce upward molecular weight shifts^{265,306}. Using this APEGS assay we detected mono- and di-palmitoylated AKAP in whole brain extracts of WT but not CS mice, where only unpalmitoylated 150 kDa AKAP was detected (Fig 3.1B).

Previous biochemical and imaging studies indicate that AKAP79/150 associates with membrane lipids, including in lipid rafts, and other post-synaptic proteins, including PSD-95 and F-actin, and is localized not only in the PSD but also the extrasynaptic membrane^{245,247,249,255,267,363}. To explore the effect of eliminating AKAP palmitoylation on its synaptic localization *in vivo*, we used differential centrifugation and detergent extraction^{104,275,363,364} to isolate subcellular fractions from hippocampal lysates of 2-3 week-old mice followed by immunoblotting (Fig 3.1C). Intriguingly, we observed a selective decrease in AKAP150 CS protein compared to WT in the synaptosomal membrane fraction (P2) and a PSD-enriched fraction (TxP) derived from P2 by Triton X-100 detergent extraction (Fig 3.1C,D). An accompanying decrease in PKA-RII regulatory subunits was also seen in TxP for CS mice (Fig 3.1E). The distribution of PSD-95 across these fractions was not significantly different between WT and CS mice with its highest levels detected in the TxP/PSD-enriched fraction as expected; however, we did observe a non-significant trend toward slightly increased PSD-95 levels in TxP for CS (Fig 3.1F). Overall, these fractionation data suggest that AKAP150 CS is less associated with the PSD-enriched fraction than WT, and thus, that palmitoylation

normally promotes AKAP150 localization in the PSD. Consistent with this idea, we combined subcellular fractionation with the APEGS palmitoylation assay in WT mice (Fig 3.1G) to reveal significant enrichment of palmitoylated AKAP150 in P2 relative to the S2 fractions and TxP relative to TxS fractions (Fig 3.1H,I). In particular, while unpalmitoylated AKAP150 predominates in whole extracts and the cytosolic/S2 fraction, mono- plus di- palmitoylated AKAP150 constitute the majority in synaptosomal/P2, perisynaptic/TxS, and PSD-enriched/TxP fractions, the latter of which contains the highest overall proportion of palmitoylated AKAP150 (Fig3.1H,I).

AKAP CS dendritic spines contain smaller AKAP150 nanodomains that exhibit reduced overlap with the PSD.

Due to the submicron dimensions of dendritic spines and organization of the PSD into even smaller nanodomains on the scale of ~ 100 nm^{7,78,79,184}, we reasoned that any changes in AKAP150 CS post-synaptic localization may be below the diffraction-limited resolution of standard confocal microscopy (~ 250 nm). Indeed, previous studies using standard microscopy revealed no differences in basal spine localization of GFP-tagged AKAP79 WT vs. CS in transfected neurons²⁴⁷. We therefore employed a custom-built, two-color Stimulated Emission Depletion (STED) nanoscope with a resolution of ~ 40 - 60 nm³⁶⁷ to assess the localization of AKAP150 relative to PSD-95 in dendritic spines of hippocampal neurons cultured from WT and CS mice (Fig 3.3). In agreement with our previous work on AKAP79 CS-GFP, standard confocal imaging revealed that AKAP150 CS and WT are both localized to dendritic spines and show substantial overlap with PSD-95; however, the improved resolution of STED revealed ~ 100 - 200 nm diameter

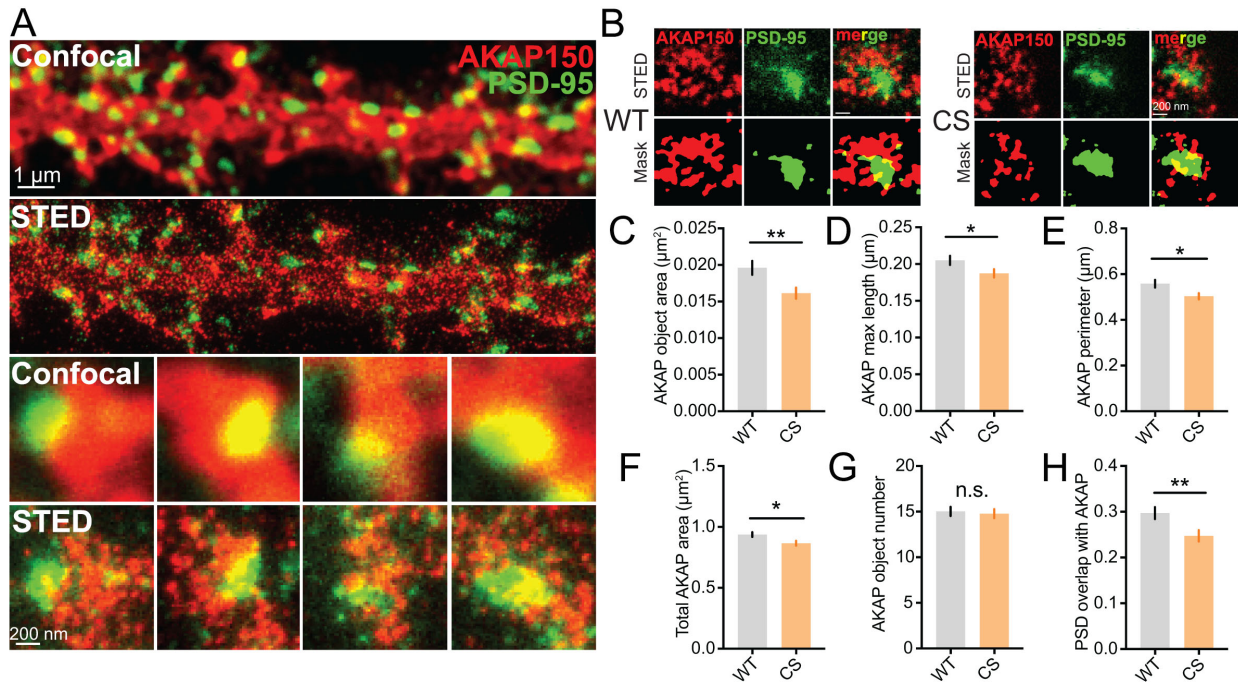


Figure 3.3: AKAP150 CS localization to the PSD is reduced.

(A and B) Confocal and STED imaging (A) and associated segmentation object masks (B) for 14–16 day *in vitro* (DIV) 14–16 hippocampal cultures from WT and CS mice stained for AKAP150 (red) and PSD-95 (green). STED images show enhanced resolution and provide better sub-synaptic visualization of AKAP150 localization relative to the PSD. (C–F) Significant decrease in AKAP object area in AKAP CS cultures (C) (WT $0.01961 \pm 0.0009 \mu\text{m}^2$, $n = 102$ spines; CS $0.01614 \pm 0.0007 \mu\text{m}^2$, $n = 106$ spines; unpaired t test $**p = 0.0043$) that was accompanied by decreases in (D) AKAP object major-axis length (WT $0.205 \pm 0.006 \mu\text{m}$, CS $0.1874 \pm 0.006 \mu\text{m}$, unpaired t test $*p = 0.0344$), (E) total AKAP perimeter (WT $0.5585 \pm 0.017 \mu\text{m}$, CS $0.5034 \pm 0.014 \mu\text{m}$, $*p = 0.0104$), and (F) AKAP compartment area within spines (WT $0.9372 \pm 0.019 \mu\text{m}^2$, CS $0.8662 \pm 0.019 \mu\text{m}^2$, unpaired t test $*p = 0.0104$). (G and H) No change is seen in AKAP object number per spine (G), but (H) AKAP CS PSD localization is reduced, as indicated by a decrease in AKAP and PSD-95 object overlap (WT 0.2971 ± 0.01 , CS 0.2474 ± 0.01 , $**p = 0.0058$). $*p < 0.05$ and $**p < 0.01$ by unpaired t test. Data are reported as mean \pm SEM.

AKAP150 clusters for both WT and CS that were not visible in confocal images and were located overlapping the PSD, closely surrounding the PSD, and also in distinct locations outside the PSD (Fig 3.3A,B). This ability of STED to resolve distinct extrasynaptic, perisynaptic and PSD clusters of AKAP150 that are not visible in standard confocal imaging parallels findings for AMPARs using STED and STORM/PALM that revealed previously unappreciated nanodomain organization^{7,78,79,184} (see also Fig 3.7). Using a custom, object-based image segmentation mask analysis method (Fig 3.3B) that we recently developed for intensity-based super-resolution imaging methods (i.e. STED, see STAR Methods) we found that the area (Fig 3.3C) and major axis length of individual AKAP150 objects (Fig 3.3D) in spines were both significantly reduced for the CS mutant compared to WT. Correspondingly, the total perimeter (Fig 3.3E) and area occupied by AKAP150 objects within spines (Fig 3.3F) were both significantly reduced for CS but with no changes in the average number of AKAP objects per spine (Fig 3.3G). Importantly, the proportional spatial overlap of AKAP150 and PSD-95 objects was also decreased for CS (Fig 3.3H) despite a small increase in total PSD area in spines (see Fig 3.7L below). Collectively, these STED imaging data are in agreement with the fractionation data presented above and indicate that AKAP150 CS localization in and around the PSD is reduced.

AKAP CS localization to recycling endosomes is decreased.

In previous work, we found that AKAP palmitoylation also controls targeting to REs. In addition, we observed that acute disruption of AKAP79/150 palmitoylation in rat hippocampal cultures resulted in enhanced basal RE fusion events in neuronal dendrites^{247,248}. Accordingly, we assessed the co-localization of AKAP150 with REs

marked by live-cell feeding with Alexa-488 labeled transferrin (TF-488) and also monitored basal exocytosis of transferrin receptor (TfR)-positive REs by expressing super-ecliptic pHluorin-tagged TfR (SEP-TfR) in WT and CS mouse dissociated hippocampal cultures (Fig 3.4). Consistent with previous work on human AKAP79, AKAP150 robustly co-localized with TF-488 positive puncta in WT mouse neurons but showed a significant decrease in RE localization in CS neurons (Fig 3.4A,B). Contrary to our previous findings showing that acute AKAP79 CS overexpression increased basal RE exocytosis, basal RE exocytosis imaged with SEP-TfR was not significantly different in CS compared to WT mouse neurons; although a slight non-significant trend toward increased exocytosis was observed (Fig 3.4C,D). Collectively, these data suggest that RE exocytosis (as read out by TfR recycling) is largely normal in CS mice despite decreased AKAP150 localization to REs.

AKAP CS mice exhibit enhanced CP-AMPA-mediated basal synaptic transmission.

Given that we observed reduced AKAP150 association with both REs and the PSD in CS mice, we wanted to explore how synaptic transmission and plasticity might be impacted. To start, we characterized basal synaptic transmission at CA1 synapses in acute, ex vivo hippocampal slices from 2-3 week-old WT and CS mice by whole-cell voltage-clamp recording of AMPAR-mediated miniature and spontaneous excitatory post-synaptic currents (mEPSCs and sEPSCs). Compared to WT, CS mice showed slightly enhanced mean mEPSC amplitude, slightly decreased mean mEPSC frequency (Fig 3.5A), and corresponding rightward shifts in the cumulative distributions of mEPSC

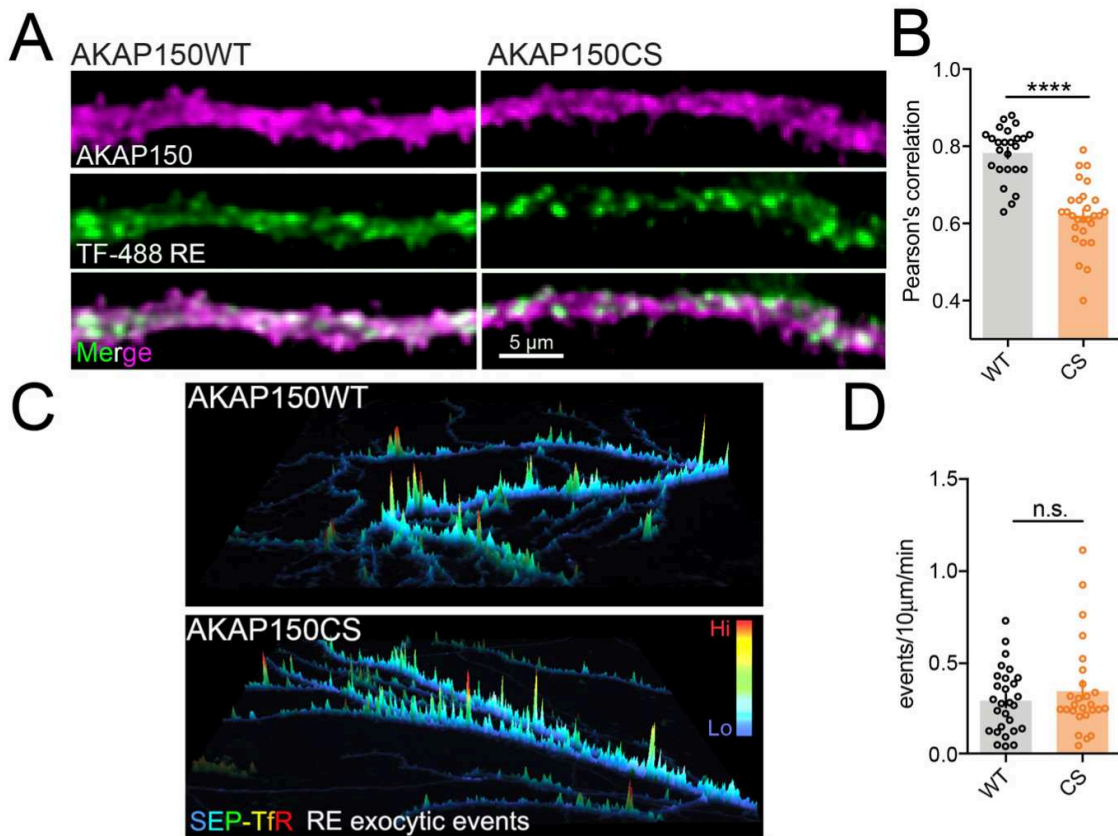


Figure 3.4: AKAP150 CS endosome localization and RE exocytosis.

(A) Max projection images of DIV14 WT or AKAP150 CS neurons labeled with Alexa488-transferrin (TF-488) to mark REs and endogenous AKAP150. (B) AKAP CS neurons show a significant decrease in AKAP co-localization with the RE marker transferrin. (C) Time composite (5 min, 0.2 Hz) images of 15-17 DIV hippocampal neurons from WT or AKAP150 CS mice showing RE exocytic events in dendrites imaged with SEP-TfR with integrated intensity plotted on the z-axis (pseudocolor: blue, low; red, high). (D) No significant difference between genotypes was detected in the number of exocytic events (defined as 2.5-fold the median fluorescence intensity) detected over 5 minutes.

amplitudes and inter-event intervals (Fig 3.5B). A similar decrease in sEPSC frequency and a non-significant trend toward increased sEPSC amplitude was observed in CS compared to WT (Fig 3.5C,D). Cultured hippocampal neurons from AKAP CS mice also exhibited slightly increased mEPSC amplitude (Fig 3.6A,B) but with no change in frequency (Fig 3.6A,C). Decreased mEPSC/sEPSC frequency could indicate a reduction in pre-synaptic release probability or a reduction in the overall number of synapses; however, analysis of CA1 dendritic spine numbers above revealed no differences between WT and CS (Fig 3.2C). We tested for changes in pre-synaptic release probability by measuring evoked AMPAR-mediated paired-pulse ratios (PPR) at Schaffer collateral (SC) synapses. We observed no differences in PPR between WT and CS in either whole-cell -70 mV EPSC (Fig 3.5E) or extracellular field excitatory post-synaptic potential (fEPSP) recordings (Fig 3.5G), thus indicating normal pre-synaptic function in CS mice. Furthermore, input-output curves for evoked AMPAR EPSC amplitude (Fig 3.5F) and fEPSP slope (Fig 3.5H) were similar for WT and CS. A normal evoked SC-CA1 input-output relationship for CS mice indicates that basal AMPAR-mediated synaptic strength is largely unaffected despite somewhat decreased frequency of spontaneous transmission. However, the small increase in mEPSC amplitude could reflect a change in AMPAR subunit composition related to synaptic incorporation of higher-conductance GluA2-lacking CP-AMPA receptors. Consistent with possible incorporation of CP-AMPA receptors at SC-CA1 synapses in CS mice, the ratio of evoked inward -70 mV AMPA peak current to outward +40 mV NMDA current (measured 50 ms after peak) was increased in CS mice relative to the corresponding ratio of peak outward +40 mV AMPA to NMDA current (Fig 3.7A), indicating the possible

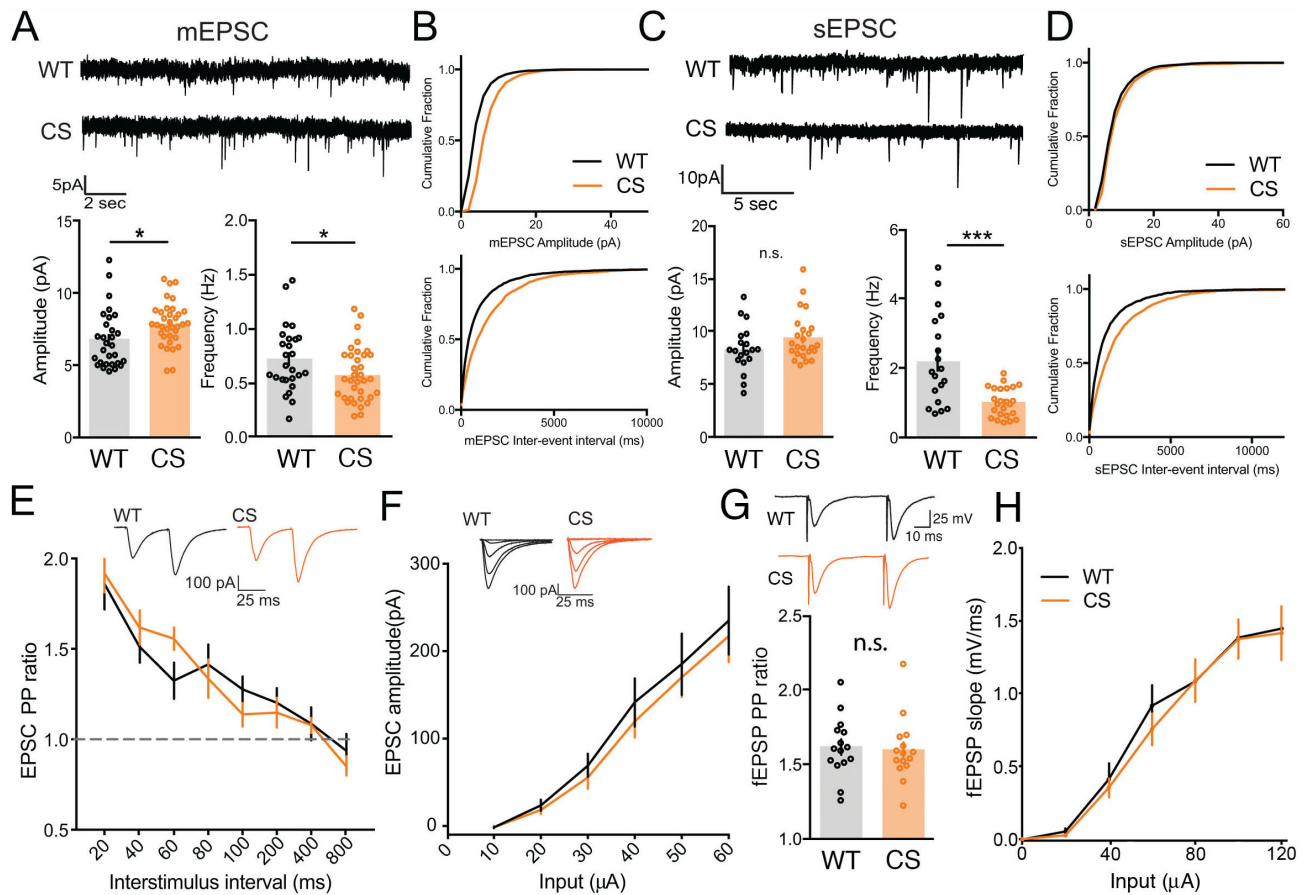


Figure 3.5: AKAP CS mice exhibit slightly increased AMPAR mEPSC amplitude and decreased frequency but normal evoked basal transmission at hippocampal CA1 synapses.

(A and B) Representative traces for mEPSC recordings with plots of mean amplitude and frequency (A) and cumulative distribution plots of mEPSC amplitude and inter-event interval (B) for CA1 neurons in acute hippocampal slices from WT and AKAP CS mice showing a slight increase in mEPSC amplitude and a slight decrease in mEPSC frequency (A: mEPSC amplitude: WT = 6.79 ± 0.371 pA n = 29 cells, CS = 7.883 ± 0.251 pA n = 35 cells, unpaired t test *p = 0.0145; mEPSC frequency: WT = 0.72 ± 0.059 Hz, CS = 0.57 ± 0.042 , unpaired t test *p = 0.0475). (C and D) Representative traces for sEPSC recording with plots of mean amplitude and frequency (C) and cumulative distribution plots of sEPSC amplitude and inter-event interval (D) for WT and CS mice showing a slight but not significant increase in sEPSC amplitude and a significant decrease in sEPSC frequency for CS mice (C: sEPSC frequency: WT 2.21 ± 0.297 Hz, n = 19 cells; CS 1.02 ± 0.0862 Hz, n = 24 cells; unpaired t test ***p = 0.0001). (E–H) No changes in SC-CA1 evoked basal AMPAR transmission are observed for CS mice in (E and G) paired-pulse ratios or (F and H) input-output curves in either whole-cell EPSC or extracellular fEPSP recordings. *p < 0.05 and ***p < 0.001 by unpaired t test. Data are reported as mean \pm SEM.

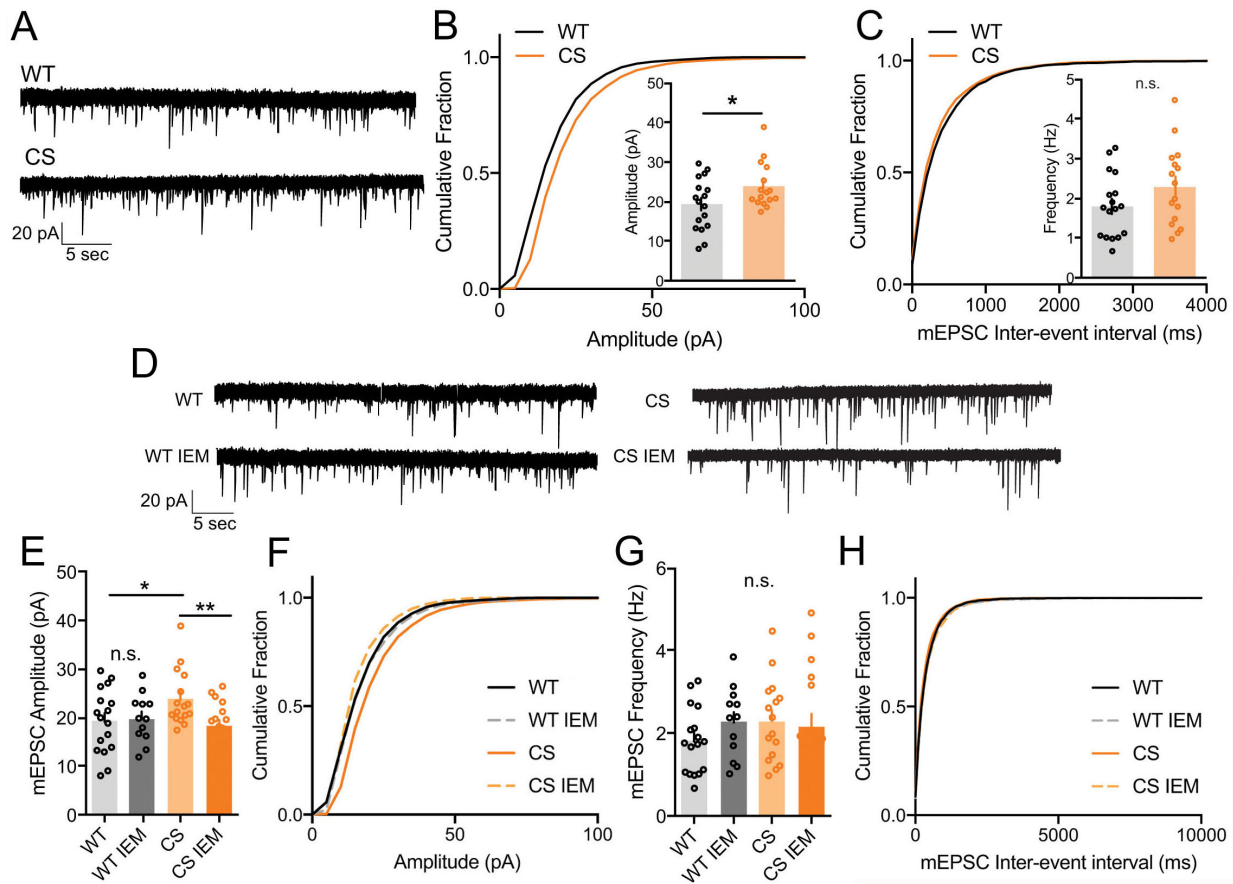


Figure 3.6: Electrophysiological characterization of AKAP CS cultures.

(A-C) Whole-cell recordings from DIV13-14 hippocampal neuron cultures from WT and CS mice. AKAP CS cultures show an enhancement in (B) mEPSC amplitude (WT=19.34 ± 1.599 n=17 cells, CS=23.86 ± 1.434 n=16, unpaired t-test p=0.0443) and no change in (C) mEPSC frequency. (D-H) AKAP CS neuron cultures also exhibit enhancement in CP-AMPA sensitivity, showing a significant decrease in mEPSC amplitude with IEM blockade of CP-AMPA receptors (CS=23.86 ± 1.434 pA n=16, CS IEM=18.42 ± 1.107 pA n=17, unpaired t-test p=0.0050). *p<0.05, **p<0.01; unpaired t-test.

presence of inwardly-rectifying CP-AMPA receptors in CS mice. Yet, increased AMPA/NMDA ratios can arise not only from enhanced AMPAR function but also from decreased NMDAR function. However, the input-output relationship for evoked NMDAR EPSCs revealed no significant differences in basal NMDAR transmission between CS and WT mice, with if anything a trend toward increased NMDAR function in CS (Fig 3.7B).

Taken together, these data suggest that the increases in mEPSC amplitude and AMPA/NMDA ratio observed in CS mice may be attributable to synaptic CP-AMPA receptors. To directly test whether synaptic AMPAR subunit composition is different in CS mice, we utilized two approaches. First, we determined the current/voltage (I/V) relationship for AMPAR EPSCs over a range of holding potentials from -70 to +40mV. CP-AMPA receptors exhibit inward-rectification due to block of outward current by intracellular polyamines. As expected, WT mice displayed a linear AMPA EPSC I/V relationship, which is characteristic of GluA2-containing AMPARs. By contrast, SC-CA1 transmission in CS mice exhibited an inward-rectifying AMPA I/V relationship, which is indicative of GluA2-lacking CP-AMPA receptors (Fig 3.7C). Inward-rectification in CS mice was also quantified as a significantly enhanced -70mV/+40mV AMPA EPSC rectification index (Fig 3.7D). Second, we applied NASPM, an extracellular polyamine, which selectively blocks inward current mediated by CP-AMPA receptors. Consistent with CS mice containing a greater number of synaptic CP-AMPA receptors, application of NASPM blocked ~40% of the inward AMPA EPSC in CS but not WT mice (Fig 3.7E). Furthermore, while mEPSC amplitude and frequency measured in WT mouse cultured hippocampal neurons were insensitive to the CP-AMPA receptor blocker IEM1460; the basal enhancement of mEPSC amplitude in

CS cultured neurons was inhibited/reversed by IEM1460 application with no impact on frequency (Fig 3.6D-H).

Finally, STED imaging and object-based segmentation analysis of surface GluA1 (sGluA1) and PSD-95 antibody staining (Fig 3.7F) revealed an increase in sGluA1 object area (Fig 3.7G) and major axis length (Fig 3.7H) but with no change in the average number of sGluA1 objects per spine for CS compared to WT (Fig 3.7I). However, the total perimeter (Fig 3.7J) and area occupied by sGluA1 objects (Fig 3.7K) were both increased for CS. In addition, increased sGluA1 clustering in CS neurons was also accompanied by an increase in total area occupied by PSD-95 objects in spines (Fig 3.7L), perhaps explaining why the proportional overlap of sGluA1 with PSD-95 remained similar between CS and WT (Fig 3.7M). Overall, these sGluA1 STED imaging results are consistent with increased post-synaptic GluA1 expression in CS cultured neurons and increased basal CP-AMPA activity measured by electrophysiology.

Previous work found that phosphorylation of GluA1 S845 by AKAP150-anchored PKA promotes and dephosphorylation by AKAP150-anchored CaN restricts CP-AMPA synaptic incorporation^{103,104,275,354}. However, immunoblotting analysis of hippocampal subcellular fractions (Fig 3.8A) revealed no significant differences between WT and CS in either total GluA1 expression (Fig 3.8B) or pS845 levels, although non-significant trends toward increased pS845 were observed across all fractions in CS mice (Fig 3.8C). Overall, these data indicate that hippocampal neurons from CS mice have increased basal GluA1 CP-AMPA synaptic activity; however, given the high single-channel conductance of these receptors, synaptic insertion of a relatively small number of S845 phosphorylated CP-AMPA receptors could account for this increased basal activity.

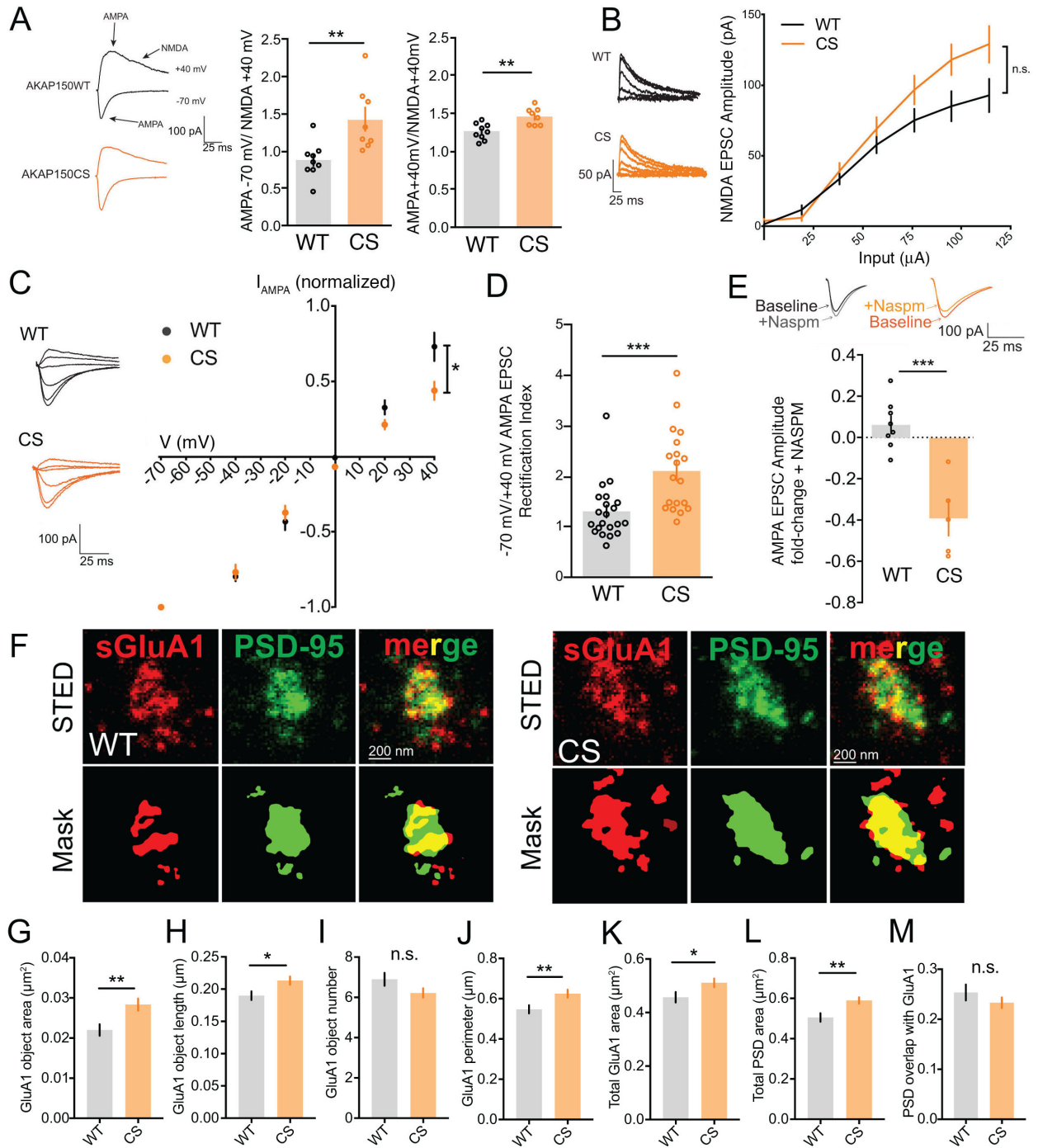


Figure 3.7: AKAP CS mice have elevated basal CP-AMPA activity at CA1 synapses.

Figure 3.7: AKAP CS mice have elevated basal CP-AMPA activity at CA1 synapses.

(A) Evoked SC-CA1 AMPA/NMDA EPSC ratios from WT and CS slices; AKAP CS mice show a substantial increase in -70 mV peak AMPA to +40 mV 50 ms after peak NMDA tail EPSC ratio and a smaller increase in the mixed AMPA and NMDA +40 mV peak to +40 mV 50 ms after peak NMDA tail EPSC ratio (-70 mV/+40 mV: WT 0.88 ± 0.080 , n = 9 cells, CS 1.43 ± 0.15 , n = 8 cells, unpaired t test $**p = 0.0052$; +40 mV: WT 1.26 ± 0.036 , CS 1.46 ± 0.040 , unpaired t test $**p = 0.0017$). (B) No change in evoked NMDA +40 mV EPSC input-output (I-O) relationship in AKAP CS. (C and D) Normalized AMPA EPSC I-V curve showing (C) decreased outward current at positive potentials (AMPA I-V at +40 mV: WT 0.73 ± 0.093 , n = 10 cells; CS 0.45 ± 0.059 , n = 9 cells; unpaired t test $*p = 0.0251$; normalized to -70 mV EPSC amplitude) and (D) increased -70 mV/+40 mV EPSC amplitude rectification index (RI: WT 1.30 ± 0.121 , n = 21; CS 2.12 ± 0.187 , n = 19; unpaired t test $***p = 0.0006$) in AKAP CS slices. (E) Inhibition of -70 mV AMPA EPSC amplitude in AKAP CS but not WT slices by 20 μ M CP-AMPA blocker NASPM (WT 0.065 ± 0.042 , n = 8 cells, CS -0.39 ± 0.084 , n = 5 cells; unpaired t test $***p = 0.0002$; fold change baseline after NASPM application). (F-I) STED imaging of cultured hippocampal neurons stained for surface GluA1 (sGluA1) and PSD-95 (F) showing for AKAP CS neurons (G) increased sGluA1 object area (WT $0.02202 \pm 0.00014 \mu\text{m}^2$, n = 125 spines; CS $0.02835 \pm 0.00015 \mu\text{m}^2$, n = 170 spines; unpaired t test $**p = 0.0032$) with (H) an increase in GluA1 object major-axis length (WT $0.19 \pm 0.0067 \mu\text{m}$, CS $0.2132 \pm 0.0064 \mu\text{m}$, $*p = 0.0132$) but with (I) no change in object number. (J and K) AKAP CS spines also have increased total perimeter (J) (WT $0.5472 \pm 0.02 \mu\text{m}$, CS $0.6252 \pm 0.02 \mu\text{m}$, $**p = 0.0070$) and (K) area occupied by sGluA1 staining in spines (WT $0.4571 \pm 0.019 \mu\text{m}^2$, CS $0.5111 \pm 0.016 \mu\text{m}^2$, $*p = 0.0359$). (L and M) The total area occupied by PSD-95 in spines is also increased in AKAP CS compared with WT (L) (WT $0.5056 \pm 0.021 \mu\text{m}^2$, CS $0.5899 \pm 0.016 \mu\text{m}^2$, $**p = 0.0013$) but with (M) no change in PSD-95 overlap with sGluA1. $*p < 0.05$, $**p < 0.01$, and $***p < 0.001$ by unpaired t test. Data are reported as mean \pm SEM.

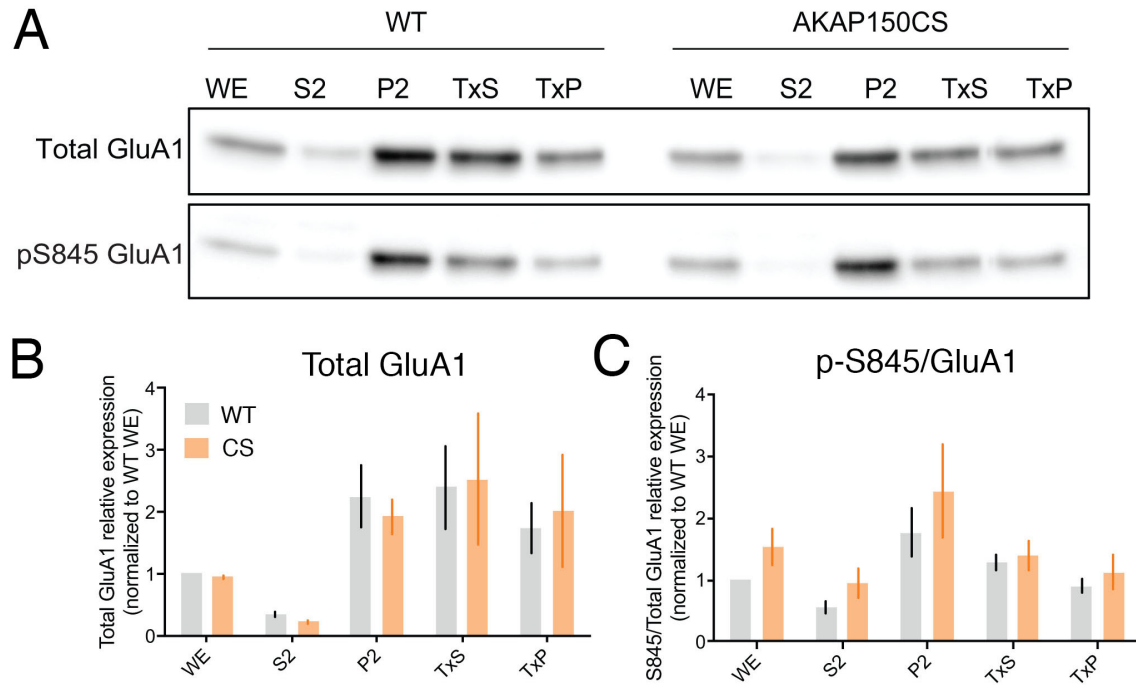


Figure 3.8: Analysis of GluA1 S845 phosphorylation.

(A) Blots from fractionation of WT and CS hippocampal lysates probed for pS845 GluA1 and GluA1 and (B,C) quantification of these blots showing no significant difference in total GluA1 protein or S845 phosphorylation although trends toward increased S845 phosphorylation are seen for CS across all fractions.

Since the majority of AMPARs in CA1 are GluA1/2 heteromers¹⁶, it would be very difficult to biochemically detect increased pS845 phosphorylation occurring in a small pool of CP-AMPARs in CS mice.

AKAP150 palmitoylation is required for expression of CP-AMPAR-dependent but not CP-AMPAR-independent LTP.

Our previous work found that AKAP150-anchored PKA and CaN modulate LTP and LTD at CA1 synapses through opposing each other in control of CP-AMPAR synaptic incorporation; however, the dependence of LTP on PKA signaling and AMPAR subunit composition is very flexible and developmentally plastic in mice between 2 and 8 weeks of age^{103,104,125,133,175,179,371}. In addition, CP-AMPAR synaptic recruitment during LTP could be affected by the strength and type of induction stimulus, which is another major variable across previous studies^{36,103,122,129,131,179,371}. Due to these factors, the contributions of GluA1 and CP-AMPARs to CA1 LTP remain unclear and controversial^{104,125,133}. Therefore, we next examined how loss of AKAP150 palmitoylation impacts LTP and LTD at CA1 synapses in 2-3 week-old mice. A standard 1x100 Hz, 1 s high frequency stimulus (HFS) protocol elicited reliable LTP of fEPSP slope (~150%) in WT slices, but failed to induce significant LTP in CS slices (Fig 3.9A,E). In contrast, LTD induced with prolonged low-frequency stimulation (LFS; 1Hz, 900 pulses, 15 min) was comparable (~60%) at CA1 synapses in WT and CS mice (Fig 3.9B,F).

To explore whether the LTP-deficit in CS mice relates to altered CP-AMPAR regulation, we used two different common whole-cell pairing LTP induction protocols that we found differentially depend on CP-AMPARs in 2-3 week-old WT mice. In

particular, we found that brief 2x100 Hz, 1 s stimulation, which is similar to HFS induction of LTP in fEPSP experiments, paired with 0 mV post-synaptic depolarization^{146,147} induced substantial LTP in WT (~200%) that was strongly impaired in CS slices and inhibited by NASPM in WT slices (Fig 3.9C,G). In contrast, LTP was similar and much greater in magnitude (~325%) for both CS and WT mice when induced with a stronger, prolonged pairing protocol (3 Hz, 90 s, 0 mV)^{129,179,371} that was largely insensitive to NASPM in WT slices (Fig 3.9D,H). These results indicate that the LTP deficits in CS mice are specifically related to impaired CP-AMPA regulation and also suggest that high-conductance CP-AMPA receptors are more important for expression of the lower levels of LTP induced with weaker stimuli versus higher levels of LTP induced with stronger stimuli, which robustly recruit GluA2-containing AMPARs.

AKAP CS mice exhibit enhanced, CP-AMPA-dependent de-depression after prior induction of LTD.

While the enhancement in basal AMPAR transmission is modest in CS mice and a strong pairing induction stimulus can overcome the LTP deficit, we wanted to examine whether prior basal CP-AMPA incorporation in CS mice was altering meta-plasticity to prevent additional CP-AMPA recruitment in response to HFS. Our previous studies found that AKAP-CaM-dependent removal of CP-AMPA receptors from CA1 synapses is required during LTD^{104,275}. Thus, having demonstrated that LTD is comparable to WT in CS mice (Fig 3.9B), we wondered whether prior induction of LTD to remove a proportion of existing synaptic AMPARs might allow CP-AMPA recruitment in response to subsequent LTP induction resulting in de-depression. With this in mind, we induced LTD with 1 Hz LFS and allowed its expression for 15 min before delivering 1x100 Hz HFS to

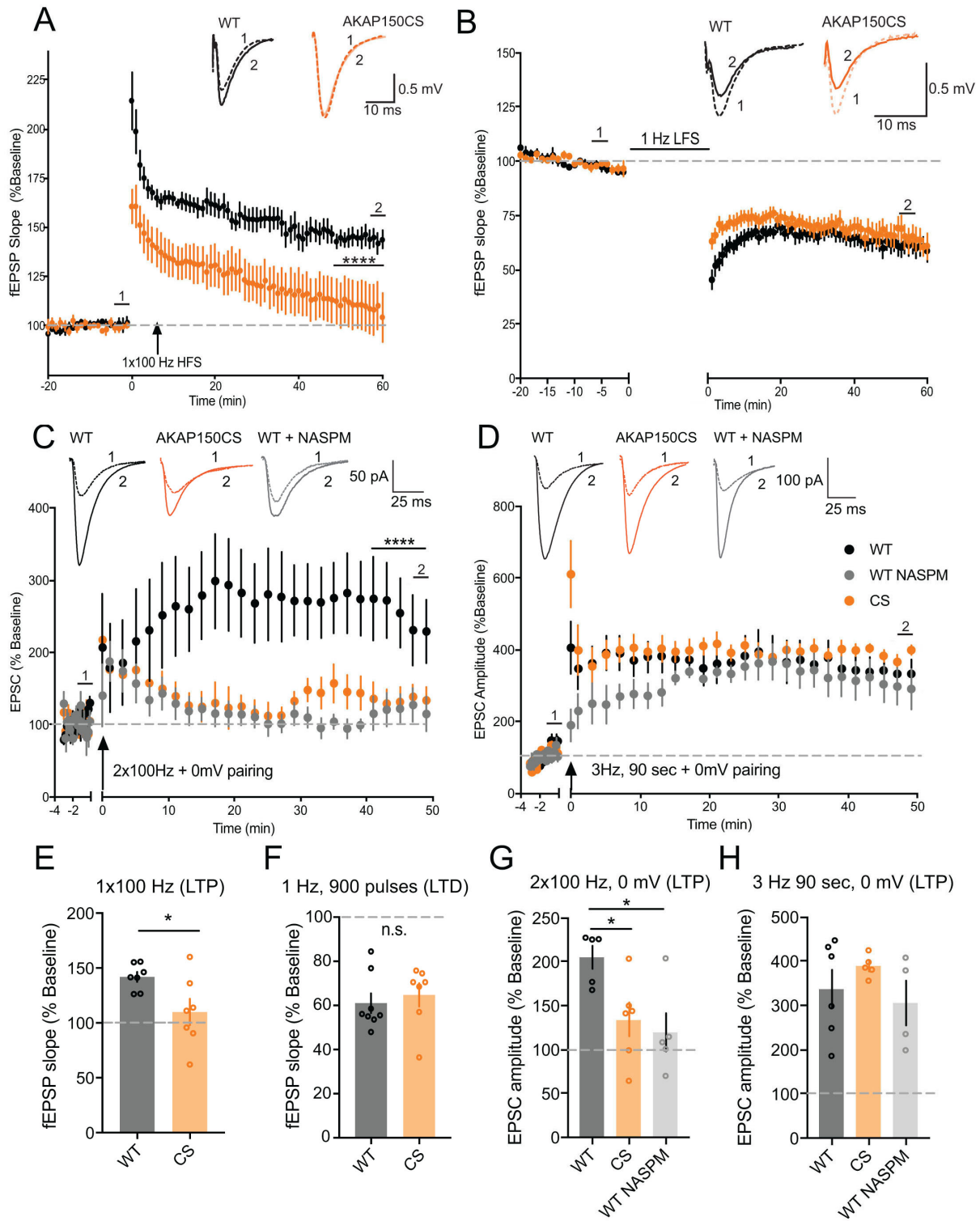


Figure 3.9: CP-AMPA-dependent LTP at CA1 synapses is impaired in AKAP CS mice.

Figure 3.9: CP-AMPA-dependent LTP at CA1 synapses is impaired in AKAP CS mice.

(**A** and **E**) SC-CA1 fEPSP slope (normalized to baseline) recorded over time for WT and AKAP CS slices (**A**) and aggregate data for measurements of normalized fEPSP slope (**E**) (averaged over the last 10 min) showing robust 1x100 Hz 1 sec HFS induction of LTP in WT (~150%) that is significantly impaired in CS (A: **** $p < 0.0001$ by 2-way ANOVA over last 10 min; E: fEPSP slope for WT = $141.9 \pm 4.55\%$ $n = 7$ slices, CS = $110 \pm 12.04\%$ $n = 7$ slices, unpaired t test last 10 min * $p = 0.028$). (**B** and **F**) SC-CA1 fEPSP slope (normalized to baseline) recorded over time for WT and AKAP CS slices (**B**) and aggregate data for measurements of normalized fEPSP slope (**F**) (averaged over the last 10 min of recording) showing 1 Hz, 900 pulses (15 min) robust induction of LTD (~60%) in both WT and CS. (**C** and **G**) Normalized EPSC amplitude (normalized to baseline) recorded over time (**C**) and aggregate data for measurements of normalized EPSC amplitude (**G**) (averaged over the last 10 min) showing CP-AMPA dependent, NASPM-sensitive LTP induced by 2x100 Hz, 1 s HFS, 0 mV pairing in WT slices is impaired in AKAP CS slices (C: 2-way ANOVA with Tukey's multiple comparisons test for last 10 min: WT NASPM versus WT **** $p < 0.0001$, WT versus CS **** $p < 0.0001$; G: WT = $204.9 \pm 3.24\%$ $n = 5$ cells, CS = $133.8 \pm 9.41\%$ $n = 6$ cells, WT NASPM = $119.6 \pm 22.45\%$ $n = 5$ cells; unpaired t test WT versus WT NASPM * $p = 0.0113$, WT versus CS * $p = 0.0362$). (**D** and **H**) Normalized EPSC amplitude (normalized to baseline) recorded over time (**D**) and aggregate data for measurements of normalized EPSC amplitude (**H**) (averaged over the last 10 min) showing CP-AMPA independent, NASPM insensitive LTP induced by 3 Hz, 90 s, 0 mV pairing in WT slices is normal in CS slices (H: WT = $337.4 \pm 44.25\%$ $n = 6$ cells, WT NASPM = $305.6 \pm 51.8\%$ $n = 4$ cells, CS = $389.1 \pm 11.25\%$ $n = 5$ cells). Data reported as mean \pm SEM.

induce LTP/de-depression. As seen in previous studies^{164,372}, HFS-induced de-depression in WT slices returned fEPSP responses back to pre-LFS baseline values within 30 min of induction (Fig 3.10A). In CS slices, not only did we observe HFS-induced de-depression, but this de-depression was also greater than that observed in WT. In addition, while NASPM had no significant impact on in WT slices, it reduced de-depression in CS slices to WT levels (Fig 3.10A,B). Thus, the basal increase in CP-AMPA synaptic activity in CS mice is altering the ability of CA1 synapses to undergo LTP and prior removal of synaptic AMPARs by LTD can restore LTP responsiveness by allowing subsequent CP-AMPA recruitment.

Summary and discussion

Dynamic protein palmitoylation has emerged as a key regulator in the subcellular positioning of proteins in neurons to coordinate precise and specific signaling^{333,334}. Here, using biochemistry, super-resolution nanoscopy and electrophysiology we demonstrate the importance of palmitoylation of the post-synaptic scaffolding molecule AKAP150 in controlling basal AMPAR synaptic subunit composition to alter LTP.

Complete gene knockout is widely used to study the effect of disrupting protein function. However, for large, multivalent scaffold protein complexes that function as structural and signaling hubs, knockouts are problematic due to disruption of multiple functions. In particular, AKAP150 KO removes the opposing signaling functions of PKA and CaN, allowing compensation that makes mechanistic interpretations difficult. Accordingly, AKAP150 null mice exhibit different and in general more limited behavioral and synaptic phenotypes than AKAP150 knock-in mice that are specifically deficient in either PKA (Δ PKA and D36) or CaN (Δ PIX) anchoring^{103,104,275,281-283,354,361}. Thus, here

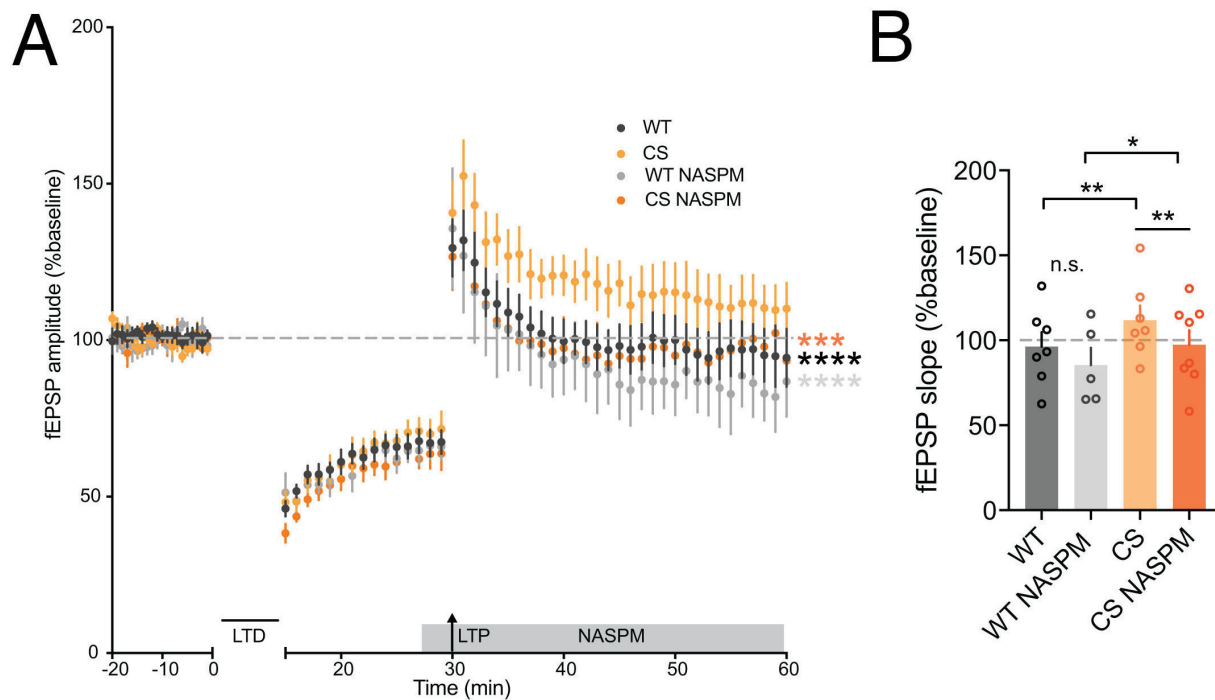


Figure 3.10: AKAP CS mice can undergo CP-AMPA-dependent de-depression at CA1 synapses.

(**A** and **B**) fEPSP slope (normalized to baseline) recorded over time (**A**) and aggregate data for measurements of normalized fEPSP slope (**B**) (averaged over last 10 min) showing that de-depression (induced by 1 Hz, 900 pulses LFS-LTD followed by 1x100 Hz, 1 s HFS-LTP 15 min later) is enhanced in CS mice (A: over last 10 min CS versus WT **** $p < 0.0001$ by 2-way ANOVA with Tukey's multiple comparisons; B: WT $96.27 \pm 8.537\%$, $n = 7$ slices, CS $111.8 \pm 8.638\%$, $n = 7$ slices; unpaired t test CS versus WT *** $p = 0.0010$). CS but not WT de-depression is sensitive to CP-AMPA blockade with NASPM (A: over last 10 min CS NASPM versus CS *** $p < 0.001$, WT NASPM versus CS **** $p < 0.0001$ by 2-way ANOVA with Tukey's multiple comparisons; B: WT NASPM $85.42 \pm 10.23\%$, $n = 5$ slices, CS NASPM $97.46 \pm 8.487\%$, $n = 8$ slices; unpaired t tests WT NASPM versus WT $p > 0.05$ [n.s.], CS NASPM versus CS ** $p = 0.0016$, WT NASPM versus CS NASPM * $p = 0.0377$). Data are reported as mean \pm SEM.

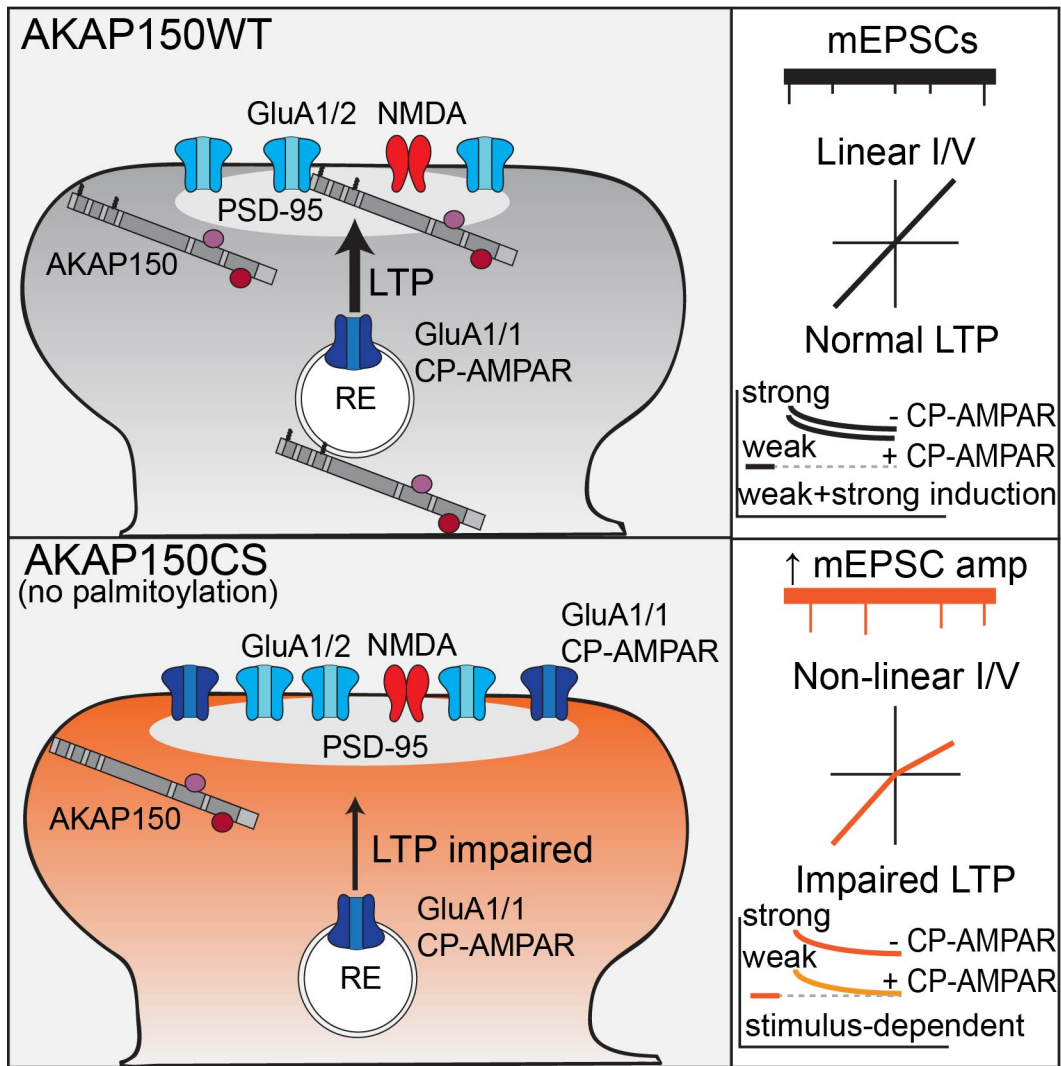


Figure 3.11: Summary of findings from Chapter III.

AKAP CS mice show increased mEPSC amplitude and have increased basal insertion of CP-AMPA receptors. Palmitoylation of AKAP controls AKAP synapse organization and occupancy, as well as AMPAR surface expression. AKAP CS mice show a selective disturbance in CP-AMPA dependent LTP, while maintaining CP-AMPA independent LTP and LTD.

we generated palmitoylation-deficient AKAP CS knock-in mice to specifically address the role of palmitoylation in controlling AKAP150 post-synaptic targeting and AMPAR regulation (Fig 3.11).

AKAP150 palmitoylation and PKA/CaN anchoring in control of basal CP-AMPAR incorporation

Importantly, we observed a very specific synaptic phenotype in AKAP CS animals that is distinct from, but overlapping with, phenotypes observed in either AKAP-PKA or -CaN anchoring-deficient mice. In particular, both CS and CaN anchoring-deficient Δ PIX mice^{104,275} exhibit increased basal synaptic CP-AMPAR activity. However, despite Δ PIX mice exhibiting significantly enhanced GluA1 S845 phosphorylation and stronger EPSC inward rectification than CS mice²⁷⁵, altered AMPAR subunit composition is only associated with increased mEPSC amplitude in CS mice. In addition, while blocking CP-AMPARs with IEM1460 in neurons cultured from WT mice had no impact on mEPSC activity, IEM1460 reduced basal mEPSC amplitude and frequency in Δ PIX mouse neurons to below WT levels³⁵⁴. Yet, in CS cultured neurons IEM1460 only reduced elevated mEPSC activity back to WT levels. Thus, in Δ PIX mice the impact of CP-AMPARs on basal synaptic strength is offset by an accompanying, compensatory loss of GluA2-containing receptors, but in CS mice, while a smaller number of CP-AMPARs are added to synapses, little or no compensatory removal of GluA2-containing receptors is occurring. Overall, the impacts of loss of AKAP palmitoylation on basal AMPAR transmission are similar but clearly not identical to those resulting from loss of AKAP-CaN anchoring.

AKAP150 palmitoylation and PKA/CaN anchoring in CP-AMPA meta-plasticity that controls LTP/LTD balance

In contrast, the CA1 LTP phenotypes in CS and Δ PIX mice are drastically different, with Δ PIX mice showing strongly enhanced²⁷⁵ and CS mice exhibiting strongly impaired HFS-induced LTP. The relatively modest enhancement in basal AMPAR transmission in CS mice is unlikely to occlude LTP, and given our previous observations of enhanced CP-AMPA-dependent LTP in Δ PIX mice, prior basal incorporation of CP-AMPA alone cannot account for impaired LTP in CS mice. However, a key difference between the plasticity landscapes of these two knock-in mice is the lack of LFS-induced LTD in Δ PIX but not CS mice. In Δ PIX mice, loss of AKAP-CaN anchoring impairs CP-AMPA removal from synapses to alter meta-plasticity at CA1 synapses in favor of LTP > LTD^{104,275}. In contrast, in CS mice LTD and CP-AMPA synaptic removal mechanisms appear to be intact, pointing more toward a specific deficit in recruitment of additional CP-AMPA to support LTP. Indeed, we were able to further link the LTP deficit in CS mice specifically to CP-AMPA dysfunction by showing that it could be overcome by using a strong, prolonged whole-cell pairing induction stimulus that did not require CP-AMPA recruitment in WT mice. In addition, we were able to establish that elevated basal CP-AMPA activity in CS mice was contributing to the inability of HFS to recruit additional CP-AMPA by showing that prior LTD induction to remove synaptic AMPARs allowed subsequent HFS to induce LTP/de-depression that was in part mediated by CP-AMPA. Thus, overall, loss of AKAP150 palmitoylation increases basal CP-AMPA synaptic incorporation but impairs additional recruitment to alter CA1 meta-plasticity in favor of LTD > LTP.

Interestingly, prior characterization of PKA anchoring-deficient AKAP150 knock-in mice also found deficits in LTP related to impaired CP-AMPA recruitment, but only in adult (~8 week-old) and not juvenile (2-4 week-old) mice^{103,104}. In particular, while HFS-induced LTP at ~2 weeks of age was strongly inhibited by CP-AMPA antagonists in WT mice, LTP was neither impaired nor sensitive to CP-AMPA antagonists in Δ PKA mice¹⁰⁴. These studies, along with a number of other studies of CA1 LTP using GluA1 knockout mice, S845A knock-in mice, and subunit replacement approaches, indicate the dependencies of LTP on PKA signaling, S845 phosphorylation, and AMPAR subunit-composition are flexible and developmentally plastic in juvenile animals^{36,122,125,129,167,171,172,175,179,371}. Thus, it is remarkable that the compensatory shift to HFS-LTP recruitment of GluA2-containing AMPARs that is observed in juvenile GluA1 knockout, S845A, and AKAP150 Δ PKA/D36 mice is not occurring in CS mice, where the LTP deficit can only be overcome by prolonged whole-cell pairing that recruits GluA2-containing AMPARs even in WT mice. Importantly, our present findings demonstrating that CP-AMPA recruitment depends strongly on LTP induction stimulus strength in general agreement with previous observations made across several different ages^{103,131,179,371} and could explain discrepancies in previous studies of juvenile rodents that observed CP-AMPA recruitment for LTP induced with comparatively weaker^{36,122,167} but not stronger pairing protocols¹²⁹.

Interestingly, at this same early developmental age when LTP is normal in Δ PKA, D36, and S845A mice, LFS-LTD is impaired because AKAP-PKA anchoring and S845 phosphorylation are needed to promote transient recruitment of CP-AMPA to CA1 synapses during LTD induction prior to their rapid removal by AKAP-anchored

CaN^{103,104,169,172}. These LTD findings at CA1 synapses are in accordance with studies in other brain regions, including in the amygdala, ventral tegmentum, and nucleus accumbens, where CP-AMPA synaptic incorporation not only supports synaptic potentiation but can also prime synapses for LTD/de-potential^{201,355}. Accordingly, in CS mice basal CP-AMPA incorporation may prime synapses to undergo normal LTD through AKAP-CaN-mediated removal with no need for additional CP-AMPA recruitment. Consistent with effective synaptic removal of CP-AMPA by LTD in CS mice, prior LFS induction of LTD allowed subsequent HFS induction of LTP/depression to recruit CP-AMPA back to CA1 synapses.

AKAP palmitoylation and signaling in multiple locations during LTP and LTD

Our prior studies found that palmitoylation of human AKAP79 is required for its localization to dendritic REs^{247,248}, a compartment that is known to deliver GluA1 to the PM in support of LTP^{143,144,148}. In addition, acute AKAP79 CS overexpression in rat hippocampal neurons increased both basal RE exocytosis and synaptic CP-AMPA activity. Here, while we also observed decreased AKAP150 CS RE localization and increased basal CP-AMPA activity in AKAP CS mice, we did not observe increased basal RE exocytosis. Thus, AKAP CS mice exhibit alterations in GluA1 CP-AMPA regulation even in the absence of more widespread RE trafficking dysfunction. However, we found that palmitoylation is also required for normal AKAP150 association with the PSD, as shown by reduced co-localization and co-fractionation of AKAP150 CS with PSD-95. Thus, impaired LTP in AKAP CS mice is likely related to decreased AKAP signaling in not only REs but also the PSD. In contrast, AKAP79/150 localization to the extrasynaptic PM, where AMPARs are endocytosed during LTD^{220,373}, is not impacted

by loss of palmitoylation. Thus, it is tempting to speculate that AKAP-PKA signaling that promotes CP-AMPA synaptic incorporation during LTP requires AKAP localization to REs and the PSD to promote recycling and synaptic retention of receptors, while AKAP-CaN signaling that removes CP-AMPA during LTD only requires extrasynaptic membrane targeting.

Accordingly, our prior work found that chemical LTP stimulation increased AKAP palmitoylation and localization to dendritic spines. Furthermore, overexpression of the AKAP79 CS mutant or knock-down of its palmitoylating enzyme DHHC2 acutely interfered with a number of cellular correlates of LTP in cultured neurons including spine enlargement, RE exocytosis, GluA1 surface delivery, and mEPSC potentiation^{247,248}. In contrast, chemical LTD stimulation decreased AKAP palmitoylation and localization to spines in coordination with spine shrinkage. Consistent with AKAP depalmitoylation favoring LTD > LTP as observed here in AKAP CS mice, AKAP79 CS did not interfere with GluA1 endocytosis and was even more sensitive than WT to removal from spines by chemical LTD²⁴⁷. In addition, overexpression of a constitutively lipidated AKAP79 mutant prevented both AKAP removal from spines and spine shrinkage following chemical LTD²⁶⁵. Thus, based also on our findings here *ex vivo*, AKAP79/150 palmitoylation is required to support LTP but not LTD.

However, the observation that CS, but not WT mice, robustly recruit CP-AMPA recently removed by LTD back to CA1 synapses during HFS-induced de-depression could reflect a loss of AKAP-CaN in REs allowing for enhanced GluA1 recycling and synaptic incorporation mediated by a pool of PKA other than that anchored to AKAP79/150 or possibly other kinases like PKG, PKC, or CaMKII^{173,174,374}. Accordingly,

loss of AKAP-CaN phosphatase signaling in REs, in addition to in the PSD, could also contribute to the increases in basal synaptic GluA1 surface expression and CP-AMPA activity in AKAP CS mice by increasing receptors within the recycling pool and then also biasing PSD signaling toward receptor retention. All things considered, it is remarkable that such a specific perturbation of AKAP79/150 intracellular targeting caused by loss of palmitoylation has such a dramatic impact on synaptic plasticity, thus further underscoring how critical scaffold proteins and their organization of localized signaling pathways are for controlling neuronal function.

CHAPTER IV

EXPLORING FURTHER MECHANISMS OF AMPAR REGULATION IN AKAP CS MICE

Introduction

Our previously published work characterized the phenotypes of AKAP CS mice. Interestingly, losing AKAP150 palmitoylation results in both a basal and activity-induced phenotype at the level of CP-AMPA regulation. CP-AMPA regulation via phosphorylation is very well studied and depends on mechanisms of recruitment basally and during activities involving AKAP-anchored enzymes^{1,104,275}. However, we only examined AMPAR synaptic localization and transmission in AKAP CS mutants. It is still unknown if perturbing palmitoylated AKAP signaling could also influence AMPAR localization or occupancy within internal compartments or at the extrasynaptic membrane. Further, CP-AMPA dependent LTP is specifically impaired in AKAP CS mice (Fig 3.9C-H) but how does this specifically affect receptor localization or function after LTP? Thus, our previous studies did not fully explore AMPAR-mediated transmission following LTP.

In our initial characterization of AKAP CS mice, we saw a slight decrease in mEPSC frequency but a larger decrease in sEPSC frequency (Fig 3.5C,D). There are a few scenarios that can result in decreased mEPSC and/or sEPSC frequency. Decreased frequency can occur due to fewer synapses, however, we provided evidence against this by showing that there was no difference in spine number or size (Fig 3.2C-H). We did not count active synapses, which could be achieved by staining with PSD-95 and a presynaptic marker and counting overlapping puncta per stretch of dendrite. Nonetheless, a frequency effect could also be observed due to a change in release

probability, but this does not seem likely because we saw no difference in PPRs in slices from AKAP CS animals (Fig 3.5E,G). Lower sEPSC frequency could also be due to decreased firing activity in the hippocampal circuit. If this is the case, could such decreased firing be a driving force for incorporating more CP-AMPARs, mimicking a homeostatic scaling phenotype? Homeostatic scaling is a form of plasticity where neurons can either scale-up or scale-down synaptic responses in order to maintain firing patterns, connectivity and other forms of plasticity (like Hebbian plasticity) over extended periods of time. There is precedent for AKAP79/150 signaling to be important for homeostatic scaling-up³⁵⁴. Like Hebbian plasticity, mechanisms of homeostatic plasticity are regulated by Ca^{2+} influx through NMDARs and LTCCs and are conferred through changes in AMPAR localization and function^{107,108,352,375-378}, including the regulation of the synaptic incorporation of CP-AMPARs^{108,353,379,380}. Our laboratory has shown that AKAP-anchored enzymes influence CP-AMPAR synaptic incorporation so it is not surprising that AKAP79/150 plays a role in scaling-up. Both the Δ PIX and Δ PKA AKAP mutants are unable to scale-up, due to already enhanced basal CP-AMPAR levels and inability to recruit CP-AMPARs to the synapse respectively³⁵⁴. It is unknown then how mislocalizing AKAP and its signaling enzymes with the CS mutation could influence mechanisms of homeostatic plasticity.

Aims

- Determine the effect of chronic activity manipulation on AMPAR function in AKAP150 palmitoylation mutant
- Characterize the receptor milieu that may be contributing to altered meta-plasticity in AKAP CS mice

Materials and methods

TBOA recordings

A baseline was established (~5 minute) in whole-cell mode with K-gluconate internal (in mM: 137 K-gluconate, 5 KCl, 10 HEPES, 4 ATP-Mg₂, 0.5 GTP-Na₂, 10 phosphocreatine, ~280-290 Osm) followed by perfusion of ACSF containing 20 μM TBOA by gravity flow and recorded for up to 10 minutes with *threo*-β-Benzyloxyaspartic acid (TBOA). In the NASPM and TBOA condition, 20 μM NASPM was added along side the TBOA.

Chronic NASPM treatments in culture

20 μM NASPM was added to the media of cultures 24 hours before recording. Cells were returned to the incubator and recorded from ~23-25 hours post-treatment in standard ACSF with CsMe (Chapter III) internal.

cLTP in culture

30 min pre-incubation in ACSF, then transferred to cLTP ACSF containing 2 mM Ca²⁺, 0 Mg²⁺, 200 μM glycine, 50 μM picrotoxin for 10 minutes and back to normal ACSF for 20-30 minute recovery. Controls maintained in normal ACSF with 2 mM Ca²⁺ and 1 mM Mg²⁺. For electrophysiology, cells were then transferred to recording ACSF containing TTX and picrotoxin to record mEPSCs with CsMe (see Chapter 3 Materials and Methods) internal for up to 1 hour after recovery.

Table 4.1: Key resources table

REAGENT or RESOURCE	SOURCE	IDENTIFIER
Chemicals, Peptides, and Recombinant Proteins		
DL- <i>threo</i> - β -Benzyloxyaspartic acid (DL-TBOA)	Tocris Bioscience	Cat#1223
Glycine	Fisher Scientific	Cat#BP381-5
Tetrodotoxin (TTX)	Tocris Bioscience	Cat# 1078
Picrotoxin	Tocris Bioscience	Cat# 1128
NASPM trihydrochloride	Tocris Bioscience	Cat# 2766
IEM 1460	Tocris Bioscience	Cat# 1636

Results

AKAP CS animals have normal extrasynaptic receptor composition.

Previously, we found that AKAP CS mice exhibited an increase in surface GluA1 expression in hippocampal neurons, as well as enhanced inward rectification and therefore CP-AMPA contribution to baseline transmission at CA1 synapses. While in preliminary experiments I observed that internal stores are not lacking for GluA1-containing receptors (data not shown) and depotentiation is successful in field recordings from these mice (Fig 3.10), extrasynaptic receptors need to be considered as well. There is a wealth of research indicating that lateral diffusion from extrasynaptic receptor pools contributes to recruitment of receptors to the synapse (see above in introduction). To understand if extrasynaptic receptor contribution or subunit composition was altered in the AKAP CS mutant, after establishing baseline EPSCs using whole-cell patch-clamp recordings, the excitatory amino acid transporter blocker TBOA was applied to produce glutamate spillover that activates extrasynaptic AMPARs, resulting in an enhancement to the EPSC (Fig 4.1 A). There was no difference between WT and CS in response to activation of extrasynaptic receptors through indirect action of TBOA (Fig 4.1 B). Further, if the CP-AMPA antagonist NASPM is applied during TBOA treatment (Fig 4.1C,D), there is also no difference between WT and CS, indicating that CP-AMPA receptors are largely not present at extrasynaptic sites in either WT or CS mice.

CP-AMPA involvement in basal transmission in AKAP CS animals.

The basal CP-AMPA phenotype that was observed in CS mice showed enhanced GluA1 surface receptor levels in cultured hippocampal neurons that were

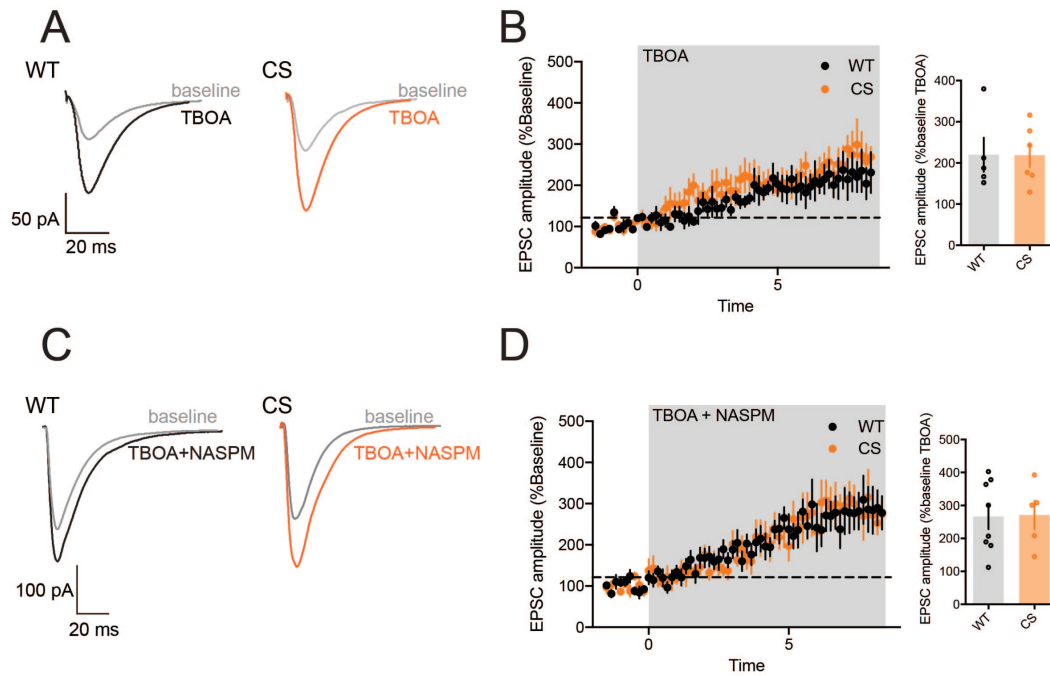


Figure 4.1: Normal TBOA response in AKAP CS mice.

(A,B) WT and CS mice respond with increased evoked EPSCs in response to TBOA (WT n=5, CS n=6). (C,D) NASPM applied alongside TBOA does not have any effect on TBOA induced increase in evoked EPSCs in either WT or CS slices (WT n=8, CS n=5). Data reported as mean \pm SEM.

also reflected in IEM-sensitive contributions to mEPSC amplitude (Figs 3.5A&3.6A,B). However, it is unclear if this is a byproduct of aberrant receptor trafficking or if the system relies on the enhanced signaling conferred by the increased conductance and Ca^{2+} -permeability of the receptor. To start to understand the requirement of CP-AMPARs basally, we blocked CP-AMPARs in cultures for 24 hours with NASPM and then recorded mEPSCs (Fig 4.2A). WT cells do not have any significant difference in mEPSC amplitude or frequency following chronic NASPM treatment, consistent with a lack of substantial signaling by synaptic CP-AMPARs under basal conditions. In contrast, AKAP CS cultures exhibited a significant increase in mEPSC frequency, but with no change in amplitude following chronic NASPM treatment (Fig 4.2B,C). This preliminary data indicates that CS cultures depend on CP-AMPAR transmission basally because when these receptors are blocked, the cells must compensate by increasing AMPAR transmission.

Impaired response to cLTP in AKAP CS mouse cultures.

Because there seems to be a disruption in proper AMPAR handling at the synapse, we wanted to know if CP-AMPARs could be properly delivered to the synapse in an activity-dependent manner in AKAP CS cultures. LTP could be failing in these cells due to already have having potentiated synapses and/or simply synapses already containing CP-AMPARs (i.e. altered meta-plastic state) that have no place to insert new AMPARs. Alternatively, new AMPARs that are delivered may not provide a change in current and/or Ca^{2+} influx because they are just redundantly replacing receptors with their same quality. We see no difference in S845 phosphorylation in CS hippocampal fractionations basally (Fig 3.8), though we have not examined this particular

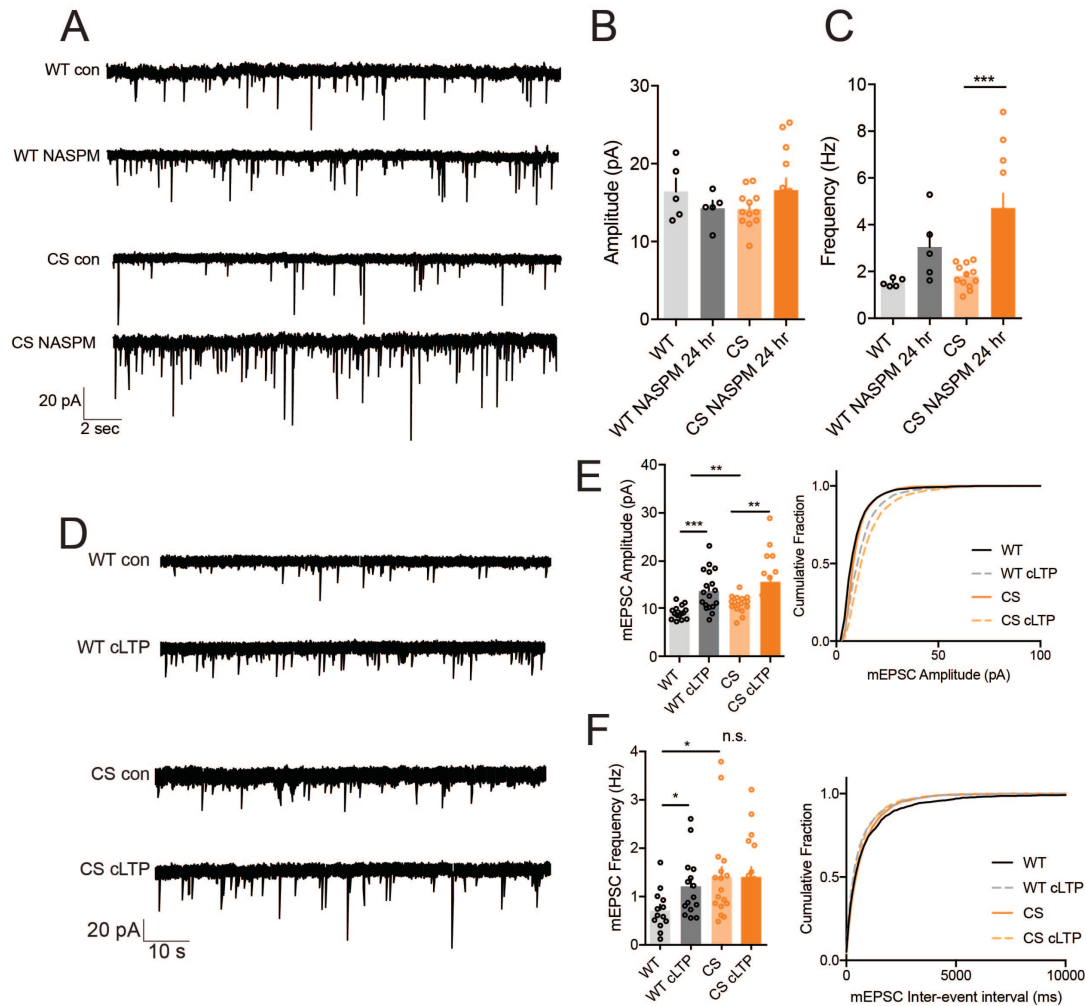


Figure 4.2: AMPAR-minis after chronic CP-AMPA blockade and cLTP.

DIV13-14 culture recordings from mouse hippocampal neurons from WT and CS mice. (A-C) 24 hours of 20 μ M NASPM does not affect WT mEPSCs, but significantly increases AKAP CS mEPSC frequency (CS con: 1.802 ± 0.1475 Hz, CS NASPM: 4.715 ± 0.6237 Hz, **** $p < 0.0001$, WT $n = 5$, CS $n = 12$)(C). (D-F) cLTP (200 μ M glycine, 50 μ M picrotoxin, $-Mg^{2+}$ for 10 min) increases WT mEPSC amplitude (E) (Amplitude WT: 9.207 ± 0.3548 pA, WT cLTP: 13.71 ± 0.9802 pA, CS: 10.99 ± 0.4182 pA, CS cLTP: 15.58 ± 1.304 pA; WT $n = 15$, WT cLTP $n = 18$, CS $n = 17$, CS cLTP $n = 17$; WT vs WT cLTP *** $p = 0.0004$, WT vs CS ** $p = 0.0032$, CS vs CS cLTP ** $p = 0.0021$) and frequency (F) (Frequency: WT: 0.7033 ± 0.1165 Hz, WT cLTP: 1.19 ± 0.1623 Hz, CS: 1.388 ± 0.2252 Hz, CS cLTP: 1.399 ± 0.1983 Hz; WT $n = 13$, WT cLTP $n = 15$, CS $n = 17$, CS cLTP $n = 17$; WT vs WT cLTP * $p = 0.0257$, CS vs CS cLTP $p = 0.9694$ [n.s.], WT vs CS * $p = 0.0202$) while only affecting AKAP CS mEPSC amplitude. * $p < 0.05$, ** $p < 0.01$, *** $p < 0.001$, **** $p < 0.00001$ one-way ANOVA with Tukey's multiple comparison test. Data are reported as mean \pm SEM.

phosphorylation site during or after LTP/cLTP. Then again, AKAP CS mice could deliver GluA1-lacking receptors that would not confer synapse strengthening. Even still, we could be observing impaired forward trafficking of receptors in CS cells when there is a high demand and enhanced stress on the system due to a lack of receptors in the trafficking pool or a problem with insertion/diffusion mechanisms. As a preliminary attempt to try and approach this question, we wanted to assess activity-dependent AMPAR recruitment with electrophysiology. Cultures show an increase in both mEPSC amplitude and frequency basally in AKAP CS cultures (Fig 3.6A-C&Fig 4.2D-F), as observed previously. In response to cLTP, WT neurons respond with a significant increase in both amplitude and frequency of mEPSCs (Fig 4.2D-F), while CS neurons only show a significant increase in amplitude and not frequency.

Conclusions and discussion

We found that extrasynaptic AMPAR levels and composition appear normal in AKAP CS slices. Also, at 2-3 weeks of age, extrasynaptic receptors appear to be largely CI-AMPARs, as shown by insensitivity to CP-AMPAR blockade paired with TBOA treatment. While this information is important for more completely understanding the total surface receptor compliment and thus the extra-synaptic contribution to the meta-plastic state of the neuron, it only tells us what is happening basally. Further work will need to be done to characterize lateral diffusion in the mutant, perhaps by crosslinking surface receptors and measuring the response to activity (as in¹⁵⁵).

We have just begun to think about how AKAP-mediated mechanisms of homeostatic scaling may be altered in AKAP CS animals. We observed in very preliminary experiments that 24 hour NASPM treatment resulted in enhanced mEPSC

frequency and a trend towards increased amplitude. This observation is intriguing and merits further exploration, by way of increased replicates and follow-up experiments. It would be interesting to observe the effect of standard scaling treatments (such as chronic TTX or TTX with NMDAR blockade) on CS cells, which our lab has used previously to understand the role of AKAP-anchored enzymes in scaling³⁵⁴. I predict that AKAP CS cells will be able to more effectively scale-down than scale-up, mimicking the LTD and LTP phenotypes outlined above. However, while there is considerable overlap, not all of the same mechanisms that control Hebbian plasticity equally control homeostatic plasticity. In this way, we can further understand the role of AKAP palmitoylation in the larger plasticity context.

AKAP CS cultures can respond normally in mEPSC amplitude increase to cLTP, but not in frequency. Post-synaptically, enhanced amplitude is often associated with increased channel properties (like single-channel conductance) and frequency is associated with synapse unsilencing. With this in mind, neurons lacking AKAP palmitoylation could have issues unsilencing synapses, perhaps due to a problem with AMPAR forward trafficking and/or receptor retention at the synapse following cLTP. With an already enhanced mEPSC frequency, CS cells could have few silent synapses left to be unsilenced in response to cLTP. However, in acute slice, we observed only an increase in mEPSC amplitude and, in fact, a decrease in both mEPSC and sEPSC frequency (Fig 3.5A,B) basally. It is unclear why these differences are present. More experiments will need to be done to understand these differences between slice and culture. One huge consideration with comparing cultures to slice is that the slice preserves the circuitry of the hippocampus and it is possible that the circuit dynamics

are altered in AKAP CS intact animals in a way that could contribute a great deal to mEPSC/sEPSC frequency. Additionally, we previously examined the effect of NASPM on slices following LTP, but to more directly understand the dynamics of CP-AMPARs specifically in slices from WT and CS mice, we can use rectification measurements following the different LTP paradigms to understand if and for how long CP-AMPARs are recruited and if they are eventually replaced by CI-AMPARs as seen in previous studies⁵⁰.

CHAPTER V

CONCLUSIONS AND FUTURE DIRECTIONS

Broad implications

The work in this thesis details several fundamental mechanisms of cellular and molecular synaptic biology. The studies here identify a molecular mechanism for controlling substrate phosphorylation through anchoring of scaffolding molecules near substrates and activity-dependent signals. Further, this thesis work shows a specific requirement for different types of receptors both during basal conditions and activity-dependent plasticity. Unexpectedly, this work also identified multiple LTP mechanisms that differentially recruit receptors for expression. Ultimately, the current study highlights the importance of a single protein's palmitoylation state using a transgenic mouse model that was among the first described to precisely perturb palmitoylation of an individual protein. More broadly, this work identifies a signaling mechanism that has the potential to be important for learning and memory.

Key findings

AKAP CS young mice display an elevated AMPAR-mediated basal transmission, due to the aberrant insertion of CP-AMPA receptors as evidenced by enhanced mEPSCs, increased AMPAR rectification, sensitivity to the CP-AMPA receptor blocker NASPM, and increased synaptic GluA1-AMPA receptors by super-resolution imaging. AKAP79/150 palmitoylation is also important for the protein's subsynaptic organization, with less AKAP in synapses in AKAP CS cultures as shown by STED imaging and biochemical subcellular fractionation. Further, plasticity induced in acute hippocampal slices shows a

divergent response to either CP-AMPA dependent or independent stimuli, failing at CP-AMPA dependent stimuli and competence at CP-AMPA independent stimuli.

AKAP CS cultures show increases in mEPSC amplitude mirroring WT cultures after cLTP, but no increase in frequency, unlike WT cultures. AKAP CS cultures also show increased mEPSC amplitude and frequency and this increase can be blocked with CP-AMPA blockers. It also appears that these elevated levels of CP-AMPA in CS mouse neurons are impacting basal neuronal signaling functions because, unlike WT, CS neurons will scale-up in response to long-term CP-AMPA blockade.

Remaining questions and future directions

AMPA trafficking and the recycling endosome

While the requirement of CP-AMPA involvement during plasticity has been a source of confusion and even controversy, evidence of the delivery of these receptors to the synapse provides a platform to support hypotheses about the input-specificity of long-term synaptic plasticity. An attractive idea is that newly recruited receptors could act as a tag for recently potentiated synapses to support and initiate long-term changes in synapse structure, local protein synthesis and gene expression^{381,382}. Nonetheless, CP-AMPA involvement needs to be studied during different types of plasticity and different behavioral paradigms under specific conditions taking into consideration that age, brain area and stimulus intensity will affect CP-AMPA involvement. It is still unknown what CP-AMPA Ca^{2+} could be providing during both LTP and LTD. In a way, CP-AMPA could act as indicators and influencers of meta-plastic state, acting as a way for synapse specific control of meta-plasticity, like the fine focus on a microscope or the above mentioned tag.

AKAP150 CS knock-in results in differential exocytosis phenotypes than what we previously observed with acute AKAP79 CS overexpression or DHHC2 knockdown in rat cells^{247,248}. While AKAP79 CS showed elevated basal RE exocytosis and a lack of further cLTP-induced exocytosis with overexpression, in AKAP150 CS mice we see normal basal trafficking and enhancement in RE exocytosis with cLTP. This result makes sense if one considers that trafficking and recycling through intracellular pathways is important for many aspects of normal cellular function and chronic manipulations (i.e. knock-in) allow more time for compensation than transient manipulations (i.e. overexpression). Further, AMPARs are not the only endosome residents and the basal synaptic AMPAR enhancement we observe could be independent of this pathway. Alternatively, if AKAP79/150 palmitoylation is involved in proper delivery of AMPARs and when it is unable to be palmitoylated this forward trafficking could be altered via endosomal mechanisms that are specific only for particular cargos (such as AKAP-interacting cargos). We know that AKAP79/150 interacts with a myriad of other synaptic proteins so there could be other proteins that are dysregulated in this mutant in a similar manner. We do not know the entire protein composition of the RE and in future it would be interesting to determine what these proteins are and how they may change when AKAP is unable to be palmitoylated. It would also be interesting to understand if AKAP interacts with different binding partners within different compartments, like the synapse versus at endosomes, and depending on its palmitoylation state. We also do not know if AKAP-anchored enzymes can signal at endosomes to affect the cargo, trafficking or the endosome itself. The RE is an exciting and important intracellular compartment that merits much further study.

The CS frequency dilemma

We found that AKAP CS slices have decreased mEPSC and sEPSC frequency compared to WT. Frequency disruptions, as mentioned above, could hint at a circuit level disruption. If the hippocampal circuit is somehow perturbed in AKAP CS mice, this could initiate homeostatic plasticity mechanisms to compensate for a potential decreased activity level. We preliminarily observed that CS cultures highly depend on CP-AMPA activity, because when CP-AMPA receptors are chronically blocked, there is a scaling-up phenotype. Still to be examined is what happens when AKAP CS cultures are exposed to traditional synaptic scaling conditions. We would expect if there is an overlap between the Hebbian CP-AMPA dependent LTP and homeostatic scaling up then CS cells will either already be scaled-up or will be unable to scale-up via mechanisms controlling CP-AMPA trafficking and synaptic retention. In parallel, future work needs to be done to characterize the intrinsic activity of CA1 neurons and other regions within the hippocampal tri-synaptic loop (CA3 neurons, Dentate cells) in AKAP CS mice. Another interesting experiment would be to study inhibitory transmission to see if AKAP79/150 palmitoylation also influences GABAergic synapses and neuronal excitability/inhibitory balance. This could provide a wealth of additional information about how AKAP palmitoylation affects signaling at the circuit level.

Age-dependent and behavioral outcomes of AKAP palmitoylation disruption

Much of the analysis of hippocampal-relevant behaviors is done in older animals (8 weeks+). The experiments in Chapter III and IV of this thesis describe phenotypes in cultures or young mice (2-3 weeks old). To understand the effect of AKAP palmitoylation on hippocampal behaviors, it will need to be determined if the CP-

AMPA phenotype seen here in younger animals is maintained or changes with age. The ultimate goal is to administer a battery of hippocampal-dependent behavioral tasks on AKAP CS mice to determine if AKAP palmitoylation is important for learning and memory behaviors *in vivo*.

Intact LTD: AKAP's palmitoylation state and signaling mechanisms during LTD

LTD is intact in CS mice but what is the mechanism of this LTD? CaMKII is important in both LTP and LTD³⁸³. Recently, our laboratory and others showed that LTD initiates AKAP79/150 depalmitoylation and subsequent removal from spines through a CaMKII mediated mechanism that promotes its depalmitoylation²⁶⁵. While we also know that AKAP CS is more easily removed from the membrane and spines when its depalmitoylated^{247,264} and LTD is still intact in AKAP CS mice, it is unknown if the mechanism of LTD in CS differs from WT. Future work will need to be done to determine if: this CaMKII mechanism is still intact, if the basally enhanced levels of CP-AMPARs are removed with LTD stimulation, if a transient population of CP-AMPARs are recruited and/or required for LTD, and if this basal enhancement also alters meta-plasticity with a bias toward LTD.

Spatial and temporal control of AKAP palmitoylation

While this study examines the effect of blocking all AKAP150 palmitoylation from birth, it limits the conclusions that can be drawn about dynamic AKAP palmitoylation-depalmitoylation cycling. It will be important to study how AKAP depalmitoylation compares to the current approach of blocking palmitoylation through mutation. We are currently technically limited in our ability to study this dynamic process due to no specific pharmacological treatments that target individual protein palmitoylation. It would

be advantageous to have a system to selectively ablate palmitoylation of a particular protein, ideally with high spatial and temporal control. Certainly, it has become vitally important to understand the flip side of palmitoylation of AKAP79/150; the depalmitoylating PPT enzyme for AKAP still needs to be discovered. In this way, understanding the dynamic nature of AKAP palmitoylation will be more complete.

This knock-in mutation approach was useful in examining the effect of altering all nodes of palmitoylation-targeting of AKAP. As a consequence this method limited the ability to parse apart contributions of AKAP palmitoylation to each individual signaling node, such as at the core PSD or at REs. In the future, the contribution of palmitoylated AKAP to these two subsynaptic locations could be studied using recruitment techniques (such as with a light-induced dimerization system) of AKAP either palmitoylation competent or incompetent to either the PSD or to REs. A technique such as this can help answer questions about the location dependence of signaling to specific phenotypic observations in AKAP CS neurons (i.e. can recruiting palmitoylation competent AKAP to REs or the core PSD during CP-AMPA dependent LTP rescue the LTP? Or does recruiting palmitoylation competent AKAP to the core PSD provide enough bi-directional control by PKA and CaN to exclude CP-AMPA receptors basally to rescue the increased CP-AMPA basal phenotype?) As for the palmitoylation field, further advancement in palmitoylation detection will be required to directly visualize palmitoylation *in situ*. This will not only help with monitoring in real time the palmitoylation state of AKAP79/150, but also with any other palmitoylated protein and even multiple proteins at once. It would be ideal to have an optical reporter of AKAP79/150 palmitoylation so we can visualize the dynamic palmitoylation state of this

key scaffold protein in living cells, tissues or living organisms in response to a variety of manipulations.

REFERENCES

1. Purkey, A. M. *et al.* AKAP150 Palmitoylation Regulates Synaptic Incorporation of Ca²⁺-Permeable AMPA Receptors to Control LTP. *Cell Reports* **25**, 974–987.e4 (2018).
2. Scoville, W. B. & Milner, B. Loss of recent memory after bilateral hippocampal lesions. *J. Neurol. Neurosurg. Psychiatry* **20**, 11–21 (1957).
3. Mayford, M., Siegelbaum, S. A. & Kandel, E. R. Synapses and memory storage. *Cold Spring Harbor Perspectives in Biology* **4**, (2012).
4. Nicoll, R. A. A Brief History of Long-Term Potentiation. *Neuron* **93**, 281–290 (2017).
5. Watanabe, S. *et al.* Ultrafast endocytosis at mouse hippocampal synapses. *Nature* **504**, 242–247 (2013).
6. Park, H., Li, Y. & Tsien, R. W. Influence of synaptic vesicle position on release probability and exocytotic fusion mode. *Science* **335**, 1362–1366 (2012).
7. Tang, A.-H. *et al.* A trans-synaptic nanocolumn aligns neurotransmitter release to receptors. *Nature* **536**, 210–214 (2016).
8. Maschi, D. & Klyachko, V. A. Spatiotemporal Regulation of Synaptic Vesicle Fusion Sites in Central Synapses. *Neuron* **94**, 65–73.e3 (2017).
9. Südhof, T. C. The presynaptic active zone. *Neuron* **75**, 11–25 (2012).
10. Biederer, T., Kaeser, P. S. & Blanpied, T. A. Transcellular Nanoalignment of Synaptic Function. *Neuron* **96**, 680–696 (2017).
11. Zuber, B., Nikonenko, I., Klauser, P., Müller, D. & Dubochet, J. The mammalian central nervous synaptic cleft contains a high density of periodically organized complexes. *Proceedings of the National Academy of Sciences* **102**, 19192–19197 (2005).
12. Lucić, V., Yang, T., Schweikert, G., Förster, F. & Baumeister, W. Morphological characterization of molecular complexes present in the synaptic cleft. *Structure* **13**, 423–434 (2005).
13. Sheng, M. & Hoogenraad, C. C. The Postsynaptic Architecture of Excitatory Synapses: A More Quantitative View. *Annu. Rev. Biochem.* **76**, 823–847 (2007).

14. Chen, X. *et al.* Mass of the postsynaptic density and enumeration of three key molecules. *Proceedings of the National Academy of Sciences* **102**, 11551–11556 (2005).
15. Traynelis, S. F. *et al.* Glutamate Receptor Ion Channels: Structure, Regulation, and Function. *Pharmacological Reviews* **62**, 405–496 (2010).
16. Lu, W. *et al.* Subunit composition of synaptic AMPA receptors revealed by a single-cell genetic approach. *Neuron* **62**, 254–268 (2009).
17. Lisman, J. E., Raghavachari, S. & Tsien, R. W. The sequence of events that underlie quantal transmission at central glutamatergic synapses. *Nat Rev Neurosci* **8**, 597–609 (2007).
18. Garcia-Nafria, J., Herguedas, B., Watson, J. F. & Greger, I. H. The dynamic AMPA receptor extracellular region: a platform for synaptic protein interactions. *The Journal of Physiology* **594**, 5449–5458 (2016).
19. Meyerson, J. R. *et al.* Structural mechanism of glutamate receptor activation and desensitization. *Nature* **514**, 328–334 (2014).
20. Shepherd, J. D. & Huganir, R. L. The Cell Biology of Synaptic Plasticity: AMPA Receptor Trafficking. *Annu. Rev. Cell Dev. Biol.* **23**, 613–643 (2007).
21. Benke, T. & Traynelis, S. F. AMPA-Type Glutamate Receptor Conductance Changes and Plasticity: Still a Lot of Noise. *Neurochem Res* (2018). doi:10.1007/s11064-018-2491-1
22. Henley, J. M. & Wilkinson, K. A. Synaptic AMPA receptor composition in development, plasticity and disease. *Nat Rev Neurosci* **17**, 337–350 (2016).
23. Higuchi, M. *et al.* Point mutation in an AMPA receptor gene rescues lethality in mice deficient in the RNA-editing enzyme ADAR2. *Nature* **406**, 78–81 (2000).
24. Isaac, J. T. R., Ashby, M. C. & McBain, C. J. The role of the GluR2 subunit in AMPA receptor function and synaptic plasticity. *Neuron* **54**, 859–871 (2007).
25. Blaschke, M. *et al.* A single amino acid determines the subunit-specific spider toxin block of alpha-amino-3-hydroxy-5-methylisoxazole-4-propionate/kainate receptor channels. *Proceedings of the National Academy of Sciences* **90**, 6528–6532 (1993).
26. Bowie, D. & Mayer, M. L. Inward rectification of both AMPA and kainate subtype glutamate receptors generated by polyamine-mediated ion channel block. *Neuron* **15**, 453–462 (1995).

27. Herlitze, S. *et al.* Argiotoxin detects molecular differences in AMPA receptor channels. *Neuron* **10**, 1131–1140 (1993).
28. Tóth, K. & McBain, C. J. Afferent-specific innervation of two distinct AMPA receptor subtypes on single hippocampal interneurons. *Nature Neuroscience* **1**, 572–578 (1998).
29. Washburn, M. S. & Dingledine, R. Block of alpha-amino-3-hydroxy-5-methyl-4-isoxazolepropionic acid (AMPA) receptors by polyamines and polyamine toxins. *J. Pharmacol. Exp. Ther.* **278**, 669–678 (1996).
30. Washburn, M. S., Numberger, M., Zhang, S. & Dingledine, R. Differential dependence on GluR2 expression of three characteristic features of AMPA receptors. *The Journal of Neuroscience* **17**, 9393–9406 (1997).
31. Koike, M., Iino, M. & Ozawa, S. Blocking effect of 1-naphthyl acetyl spermine on Ca²⁺-permeable AMPA receptors in cultured rat hippocampal neurons. *Neurosci. Res.* **29**, 27–36 (1997).
32. Magazanik, L. G. *et al.* Block of open channels of recombinant AMPA receptors and native AMPA/kainate receptors by adamantane derivatives. *The Journal of Physiology* **505 (Pt 3)**, 655–663 (1997).
33. Kumar, S. S., Bacci, A., Kharazia, V. & Huguenard, J. R. A developmental switch of AMPA receptor subunits in neocortical pyramidal neurons. *Journal of Neuroscience* **22**, 3005–3015 (2002).
34. Liu, S. Q. & Cull-Candy, S. G. Synaptic activity at calcium-permeable AMPA receptors induces a switch in receptor subtype. *Nature* **405**, 454–458 (2000).
35. Terashima, A. *et al.* An essential role for PICK1 in NMDA receptor-dependent bidirectional synaptic plasticity. *Neuron* **57**, 872–882 (2008).
36. Plant, K. *et al.* Transient incorporation of native GluR2-lacking AMPA receptors during hippocampal long-term potentiation. *Nature Neuroscience* **9**, 602–604 (2006).
37. Cull-Candy, S., Kelly, L. & Farrant, M. Regulation of Ca²⁺-permeable AMPA receptors: synaptic plasticity and beyond. *Current Opinion in Neurobiology* **16**, 288–297 (2006).
38. Liu, S. J. & Zukin, R. S. Ca²⁺-permeable AMPA receptors in synaptic plasticity and neuronal death. *Trends in Neurosciences* **30**, 126–134 (2007).
39. Lüscher, B., Fuchs, T. & Kilpatrick, C. L. GABA_A receptor trafficking-mediated plasticity of inhibitory synapses. *Neuron* **70**, 385–409 (2011).

40. Zhu, J. J., Esteban, J. A., Hayashi, Y. & Malinow, R. Postnatal synaptic potentiation: delivery of GluR4-containing AMPA receptors by spontaneous activity. *Nature Neuroscience* **3**, 1098–1106 (2000).
41. Kennedy, M. J. & Ehlers, M. D. Organelles and trafficking machinery for postsynaptic plasticity. *Annu. Rev. Neurosci.* **29**, 325–362 (2006).
42. Mattison, H. A. *et al.* Evidence of calcium-permeable AMPA receptors in dendritic spines of CA1 pyramidal neurons. *Journal of Neurophysiology* **112**, 263–275 (2014).
43. Brorson, J. R., Li, D. & Suzuki, T. Selective expression of heteromeric AMPA receptors driven by flip-flop differences. *Journal of Neuroscience* **24**, 3461–3470 (2004).
44. Greger, I. H., Khatri, L., Kong, X. & Ziff, E. B. AMPA receptor tetramerization is mediated by Q/R editing. *Neuron* **40**, 763–774 (2003).
45. Mansour, M., Nagarajan, N., Nehring, R. B., Clements, J. D. & Rosenmund, C. Heteromeric AMPA receptors assemble with a preferred subunit stoichiometry and spatial arrangement. *Neuron* **32**, 841–853 (2001).
46. Rossmann, M. *et al.* Subunit-selective N-terminal domain associations organize the formation of AMPA receptor heteromers. *EMBO J.* **30**, 959–971 (2011).
47. Greger, I. H., Khatri, L. & Ziff, E. B. RNA editing at arg607 controls AMPA receptor exit from the endoplasmic reticulum. *Neuron* **34**, 759–772 (2002).
48. Greger, I. H. & Esteban, J. A. AMPA receptor biogenesis and trafficking. *Current Opinion in Neurobiology* **17**, 289–297 (2007).
49. Mah, S. J., Cornell, E., Mitchell, N. A. & Fleck, M. W. Glutamate receptor trafficking: endoplasmic reticulum quality control involves ligand binding and receptor function. *Journal of Neuroscience* **25**, 2215–2225 (2005).
50. Shi, S., Hayashi, Y., Esteban, J. A. & Malinow, R. Subunit-specific rules governing AMPA receptor trafficking to synapses in hippocampal pyramidal neurons. *Cell* **105**, 331–343 (2001).
51. Passafaro, M., Piëch, V. & Sheng, M. Subunit-specific temporal and spatial patterns of AMPA receptor exocytosis in hippocampal neurons. *Nature Neuroscience* **4**, 917–926 (2001).
52. Henley, J. M., Barker, E. A. & Glebov, O. O. Routes, destinations and delays: recent advances in AMPA receptor trafficking. *Trends in Neurosciences* **34**, 258–268 (2011).

53. Sheng, M. & Kim, E. The postsynaptic organization of synapses. *Cold Spring Harbor Perspectives in Biology* **3**, (2011).
54. Leonard, A. S., Davare, M. A., Horne, M. C., Garner, C. C. & Hell, J. W. SAP97 is associated with the alpha-amino-3-hydroxy-5-methylisoxazole-4-propionic acid receptor GluR1 subunit. *J. Biol. Chem.* **273**, 19518–19524 (1998).
55. Sheng, M. & Sala, C. PDZ domains and the organization of supramolecular complexes. *Annu. Rev. Neurosci.* **24**, 1–29 (2001).
56. Xu, W. PSD-95-like membrane associated guanylate kinases (PSD-MAGUKs) and synaptic plasticity. *Current Opinion in Neurobiology* **21**, 306–312 (2011).
57. Zheng, C.-Y., Seabold, G. K., Horak, M. & Petralia, R. S. MAGUKs, Synaptic Development, and Synaptic Plasticity. *The Neuroscientist* **17**, 493–512 (2011).
58. Beique, J.-C. & Andrade, R. PSD-95 regulates synaptic transmission and plasticity in rat cerebral cortex. *The Journal of Physiology* **546**, 859–867 (2003).
59. El-Husseini, A. E., Schnell, E., Chetkovich, D. M., Nicoll, R. A. & Brecht, D. S. PSD-95 involvement in maturation of excitatory synapses. *Science* **290**, 1364–1368 (2000).
60. Lu, W. & Roche, K. W. Posttranslational regulation of AMPA receptor trafficking and function. *Current Opinion in Neurobiology* **22**, 470–479 (2012).
61. Diering, G. H. & Huganir, R. L. The AMPA Receptor Code of Synaptic Plasticity. *Neuron* **100**, 314–329 (2018).
62. Banke, T. G. *et al.* Control of GluR1 AMPA receptor function by cAMP-dependent protein kinase. *Journal of Neuroscience* **20**, 89–102 (2000).
63. Diering, G. H., Heo, S., Hussain, N. K., Liu, B. & Huganir, R. L. Extensive phosphorylation of AMPA receptors in neurons. *Proc. Natl. Acad. Sci. U.S.A.* **113**, E4920–7 (2016).
64. Dong, H. *et al.* GRIP: a synaptic PDZ domain-containing protein that interacts with AMPA receptors. *Nature* **386**, 279–284 (1997).
65. Dong, H. *et al.* Characterization of the glutamate receptor-interacting proteins GRIP1 and GRIP2. *Journal of Neuroscience* **19**, 6930–6941 (1999).
66. Srivastava, S. & Ziff, E. B. ABP: a novel AMPA receptor binding protein. *Ann. N. Y. Acad. Sci.* **868**, 561–564 (1999).

67. Xia, J., Chung, H. J., Wihler, C., Huganir, R. L. & Linden, D. J. Cerebellar long-term depression requires PKC-regulated interactions between GluR2/3 and PDZ domain-containing proteins. *Neuron* **28**, 499–510 (2000).
68. Dev, K. K. *et al.* PICK1 interacts with and regulates PKC phosphorylation of mGLUR7. *Journal of Neuroscience* **20**, 7252–7257 (2000).
69. Lüscher, C. *et al.* Role of AMPA receptor cycling in synaptic transmission and plasticity. *Neuron* **24**, 649–658 (1999).
70. Lee, S. H., Liu, L., Wang, Y. T. & Sheng, M. Clathrin adaptor AP2 and NSF interact with overlapping sites of GluR2 and play distinct roles in AMPA receptor trafficking and hippocampal LTD. *Neuron* **36**, 661–674 (2002).
71. Lüthi, A. *et al.* Hippocampal LTD expression involves a pool of AMPARs regulated by the NSF-GluR2 interaction. *Neuron* **24**, 389–399 (1999).
72. Nishimune, A. *et al.* NSF binding to GluR2 regulates synaptic transmission. *Neuron* **21**, 87–97 (1998).
73. Noël, J. *et al.* Surface expression of AMPA receptors in hippocampal neurons is regulated by an NSF-dependent mechanism. *Neuron* **23**, 365–376 (1999).
74. Song, I. *et al.* Interaction of the N-ethylmaleimide-sensitive factor with AMPA receptors. *Neuron* **21**, 393–400 (1998).
75. Osten, P. *et al.* The AMPA receptor GluR2 C terminus can mediate a reversible, ATP-dependent interaction with NSF and alpha- and beta-SNAPs. *Neuron* **21**, 99–110 (1998).
76. Chung, H. J., Xia, J., Scannevin, R. H., Zhang, X. & Huganir, R. L. Phosphorylation of the AMPA receptor subunit GluR2 differentially regulates its interaction with PDZ domain-containing proteins. *Journal of Neuroscience* **20**, 7258–7267 (2000).
77. Matsuda, S., Mikawa, S. & Hirai, H. Phosphorylation of serine-880 in GluR2 by protein kinase C prevents its C terminus from binding with glutamate receptor-interacting protein. *Journal of Neurochemistry* **73**, 1765–1768 (1999).
78. MacGillavry, H. D., Song, Y., Raghavachari, S. & Blanpied, T. A. Nanoscale scaffolding domains within the postsynaptic density concentrate synaptic AMPA receptors. *Neuron* **78**, 615–622 (2013).
79. Nair, D. *et al.* Super-resolution imaging reveals that AMPA receptors inside synapses are dynamically organized in nanodomains regulated by PSD95. *Journal of Neuroscience* **33**, 13204–13224 (2013).

80. Tarusawa, E. *et al.* Input-specific intrasynaptic arrangements of ionotropic glutamate receptors and their impact on postsynaptic responses. *Journal of Neuroscience* **29**, 12896–12908 (2009).
81. Lisman, J. Glutamatergic synapses are structurally and biochemically complex because of multiple plasticity processes: long-term potentiation, long-term depression, short-term potentiation and scaling. *Philos. Trans. R. Soc. Lond., B, Biol. Sci.* **372**, (2017).
82. Chen, X. *et al.* Organization of the Core Structure of the Postsynaptic Density. *Proc. Natl. Acad. Sci. U.S.A.* **105**, 4453–4458 (2008).
83. Broadhead, M. J. *et al.* PSD95 nanoclusters are postsynaptic building blocks in hippocampus circuits. *Sci Rep* **6**, 24626 (2016).
84. Chen, X. *et al.* PSD-95 is required to sustain the molecular organization of the postsynaptic density. *Journal of Neuroscience* **31**, 6329–6338 (2011).
85. Heine, M. *et al.* Surface mobility of postsynaptic AMPARs tunes synaptic transmission. *Science* **320**, 201–205 (2008).
86. Adesnik, H., Nicoll, R. A. & England, P. M. Photoinactivation of native AMPA receptors reveals their real-time trafficking. *Neuron* **48**, 977–985 (2005).
87. Ehlers, M. D., Heine, M., Groc, L., Lee, M.-C. & Choquet, D. Diffusional Trapping of GluR1 AMPA Receptors by Input-Specific Synaptic Activity. *Neuron* **54**, 447–460 (2007).
88. Kerr, J. M. & Blanpied, T. A. Subsynaptic AMPA receptor distribution is acutely regulated by actin-driven reorganization of the postsynaptic density. *Journal of Neuroscience* **32**, 658–673 (2012).
89. Opazo, P., Sainlos, M. & Choquet, D. Regulation of AMPA receptor surface diffusion by PSD-95 slots. *Current Opinion in Neurobiology* **22**, 453–460 (2012).
90. Santamaria, F., Gonzalez, J., Augustine, G. J. & Raghavachari, S. Quantifying the effects of elastic collisions and non-covalent binding on glutamate receptor trafficking in the post-synaptic density. *PLoS Comput. Biol.* **6**, e1000780 (2010).
91. Li, T. P. & Blanpied, T. A. Control of Transmembrane Protein Diffusion within the Postsynaptic Density Assessed by Simultaneous Single-Molecule Tracking and Localization Microscopy. *Front Synaptic Neurosci* **8**, 19 (2016).
92. Greger, I. H., Watson, J. F. & Cull-Candy, S. G. Structural and Functional Architecture of AMPA-Type Glutamate Receptors and Their Auxiliary Proteins. *Neuron* **94**, 713–730 (2017).

93. Kato, A. S. *et al.* Hippocampal AMPA receptor gating controlled by both TARP and cornichon proteins. *Neuron* **68**, 1082–1096 (2010).
94. Sumioka, A., Yan, D. & Tomita, S. TARP phosphorylation regulates synaptic AMPA receptors through lipid bilayers. *Neuron* **66**, 755–767 (2010).
95. Tomita, S., Stein, V., Stocker, T. J., Nicoll, R. A. & Brecht, D. S. Bidirectional synaptic plasticity regulated by phosphorylation of stargazin-like TARPs. *Neuron* **45**, 269–277 (2005).
96. Gray, J. A. *et al.* Distinct modes of AMPA receptor suppression at developing synapses by GluN2A and GluN2B: single-cell NMDA receptor subunit deletion in vivo. *Neuron* **71**, 1085–1101 (2011).
97. Hebb, D. O. *The Organization of Behavior*. (Wiley, 1949).
98. Bliss, T. V. & Lomo, T. Long-lasting potentiation of synaptic transmission in the dentate area of the anaesthetized rabbit following stimulation of the perforant path. *The Journal of Physiology* **232**, 331–356 (1973).
99. Huganir, R. L. & Nicoll, R. A. AMPARs and synaptic plasticity: the last 25 years. *Neuron* **80**, 704–717 (2013).
100. Kessels, H. W. & Malinow, R. Synaptic AMPA receptor plasticity and behavior. *Neuron* **61**, 340–350 (2009).
101. Opazo, P. & Choquet, D. A three-step model for the synaptic recruitment of AMPA receptors. *Mol. Cell. Neurosci.* **46**, 1–8 (2011).
102. Newpher, T. M. & Ehlers, M. D. Glutamate Receptor Dynamics in Dendritic Microdomains. *Neuron* **58**, 472–497 (2008).
103. Lu, Y. *et al.* Age-dependent requirement of AKAP150-anchored PKA and GluR2-lacking AMPA receptors in LTP. *EMBO J.* **26**, 4879–4890 (2007).
104. Sanderson, J. L., Gorski, J. A. & Dell'Acqua, M. L. NMDA Receptor-Dependent LTD Requires Transient Synaptic Incorporation of Ca²⁺-Permeable AMPARs Mediated by AKAP150-Anchored PKA and Calcineurin. *Neuron* **89**, 1000–1015 (2016).
105. Clem, R. L. & Barth, A. Pathway-specific trafficking of native AMPARs by in vivo experience. *Neuron* **49**, 663–670 (2006).
106. Ju, W. *et al.* Activity-dependent regulation of dendritic synthesis and trafficking of AMPA receptors. *Nature Neuroscience* **7**, 244–253 (2004).

107. Thiagarajan, T. C., Lindskog, M. & Tsien, R. W. Adaptation to synaptic inactivity in hippocampal neurons. *Neuron* **47**, 725–737 (2005).
108. Sutton, M. A. *et al.* Miniature neurotransmission stabilizes synaptic function via tonic suppression of local dendritic protein synthesis. *Cell* **125**, 785–799 (2006).
109. Kauer, J. A., Malenka, R. C. & Nicoll, R. A. A persistent postsynaptic modification mediates long-term potentiation in the hippocampus. *Neuron* **1**, 911–917 (1988).
110. Muller, D., Joly, M. & Lynch, G. Contributions of quisqualate and NMDA receptors to the induction and expression of LTP. *Science* **242**, 1694–1697 (1988).
111. Carter, A. G. & Regehr, W. G. Quantal events shape cerebellar interneuron firing. *Nature Neuroscience* **5**, 1309–1318 (2002).
112. Geiger, J. R., Lübke, J., Roth, A., Frotscher, M. & Jonas, P. Submillisecond AMPA receptor-mediated signaling at a principal neuron-interneuron synapse. *Neuron* **18**, 1009–1023 (1997).
113. Walker, H. C., Lawrence, J. J. & McBain, C. J. Activation of kinetically distinct synaptic conductances on inhibitory interneurons by electrotonically overlapping afferents. *Neuron* **35**, 161–171 (2002).
114. Geiger, J. R. *et al.* Relative abundance of subunit mRNAs determines gating and Ca²⁺ permeability of AMPA receptors in principal neurons and interneurons in rat CNS. *Neuron* **15**, 193–204 (1995).
115. Swanson, G. T., Kamboj, S. K. & Cull-Candy, S. G. Single-channel properties of recombinant AMPA receptors depend on RNA editing, splice variation, and subunit composition. *The Journal of Neuroscience* **17**, 58–69 (1997).
116. Rozov, A. & Burnashev, N. Polyamine-dependent facilitation of postsynaptic AMPA receptors counteracts paired-pulse depression. *Nature* **401**, 594–598 (1999).
117. Rozov, A., Zilberter, Y., Wollmuth, L. P. & Burnashev, N. Facilitation of currents through rat Ca²⁺-permeable AMPA receptor channels by activity-dependent relief from polyamine block. *The Journal of Physiology* **511 (Pt 2)**, 361–377 (1998).
118. Tóth, K., Soares, G., Lawrence, J. J., Philips-Tansey, E. & McBain, C. J. Differential mechanisms of transmission at three types of mossy fiber synapse. *Journal of Neuroscience* **20**, 8279–8289 (2000).

119. Kamboj, S. K., Swanson, G. T. & Cull-Candy, S. G. Intracellular spermine confers rectification on rat calcium-permeable AMPA and kainate receptors. *The Journal of Physiology* **486 (Pt 2)**, 297–303 (1995).
120. Koh, D. S., Burnashev, N. & Jonas, P. Block of native Ca(2+)-permeable AMPA receptors in rat brain by intracellular polyamines generates double rectification. *The Journal of Physiology* **486 (Pt 2)**, 305–312 (1995).
121. Mahanty, N. K. & Sah, P. Calcium-permeable AMPA receptors mediate long-term potentiation in interneurons in the amygdala. *Nature* **394**, 683–687 (1998).
122. Yang, Y., Wang, X.-B. & Zhou, Q. Perisynaptic GluR2-lacking AMPA receptors control the reversibility of synaptic and spines modifications. *Proc. Natl. Acad. Sci. U.S.A.* **107**, 11999–12004 (2010).
123. Jaafari, N., Henley, J. M. & Hanley, J. G. PICK1 mediates transient synaptic expression of GluA2-lacking AMPA receptors during glycine-induced AMPA receptor trafficking. *Journal of Neuroscience* **32**, 11618–11630 (2012).
124. Rozov, A., Sprengel, R. & Seeburg, P. H. GluA2-lacking AMPA receptors in hippocampal CA1 cell synapses: evidence from gene-targeted mice. *Front Mol Neurosci* **5**, 22 (2012).
125. Granger, A. J., Shi, Y., Lu, W., Cerpas, M. & Nicoll, R. A. LTP requires a reserve pool of glutamate receptors independent of subunit type. *Nature* **493**, 495–500 (2013).
126. Renner, M. C. *et al.* Synaptic plasticity through activation of GluA3-containing AMPA-receptors. *eLife* **6**, (2017).
127. Stubblefield, E. A. & Benke, T. A. Distinct AMPA-type glutamatergic synapses in developing rat CA1 hippocampus. *Journal of Neurophysiology* **104**, 1899–1912 (2010).
128. Guire, E. S., Oh, M. C., Soderling, T. R. & Derkach, V. A. Recruitment of calcium-permeable AMPA receptors during synaptic potentiation is regulated by CaM-kinase I. *Journal of Neuroscience* **28**, 6000–6009 (2008).
129. Adesnik, H. & Nicoll, R. A. Conservation of glutamate receptor 2-containing AMPA receptors during long-term potentiation. *Journal of Neuroscience* **27**, 4598–4602 (2007).
130. Pickard, L., Noël, J., Henley, J. M., Collingridge, G. L. & Molnár, E. Developmental changes in synaptic AMPA and NMDA receptor distribution and AMPA receptor subunit composition in living hippocampal neurons. *Journal of Neuroscience* **20**, 7922–7931 (2000).

131. Gray, E. E., Fink, A. E., Sariñana, J., Vissel, B. & O'Dell, T. J. Long-term potentiation in the hippocampal CA1 region does not require insertion and activation of GluR2-lacking AMPA receptors. *Journal of Neurophysiology* **98**, 2488–2492 (2007).
132. Park, P. *et al.* Calcium-Permeable AMPA Receptors Mediate the Induction of the Protein Kinase A-Dependent Component of Long-Term Potentiation in the Hippocampus. *Journal of Neuroscience* **36**, 622–631 (2016).
133. Zhou, Z. *et al.* The C-terminal tails of endogenous GluA1 and GluA2 differentially contribute to hippocampal synaptic plasticity and learning. *Nature Neuroscience* **21**, 50–62 (2018).
134. Petrini, E. M. *et al.* Endocytic trafficking and recycling maintain a pool of mobile surface AMPA receptors required for synaptic potentiation. *Neuron* **63**, 92–105 (2009).
135. Sanes, J. R. & Lichtman, J. W. Development of the vertebrate neuromuscular junction. *Annu. Rev. Neurosci.* **22**, 389–442 (1999).
136. Gomperts, S. N., Rao, A., Craig, A. M., Malenka, R. C. & Nicoll, R. A. Postsynaptically silent synapses in single neuron cultures. *Neuron* **21**, 1443–1451 (1998).
137. Liao, D., Scannevin, R. H. & Huganir, R. Activation of silent synapses by rapid activity-dependent synaptic recruitment of AMPA receptors. *Journal of Neuroscience* **21**, 6008–6017 (2001).
138. Liao, D., Zhang, X., O'Brien, R., Ehlers, M. D. & Huganir, R. L. Regulation of morphological postsynaptic silent synapses in developing hippocampal neurons. *Nature Neuroscience* **2**, 37–43 (1999).
139. Takumi, Y., Ramírez-León, V., Laake, P., Rinvik, E. & Ottersen, O. P. Different modes of expression of AMPA and NMDA receptors in hippocampal synapses. *Nature Neuroscience* **2**, 618–624 (1999).
140. Lledo, P. Postsynaptic Membrane Fusion and Long-Term Potentiation. *Science* **279**, 399–403 (1998).
141. Lu, W. *et al.* Activation of synaptic NMDA receptors induces membrane insertion of new AMPA receptors and LTP in cultured hippocampal neurons. *Neuron* **29**, 243–254 (2001).
142. Nicoll, R. A. & Roche, K. W. Long-term potentiation: peeling the onion. *Neuropharmacology* **74**, 18–22 (2013).

143. Kennedy, M. J., Davison, I. G., Robinson, C. G. & Ehlers, M. D. Syntaxin-4 defines a domain for activity-dependent exocytosis in dendritic spines. *Cell* **141**, 524–535 (2010).
144. Hiester, B. G. *et al.* L-Type Voltage-Gated Ca²⁺ Channels Regulate Synaptic-Activity-Triggered Recycling Endosome Fusion in Neuronal Dendrites. *CellReports* **21**, 2134–2146 (2017).
145. Kelly, E. E., Horgan, C. P., McCaffrey, M. W. & Young, P. The role of endosomal-recycling in long-term potentiation. *Cell. Mol. Life Sci.* **68**, 185–194 (2011).
146. Jurado, S. *et al.* LTP requires a unique postsynaptic SNARE fusion machinery. *Neuron* **77**, 542–558 (2013).
147. Ahmad, M. *et al.* Postsynaptic complexin controls AMPA receptor exocytosis during LTP. *Neuron* **73**, 260–267 (2012).
148. Park, M., Penick, E. C., Edwards, J. G., Kauer, J. A. & Ehlers, M. D. Recycling endosomes supply AMPA receptors for LTP. *Science* **305**, 1972–1975 (2004).
149. Park, M. *et al.* Plasticity-Induced Growth of Dendritic Spines by Exocytic Trafficking from Recycling Endosomes. *Neuron* **52**, 817–830 (2006).
150. Kessels, H. W., Kopec, C. D., Klein, M. E. & Malinow, R. Roles of stargazin and phosphorylation in the control of AMPA receptor subcellular distribution. *Nature Neuroscience* **12**, 888–896 (2009).
151. McCormack, S. G., Stornetta, R. L. & Zhu, J. J. Synaptic AMPA Receptor Exchange Maintains Bidirectional Plasticity. *Neuron* **50**, 75–88 (2006).
152. Borgdorff, A. J. & Choquet, D. Regulation of AMPA receptor lateral movements. *Nature* **417**, 649–653 (2002).
153. Makino, H. & Malinow, R. AMPA receptor incorporation into synapses during LTP: the role of lateral movement and exocytosis. *Neuron* **64**, 381–390 (2009).
154. Patterson, M. A., Szatmari, E. M., Yasuda, R. & Huganir, R. L. AMPA receptors are exocytosed in stimulated spines and adjacent dendrites in a Ras-ERK-dependent manner during long-term potentiation. *Proc. Natl. Acad. Sci. U.S.A.* **107**, 15951–15956 (2010).
155. Penn, A. C. *et al.* Hippocampal LTP and contextual learning require surface diffusion of AMPA receptors. *Nature* **549**, 384–388 (2017).

156. Malenka, R. C. *et al.* An essential role for postsynaptic calmodulin and protein kinase activity in long-term potentiation. *Nature* **340**, 554–557 (1989).
157. Malinow, R., Schulman, H. & Tsien, R. W. Inhibition of postsynaptic PKC or CaMKII blocks induction but not expression of LTP. *Science* **245**, 862–866 (1989).
158. Wyllie, D. J. & Nicoll, R. A. A role for protein kinases and phosphatases in the Ca(2+)-induced enhancement of hippocampal AMPA receptor-mediated synaptic responses. *Neuron* **13**, 635–643 (1994).
159. Soderling, T. R. Calcium/calmodulin-dependent protein kinase II: role in learning and memory. *Mol. Cell. Biochem.* **127-128**, 93–101 (1993).
160. Swope, S. L., Moss, S. J., Blackstone, C. D. & Huganir, R. L. Phosphorylation of ligand-gated ion channels: a possible mode of synaptic plasticity. *FASEB J.* **6**, 2514–2523 (1992).
161. Barria, A., Muller, D., Derkach, V., Griffith, L. C. & Soderling, T. R. Regulatory phosphorylation of AMPA-type glutamate receptors by CaM-KII during long-term potentiation. *Science* **276**, 2042–2045 (1997).
162. Kameyama, K., Lee, H.-K., Bear, M. F. & Huganir, R. L. Involvement of a postsynaptic protein kinase A substrate in the expression of homosynaptic long-term depression. *Neuron* **21**, 1163–1175 (1998).
163. Lee, H. K., Kameyama, K., Huganir, R. L. & Bear, M. F. NMDA induces long-term synaptic depression and dephosphorylation of the GluR1 subunit of AMPA receptors in hippocampus. *Neuron* **21**, 1151–1162 (1998).
164. Lee, H. K., Barbarosie, M., Kameyama, K., Bear, M. F. & Huganir, R. L. Regulation of distinct AMPA receptor phosphorylation sites during bidirectional synaptic plasticity. *Nature* **405**, 955–959 (2000).
165. Kristensen, A. S. *et al.* Mechanism of Ca²⁺/calmodulin-dependent kinase II regulation of AMPA receptor gating. *Nature Neuroscience* **14**, 727–735 (2011).
166. Oh, M. C., Derkach, V. A., Guire, E. S. & Soderling, T. R. Extrasynaptic membrane trafficking regulated by GluR1 serine 845 phosphorylation primes AMPA receptors for long-term potentiation. *J. Biol. Chem.* **281**, 752–758 (2006).
167. Yang, Y., Wang, X.-B., Frerking, M. & Zhou, Q. Delivery of AMPA receptors to perisynaptic sites precedes the full expression of long-term potentiation. *Proc. Natl. Acad. Sci. U.S.A.* **105**, 11388–11393 (2008).

168. Man, H.-Y., Sekine-Aizawa, Y. & Huganir, R. L. Regulation of {alpha}-amino-3-hydroxy-5-methyl-4-isoxazolepropionic acid receptor trafficking through PKA phosphorylation of the Glu receptor 1 subunit. *Proceedings of the National Academy of Sciences* **104**, 3579–3584 (2007).
169. He, K. *et al.* Stabilization of Ca²⁺-permeable AMPA receptors at perisynaptic sites by GluR1-S845 phosphorylation. *Proc. Natl. Acad. Sci. U.S.A.* **106**, 20033–20038 (2009).
170. Esteban, J. A. AMPA receptor trafficking: a road map for synaptic plasticity. *Mol. Interv.* **3**, 375–385 (2003).
171. Lee, H.-K. *et al.* Phosphorylation of the AMPA receptor GluR1 subunit is required for synaptic plasticity and retention of spatial memory. *Cell* **112**, 631–643 (2003).
172. Lee, H.-K., Takamiya, K., He, K., Song, L. & Huganir, R. L. Specific roles of AMPA receptor subunit GluR1 (GluA1) phosphorylation sites in regulating synaptic plasticity in the CA1 region of hippocampus. *Journal of Neurophysiology* **103**, 479–489 (2010).
173. Opazo, P. *et al.* CaMKII triggers the diffusional trapping of surface AMPARs through phosphorylation of stargazin. *Neuron* **67**, 239–252 (2010).
174. Boehm, J. *et al.* Synaptic incorporation of AMPA receptors during LTP is controlled by a PKC phosphorylation site on GluR1. *Neuron* **51**, 213–225 (2006).
175. Zamanillo, D. *et al.* Importance of AMPA receptors for hippocampal synaptic plasticity but not for spatial learning. *Science* **284**, 1805–1811 (1999).
176. Meng, Y., Zhang, Y. & Jia, Z. Synaptic transmission and plasticity in the absence of AMPA glutamate receptor GluR2 and GluR3. *Neuron* **39**, 163–176 (2003).
177. Kim, C.-H. *et al.* Persistent hippocampal CA1 LTP in mice lacking the C-terminal PDZ ligand of GluR1. *Nature Neuroscience* **8**, 985–987 (2005).
178. Granger, A. J. & Nicoll, R. A. LTD expression is independent of glutamate receptor subtype. *Front Synaptic Neurosci* **6**, 15 (2014).
179. Jensen, V. *et al.* A juvenile form of postsynaptic hippocampal long-term potentiation in mice deficient for the AMPA receptor subunit GluR-A. *The Journal of Physiology* **553**, 843–856 (2003).

180. Hoffman, D. A., Sprengel, R. & Sakmann, B. Molecular dissection of hippocampal theta-burst pairing potentiation. *Proceedings of the National Academy of Sciences* **99**, 7740–7745 (2002).
181. Reisel, D. *et al.* Spatial memory dissociations in mice lacking GluR1. *Nature Neuroscience* **5**, 868–873 (2002).
182. Jia, Z. *et al.* Enhanced LTP in mice deficient in the AMPA receptor GluR2. *Neuron* **17**, 945–956 (1996).
183. Gerlai, R., Henderson, J. T., Roder, J. C. & Jia, Z. Multiple behavioral anomalies in GluR2 mutant mice exhibiting enhanced LTP. *Behav. Brain Res.* **95**, 37–45 (1998).
184. Sinnen, B. L. *et al.* Optogenetic Control of Synaptic Composition and Function. *Neuron* **93**, 646–660.e5 (2017).
185. Matsuzaki, M., Honkura, N., Ellis-Davies, G. C. R. & Kasai, H. Structural basis of long-term potentiation in single dendritic spines. *Nature* **429**, 761–766 (2004).
186. Harvey, C. D. & Svoboda, K. Locally dynamic synaptic learning rules in pyramidal neuron dendrites. *Nature* **450**, 1195–1200 (2007).
187. Lee, S.-J. R., Escobedo-Lozoya, Y., Szatmari, E. M. & Yasuda, R. Activation of CaMKII in single dendritic spines during long-term potentiation. *Nature* **458**, 299–304 (2009).
188. Okamoto, K.-I., Nagai, T., Miyawaki, A. & Hayashi, Y. Rapid and persistent modulation of actin dynamics regulates postsynaptic reorganization underlying bidirectional plasticity. *Nature Neuroscience* **7**, 1104–1112 (2004).
189. Kopec, C. D., Li, B., Wei, W., Boehm, J. & Malinow, R. Glutamate receptor exocytosis and spine enlargement during chemically induced long-term potentiation. *Journal of Neuroscience* **26**, 2000–2009 (2006).
190. Tønnesen, J., Katona, G., Rózsa, B. & Nägerl, U. V. Spine neck plasticity regulates compartmentalization of synapses. *Nature Neuroscience* **17**, 678–685 (2014).
191. Renner, M., Choquet, D. & Triller, A. Control of the postsynaptic membrane viscosity. *Journal of Neuroscience* **29**, 2926–2937 (2009).
192. Santamaria, F., Wils, S., De Schutter, E. & Augustine, G. J. Anomalous diffusion in Purkinje cell dendrites caused by spines. *Neuron* **52**, 635–648 (2006).

193. Engert, F. & Bonhoeffer, T. Dendritic spine changes associated with hippocampal long-term synaptic plasticity. *Nature* **399**, 66–70 (1999).
194. Morris, R. G., Anderson, E., Lynch, G. S. & Baudry, M. Selective impairment of learning and blockade of long-term potentiation by an N-methyl-D-aspartate receptor antagonist, AP5. *Nature* **319**, 774–776 (1986).
195. Shimshek, D. R. *et al.* Forebrain-specific glutamate receptor B deletion impairs spatial memory but not hippocampal field long-term potentiation. *Journal of Neuroscience* **26**, 8428–8440 (2006).
196. Moser, E. I., Krobort, K. A., Moser, M. B. & Morris, R. G. Impaired spatial learning after saturation of long-term potentiation. *Science* **281**, 2038–2042 (1998).
197. Whitlock, J. R., Heynen, A. J., Shuler, M. G. & Bear, M. F. Learning Induces Long-Term Potentiation in the Hippocampus. *Science* **313**, 1093–1097 (2006).
198. Rogan, M. T., Stäubli, U. V. & LeDoux, J. E. Fear conditioning induces associative long-term potentiation in the amygdala. *Nature* **390**, 604–607 (1997).
199. Nabavi, S. *et al.* Engineering a memory with LTD and LTP. *Nature* **511**, 348–352 (2014).
200. Takemoto, K. *et al.* Optical inactivation of synaptic AMPA receptors erases fear memory. *Nat. Biotechnol.* **35**, 38–47 (2017).
201. Clem, R. L. & Huganir, R. L. Calcium-permeable AMPA receptor dynamics mediate fear memory erasure. *Science* **330**, 1108–1112 (2010).
202. Clem, R. L., Anggono, V. & Huganir, R. L. PICK1 regulates incorporation of calcium-permeable AMPA receptors during cortical synaptic strengthening. *Journal of Neuroscience* **30**, 6360–6366 (2010).
203. Bellone, C. & Lüscher, C. mGluRs induce a long-term depression in the ventral tegmental area that involves a switch of the subunit composition of AMPA receptors. *Eur. J. Neurosci.* **21**, 1280–1288 (2005).
204. Bellone, C. & Lüscher, C. Cocaine triggered AMPA receptor redistribution is reversed in vivo by mGluR-dependent long-term depression. *Nature Neuroscience* **9**, 636–641 (2006).
205. Conrad, K. L. *et al.* Formation of accumbens GluR2-lacking AMPA receptors mediates incubation of cocaine craving. *Nature* **454**, 118–121 (2008).

206. Collingridge, G. L., Kehl, S. J. & McLennan, H. Excitatory amino acids in synaptic transmission in the Schaffer collateral-commissural pathway of the rat hippocampus. *The Journal of Physiology* **334**, 33–46 (1983).
207. Dudek, S. M. & Bear, M. F. Homosynaptic long-term depression in area CA1 of hippocampus and effects of N-methyl-D-aspartate receptor blockade. *Proceedings of the National Academy of Sciences* **89**, 4363–4367 (1992).
208. Collingridge, G. L., Peineau, S., Howland, J. G. & Wang, Y. T. Long-term depression in the CNS. *Nat Rev Neurosci* **11**, 459–473 (2010).
209. Massey, P. V. & Bashir, Z. I. Long-term depression: multiple forms and implications for brain function. *Trends in Neurosciences* **30**, 176–184 (2007).
210. Palmer, M. J., Irving, A. J., Seabrook, G. R., Jane, D. E. & Collingridge, G. L. The group I mGlu receptor agonist DHPG induces a novel form of LTD in the CA1 region of the hippocampus. *Neuropharmacology* **36**, 1517–1532 (1997).
211. Mulkey, R. M. & Malenka, R. C. Mechanisms underlying induction of homosynaptic long-term depression in area CA1 of the hippocampus. *Neuron* **9**, 967–975 (1992).
212. Mulkey, R. M., Endo, S., Shenolikar, S. & Malenka, R. C. Involvement of a calcineurin/ inhibitor-1 phosphatase cascade in hippocampal long-term depression. *Nature* **369**, 486–488 (1994).
213. Lüthi, A. *et al.* Bi-directional modulation of AMPA receptor unitary conductance by synaptic activity. *BMC Neurosci* **5**, 44 (2004).
214. Mulkey, R. M., Herron, C. E. & Malenka, R. C. An essential role for protein phosphatases in hippocampal long-term depression. *Science* **261**, 1051–1055 (1993).
215. Lisman, J. A mechanism for the Hebb and the anti-Hebb processes underlying learning and memory. *Proceedings of the National Academy of Sciences* **86**, 9574–9578 (1989).
216. Malenka, R. C. & Bear, M. F. LTP and LTD: an embarrassment of riches. *Neuron* (2004).
217. Blanpied, T. A., Scott, D. B. & Ehlers, M. D. Dynamics and regulation of clathrin coats at specialized endocytic zones of dendrites and spines. *Neuron* **36**, 435–449 (2002).

218. Spacek, J. & Harris, K. M. Three-dimensional organization of smooth endoplasmic reticulum in hippocampal CA1 dendrites and dendritic spines of the immature and mature rat. *The Journal of Neuroscience* **17**, 190–203 (1997).
219. Rácz, B., Blanpied, T. A., Ehlers, M. D. & Weinberg, R. J. Lateral organization of endocytic machinery in dendritic spines. *Nature Neuroscience* **7**, 917–918 (2004).
220. Beattie, E. C. *et al.* Regulation of AMPA receptor endocytosis by a signaling mechanism shared with LTD. *Nature Neuroscience* **3**, 1291–1300 (2000).
221. Carroll, R. C. *et al.* Dynamin-dependent endocytosis of ionotropic glutamate receptors. *Proceedings of the National Academy of Sciences* **96**, 14112–14117 (1999).
222. Carroll, R. C., Lissin, D. V., Zastrow, von, M., Nicoll, R. A. & Malenka, R. C. Rapid redistribution of glutamate receptors contributes to long-term depression in hippocampal cultures. *Nature Neuroscience* **2**, 454–460 (1999).
223. Ehlers, M. D. Reinsertion or degradation of AMPA receptors determined by activity-dependent endocytic sorting. *Neuron* **28**, 511–525 (2000).
224. Heynen, A. J., Quinlan, E. M., Bae, D. C. & Bear, M. F. Bidirectional, activity-dependent regulation of glutamate receptors in the adult hippocampus in vivo. *Neuron* **28**, 527–536 (2000).
225. Zhou, Q., Xiao, M. & Nicoll, R. A. Contribution of cytoskeleton to the internalization of AMPA receptors. *Proceedings of the National Academy of Sciences* **98**, 1261–1266 (2001).
226. Kim, C. H. & Lisman, J. E. A labile component of AMPA receptor-mediated synaptic transmission is dependent on microtubule motors, actin, and N-ethylmaleimide-sensitive factor. *Journal of Neuroscience* **21**, 4188–4194 (2001).
227. Seidenman, K. J., Steinberg, J. P., Haganir, R. & Malinow, R. Glutamate receptor subunit 2 Serine 880 phosphorylation modulates synaptic transmission and mediates plasticity in CA1 pyramidal cells. *Journal of Neuroscience* **23**, 9220–9228 (2003).
228. Daw, M. I. *et al.* PDZ proteins interacting with C-terminal GluR2/3 are involved in a PKC-dependent regulation of AMPA receptors at hippocampal synapses. *Neuron* **28**, 873–886 (2000).

229. Selcher, J. C., Xu, W., Hanson, J. E., Malenka, R. C. & Madison, D. V. Glutamate receptor subunit GluA1 is necessary for long-term potentiation and synapse unsilencing, but not long-term depression in mouse hippocampus. *Brain Research* **1435**, 8–14 (2012).
230. Kim, J. J., Foy, M. R. & Thompson, R. F. Behavioral stress modifies hippocampal plasticity through N-methyl-D-aspartate receptor activation. *Proceedings of the National Academy of Sciences* **93**, 4750–4753 (1996).
231. Yang, C.-H., Huang, C.-C. & Hsu, K.-S. Behavioral stress enhances hippocampal CA1 long-term depression through the blockade of the glutamate uptake. *Journal of Neuroscience* **25**, 4288–4293 (2005).
232. Wong, T. P. *et al.* Hippocampal long-term depression mediates acute stress-induced spatial memory retrieval impairment. *Proceedings of the National Academy of Sciences* **104**, 11471–11476 (2007).
233. Xu, L., Anwyl, R. & Rowan, M. J. Behavioural stress facilitates the induction of long-term depression in the hippocampus. *Nature* **387**, 497–500 (1997).
234. Staubli, U. & Scafidi, J. Studies on long-term depression in area CA1 of the anesthetized and freely moving rat. *The Journal of Neuroscience* **17**, 4820–4828 (1997).
235. Sidorov, M. S., Kaplan, E. S., Osterweil, E. K., Lindemann, L. & Bear, M. F. Metabotropic glutamate receptor signaling is required for NMDA receptor-dependent ocular dominance plasticity and LTD in visual cortex. *Proc. Natl. Acad. Sci. U.S.A.* **112**, 12852–12857 (2015).
236. Andersen, N., Krauth, N. & Nabavi, S. Hebbian plasticity in vivo: relevance and induction. *Current Opinion in Neurobiology* **45**, 188–192 (2017).
237. Volk, L., Chiu, S.-L., Sharma, K. & Huganir, R. L. Glutamate synapses in human cognitive disorders. *Annu. Rev. Neurosci.* **38**, 127–149 (2015).
238. Herring, B. E. & Nicoll, R. A. Long-Term Potentiation: From CaMKII to AMPA Receptor Trafficking. *Annu. Rev. Physiol.* **78**, 351–365 (2016).
239. Jurado, S. AMPA Receptor Trafficking in Natural and Pathological Aging. *Front Mol Neurosci* **10**, 446 (2017).
240. Wang, L. Y., Salter, M. W. & MacDonald, J. F. Regulation of kainate receptors by cAMP-dependent protein kinase and phosphatases. *Science* **253**, 1132–1135 (1991).

241. Smith, F. D. *et al.* Intrinsic disorder within an AKAP-protein kinase A complex guides local substrate phosphorylation. *eLife* **2**, e01319 (2013).
242. Smith, F. D. *et al.* Local protein kinase A action proceeds through intact holoenzymes. *Science* **356**, 1288–1293 (2017).
243. Coghlan, V. M. *et al.* Association of protein kinase A and protein phosphatase 2B with a common anchoring protein. *Science* **267**, 108–111 (1995).
244. Carr, D. W., Stofko-Hahn, R. E., Fraser, I. D., Cone, R. D. & Scott, J. D. Localization of the cAMP-dependent protein kinase to the postsynaptic densities by A-kinase anchoring proteins. Characterization of AKAP 79. *J. Biol. Chem.* **267**, 16816–16823 (1992).
245. Gomez, L. L., Alam, S., Smith, K. E., Horne, E. & Dell'Acqua, M. L. Regulation of A-kinase anchoring protein 79/150-cAMP-dependent protein kinase postsynaptic targeting by NMDA receptor activation of calcineurin and remodeling of dendritic actin. *Journal of Neuroscience* **22**, 7027–7044 (2002).
246. Li, H. *et al.* Balanced interactions of calcineurin with AKAP79 regulate Ca²⁺-calcineurin-NFAT signaling. *Nat. Struct. Mol. Biol.* **19**, 337–345 (2012).
247. Keith, D. J. *et al.* Palmitoylation of A-kinase anchoring protein 79/150 regulates dendritic endosomal targeting and synaptic plasticity mechanisms. *Journal of Neuroscience* **32**, 7119–7136 (2012).
248. Woolfrey, K. M., Sanderson, J. L. & Dell'Acqua, M. L. The palmitoyl acyltransferase DHHC2 regulates recycling endosome exocytosis and synaptic potentiation through palmitoylation of AKAP79/150. *Journal of Neuroscience* **35**, 442–456 (2015).
249. Dell'Acqua, M. L., Faux, M. C., Thorburn, J., Thorburn, A. & Scott, J. D. Membrane-targeting sequences on AKAP79 bind phosphatidylinositol-4, 5-bisphosphate. *EMBO J.* **17**, 2246–2260 (1998).
250. Hoshi, N. *et al.* AKAP150 signaling complex promotes suppression of the M-current by muscarinic agonists. *Nature Neuroscience* **6**, 564–571 (2003).
251. Zhang, J., Bal, M., Bierbower, S., Zaika, O. & Shapiro, M. S. AKAP79/150 signal complexes in G-protein modulation of neuronal ion channels. *Journal of Neuroscience* **31**, 7199–7211 (2011).
252. Schnizler, K. *et al.* Protein kinase A anchoring via AKAP150 is essential for TRPV1 modulation by forskolin and prostaglandin E2 in mouse sensory neurons. *Journal of Neuroscience* **28**, 4904–4917 (2008).

253. Wild, A. R. & Dell'Acqua, M. L. Potential for therapeutic targeting of AKAP signaling complexes in nervous system disorders. *Pharmacol. Ther.* **185**, 99–121 (2018).
254. Dacher, M., Gouty, S., Dash, S., Cox, B. M. & Nugent, F. S. A-kinase anchoring protein-calcineurin signaling in long-term depression of GABAergic synapses. *Journal of Neuroscience* **33**, 2650–2660 (2013).
255. Carr, D. W., Hausken, Z. E., Fraser, I. D., Stofko-Hahn, R. E. & Scott, J. D. Association of the type II cAMP-dependent protein kinase with a human thyroid RII-anchoring protein. Cloning and characterization of the RII-binding domain. *J. Biol. Chem.* **267**, 13376–13382 (1992).
256. Dell'Acqua, M. L., Dodge, K. L., Tavalin, S. J. & Scott, J. D. Mapping the Protein Phosphatase-2B Anchoring Site on AKAP79: BINDING AND INHIBITION OF PHOSPHATASE ACTIVITY ARE MEDIATED BY RESIDUES 315-360. *Journal of Biological Chemistry* **277**, 48796–48802 (2002).
257. Oliveria, S. F., Dell'Acqua, M. L. & Sather, W. A. AKAP79/150 Anchoring of Calcineurin Controls Neuronal L-Type Ca²⁺ Channel Activity and Nuclear Signaling. *Neuron* **55**, 261–275 (2007).
258. Oliveria, S. F., Dittmer, P. J., Youn, D.-H., Dell'Acqua, M. L. & Sather, W. A. Localized calcineurin confers Ca²⁺-dependent inactivation on neuronal L-type Ca²⁺ channels. *Journal of Neuroscience* **32**, 15328–15337 (2012).
259. Klauck, T. M., Faux, M. C., Labudda, K. & Langeberg, L. K. Coordination of three signaling enzymes by AKAP79, a mammalian scaffold protein. *Science* (1996).
260. Faux, M. C. *et al.* Mechanism of A-kinase-anchoring protein 79 (AKAP79) and protein kinase C interaction. *Biochem. J.* **343 Pt 2**, 443–452 (1999).
261. Faux, M. C. & Scott, J. D. Regulation of the AKAP79-protein kinase C interaction by Ca²⁺/Calmodulin. *J. Biol. Chem.* **272**, 17038–17044 (1997).
262. Gorski, J. A., Gomez, L. L., Scott, J. D. & Dell'Acqua, M. L. Association of an A-kinase-anchoring protein signaling scaffold with cadherin adhesion molecules in neurons and epithelial cells. *Mol. Biol. Cell* **16**, 3574–3590 (2005).
263. Tavalin, S. J. AKAP79 Selectively Enhances Protein Kinase C Regulation of GluR1 at a Ca²⁺-Calmodulin-dependent Protein Kinase II/Protein Kinase C Site. *Journal of Biological Chemistry* **283**, 11445–11452 (2008).

264. Delint-Ramirez, I. *et al.* Palmitoylation targets AKAP79 protein to lipid rafts and promotes its regulation of calcium-sensitive adenylyl cyclase type 8. *Journal of Biological Chemistry* **286**, 32962–32975 (2011).
265. Woolfrey, K. M. *et al.* CaMKII regulates the depalmitoylation and synaptic removal of the scaffold protein AKAP79/150 to mediate structural long-term depression. *Journal of Biological Chemistry* **293**, 1551–1567 (2018).
266. Bhattacharyya, S., Biou, V., Xu, W., Schlüter, O. & Malenka, R. C. A critical role for PSD-95/AKAP interactions in endocytosis of synaptic AMPA receptors. *Nature Neuroscience* **12**, 172–181 (2009).
267. Colledge, M. *et al.* Targeting of PKA to glutamate receptors through a MAGUK-AKAP complex. *Neuron* **27**, 107–119 (2000).
268. Nikandrova, Y. A., Jiao, Y., Baucum, A. J., Tavalin, S. J. & Colbran, R. J. Ca²⁺/calmodulin-dependent protein kinase II binds to and phosphorylates a specific SAP97 splice variant to disrupt association with AKAP79/150 and modulate alpha-amino-3-hydroxy-5-methyl-4-isoxazolepropionic acid-type glutamate receptor (AMPA) activity. *Journal of Biological Chemistry* **285**, 923–934 (2010).
269. Robertson, H. R., Gibson, E. S., Benke, T. A. & Dell'Acqua, M. L. Regulation of postsynaptic structure and function by an A-kinase anchoring protein-membrane-associated guanylate kinase scaffolding complex. *Journal of Neuroscience* **29**, 7929–7943 (2009).
270. Bauman, A. L. *et al.* Dynamic Regulation of cAMP Synthesis through Anchored PKA-Adenylyl Cyclase V/VI Complexes. *Molecular Cell* **23**, 925–931 (2006).
271. Efendiev, R. *et al.* AKAP79 interacts with multiple adenylyl cyclase (AC) isoforms and scaffolds AC5 and -6 to alpha-amino-3-hydroxyl-5-methyl-4-isoxazole-propionate (AMPA) receptors. *Journal of Biological Chemistry* **285**, 14450–14458 (2010).
272. Jeske, N. A. *et al.* A-kinase anchoring protein mediates TRPV1 thermal hyperalgesia through PKA phosphorylation of TRPV1. *Pain* **138**, 604–616 (2008).
273. Lin, L., Sun, W., Kung, F., Dell'Acqua, M. L. & Hoffman, D. A. AKAP79/150 impacts intrinsic excitability of hippocampal neurons through phospho-regulation of A-type K⁺ channel trafficking. *Journal of Neuroscience* **31**, 1323–1332 (2011).

274. Fraser, I. D. *et al.* Assembly of an A kinase-anchoring protein-beta(2)-adrenergic receptor complex facilitates receptor phosphorylation and signaling. *Curr. Biol.* **10**, 409–412 (2000).
275. Sanderson, J. L. *et al.* AKAP150-anchored calcineurin regulates synaptic plasticity by limiting synaptic incorporation of Ca²⁺-permeable AMPA receptors. *Journal of Neuroscience* **32**, 15036–15052 (2012).
276. Rosenmund, C. *et al.* Anchoring of protein kinase A is required for modulation of AMPA/kainate receptors on hippocampal neurons. *Nature* **368**, 853–856 (1994).
277. Tavalin, S. J. *et al.* Regulation of GluR1 by the A-kinase anchoring protein 79 (AKAP79) signaling complex shares properties with long-term depression. *Journal of Neuroscience* **22**, 3044–3051 (2002).
278. Hoshi, N., Langeberg, L. K. & Scott, J. D. Distinct enzyme combinations in AKAP signalling complexes permit functional diversity. *Nat Cell Biol* **7**, 1066–1073 (2005).
279. Hayashi, T., Rumbaugh, G. & Huganir, R. L. Differential Regulation of AMPA Receptor Subunit Trafficking by Palmitoylation of Two Distinct Sites. *Neuron* **47**, 709–723 (2005).
280. Jurado, S., Biou, V. & Malenka, R. C. A calcineurin/AKAP complex is required for NMDA receptor-dependent long-term depression. *Nature Neuroscience* **13**, 1053–1055 (2010).
281. Tunquist, B. J. *et al.* Loss of AKAP150 perturbs distinct neuronal processes in mice. *Proc. Natl. Acad. Sci. U.S.A.* **105**, 12557–12562 (2008).
282. Weisenhaus, M. *et al.* Mutations in AKAP5 disrupt dendritic signaling complexes and lead to electrophysiological and behavioral phenotypes in mice. *PLoS ONE* **5**, e10325 (2010).
283. Lu, Y. *et al.* AKAP150-anchored PKA activity is important for LTD during its induction phase. *The Journal of Physiology* **586**, 4155–4164 (2008).
284. Schmidt, M. F. & Schlesinger, M. J. Fatty acid binding to vesicular stomatitis virus glycoprotein: a new type of post-translational modification of the viral glycoprotein. *Cell* **17**, 813–819 (1979).
285. Gottlieb, C. D. & Linder, M. E. Structure and function of DHHC protein S-acyltransferases. *Biochem. Soc. Trans.* **45**, 923–928 (2017).

286. Staufenbiel, M. Ankyrin-bound fatty acid turns over rapidly at the erythrocyte plasma membrane. *Mol. Cell. Biol.* **7**, 2981–2984 (1987).
287. Sezgin, E., Levental, I., Mayor, S. & Eggeling, C. The mystery of membrane organization: composition, regulation and roles of lipid rafts. *Nat Rev Mol Cell Biol* **18**, 361–374 (2017).
288. Ernst, A. M. *et al.* S-Palmitoylation Sorts Membrane Cargo for Anterograde Transport in the Golgi. *Dev. Cell* **47**, 479–493.e7 (2018).
289. Eisenberg, S. *et al.* The role of palmitoylation in regulating Ras localization and function. *Biochem. Soc. Trans.* **41**, 79–83 (2013).
290. Mitchell, D. A. Protein palmitoylation by a family of DHHC protein S-acyltransferases. *The Journal of Lipid Research* **47**, 1118–1127 (2006).
291. Linder, M. E. & Deschenes, R. J. New insights into the mechanisms of protein palmitoylation. *Biochemistry* **42**, 4311–4320 (2003).
292. Linder, M. E. & Deschenes, R. J. Model organisms lead the way to protein palmitoyltransferases. *Journal of Cell Science* **117**, 521–526 (2004).
293. Roth, A. F. *et al.* Global Analysis of Protein Palmitoylation in Yeast. *Cell* **125**, 1003–1013 (2006).
294. Fukata, Y. & Fukata, M. Protein palmitoylation in neuronal development and synaptic plasticity. *Nat Rev Neurosci* **11**, 161–175 (2010).
295. Linder, M. E. & Deschenes, R. J. Palmitoylation: policing protein stability and traffic. *Nat Rev Mol Cell Biol* **8**, 74–84 (2007).
296. Mitchell, D. A., Mitchell, G., Ling, Y., Budde, C. & Deschenes, R. J. Mutational analysis of *Saccharomyces cerevisiae* Erf2 reveals a two-step reaction mechanism for protein palmitoylation by DHHC enzymes. *Journal of Biological Chemistry* **285**, 38104–38114 (2010).
297. Jennings, B. C. & Linder, M. E. DHHC protein S-acyltransferases use similar ping-pong kinetic mechanisms but display different acyl-CoA specificities. *Journal of Biological Chemistry* **287**, 7236–7245 (2012).
298. Rana, M. S. *et al.* Fatty acyl recognition and transfer by an integral membrane S-acyltransferase. *Science* **359**, (2018).
299. Rana, M. S., Lee, C.-J. & Banerjee, A. The molecular mechanism of DHHC protein acyltransferases. *Biochem. Soc. Trans.* **47**, 157–167 (2019).

300. Charollais, J. & Van Der Goot, F. G. Palmitoylation of membrane proteins (Review). *Mol. Membr. Biol.* **26**, 55–66 (2009).
301. Ohno, Y., Kihara, A., Sano, T. & Igarashi, Y. Intracellular localization and tissue-specific distribution of human and yeast DHHC cysteine-rich domain-containing proteins. *Biochim. Biophys. Acta* **1761**, 474–483 (2006).
302. Fukata, Y., Murakami, T., Yokoi, N. & Fukata, M. Local Palmitoylation Cycles and Specialized Membrane Domain Organization. *Curr Top Membr* **77**, 97–141 (2016).
303. Greaves, J. & Chamberlain, L. H. DHHC palmitoyl transferases: substrate interactions and (patho)physiology. *Trends in Biochemical Sciences* **36**, 245–253 (2011).
304. Noritake, J. *et al.* Mobile DHHC palmitoylating enzyme mediates activity-sensitive synaptic targeting of PSD-95. *The Journal of Cell Biology* **186**, 147–160 (2009).
305. Linder, M. E. & Jennings, B. C. Mechanism and function of DHHC S-acyltransferases. *Biochem. Soc. Trans.* **41**, 29–34 (2013).
306. Yokoi, N. *et al.* Identification of PSD-95 Depalmitoylating Enzymes. *Journal of Neuroscience* **36**, 6431–6444 (2016).
307. Won, S. J., Cheung See Kit, M. & Martin, B. R. Protein depalmitoylases. *Crit. Rev. Biochem. Mol. Biol.* **53**, 83–98 (2018).
308. Heinonen, O. *et al.* Expression of Palmitoyl Protein Thioesterase in Neurons. *Molecular Genetics and Metabolism* **69**, 123–129 (2000).
309. Ahtiainen, L., Van Diggelen, O. P., Jalanko, A. & Kopra, O. Palmitoyl protein thioesterase 1 is targeted to the axons in neurons. *J. Comp. Neurol.* **455**, 368–377 (2002).
310. Lord, C. C., Thomas, G. & Brown, J. M. Mammalian alpha beta hydrolase domain (ABHD) proteins: Lipid metabolizing enzymes at the interface of cell signaling and energy metabolism. *Biochim. Biophys. Acta* **1831**, 792–802 (2013).
311. Lin, D. & Conibear, E. ABHD17 proteins are novel protein depalmitoylases that regulate N-Ras palmitate turnover and subcellular localization. *eLife* (2015). doi:10.7554/eLife.11306.001

312. Lu, J.-Y. & Hofmann, S. L. Thematic review series: lipid posttranslational modifications. Lysosomal metabolism of lipid-modified proteins. *The Journal of Lipid Research* **47**, 1352–1357 (2006).
313. Zaręba-Kozioł, M., Figiel, I., Bartkowiak-Kaczmarek, A. & Włodarczyk, J. Insights Into Protein S-Palmitoylation in Synaptic Plasticity and Neurological Disorders: Potential and Limitations of Methods for Detection and Analysis. *Front Mol Neurosci* **11**, 175 (2018).
314. Bizzozero, O. A. Chemical analysis of acylation sites and species. *Meth. Enzymol.* **250**, 361–379 (1995).
315. Magee, A. I., Wootton, J. & de Bony, J. Detecting radiolabeled lipid-modified proteins in polyacrylamide gels. *Meth. Enzymol.* **250**, 330–336 (1995).
316. Martin, B. R. & Cravatt, B. F. Large-scale profiling of protein palmitoylation in mammalian cells. *Nat Meth* **6**, 135–138 (2009).
317. Yount, J. S., Zhang, M. M. & Hang, H. C. Visualization and Identification of Fatty Acylated Proteins Using Chemical Reporters. *Curr Protoc Chem Biol* **3**, 65–79 (2011).
318. Zhang, M. M. *et al.* Tandem fluorescence imaging of dynamic S -acylation and protein turnover. *Proc. Natl. Acad. Sci. U.S.A.* **107**, 8627–8632 (2010).
319. Martin, B. R. Chemical approaches for profiling dynamic palmitoylation. *Biochem. Soc. Trans.* **41**, 43–49 (2013).
320. Martin, B. R., Wang, C., Adibekian, A., Tully, S. E. & Cravatt, B. F. Global profiling of dynamic protein palmitoylation. *Nat Meth* **9**, 84–89 (2011).
321. Gao, X. & Hannoush, R. N. Single-cell in situ imaging of palmitoylation in fatty-acylated proteins. *Nat Protoc* **9**, 2607–2623 (2014).
322. Drisdell, R. C. & Green, W. N. Labeling and quantifying sites of protein palmitoylation. *BioTechniques* **36**, 276–285 (2004).
323. Kang, R. *et al.* Neural palmitoyl-proteomics reveals dynamic synaptic palmitoylation. *Nature* **456**, 904–909 (2008).
324. Sato, I. *et al.* Differential trafficking of Src, Lyn, Yes and Fyn is specified by the state of palmitoylation in the SH4 domain. *Journal of Cell Science* **122**, 965–975 (2009).

325. Thomas, G. M., Hayashi, T., Chiu, S.-L., Chen, C.-M. & Huganir, R. L. Palmitoylation by DHHC5/8 targets GRIP1 to dendritic endosomes to regulate AMPA-R trafficking. *Neuron* **73**, 482–496 (2012).
326. Forrester, M. T. *et al.* Site-specific analysis of protein S-acylation by resin-assisted capture. *J. Lipid Res.* **52**, 393–398 (2011).
327. Zhou, B., An, M., Freeman, M. R. & Yang, W. Technologies and Challenges in Proteomic Analysis of Protein S-acylation. *J Proteomics Bioinform* **7**, 256–263 (2014).
328. Percher, A. *et al.* Mass-tag labeling reveals site-specific and endogenous levels of protein S-fatty acylation. *Proc. Natl. Acad. Sci. U.S.A.* **113**, 4302–4307 (2016).
329. Sanders, S. S. *et al.* Curation of the Mammalian Palmitoylome Indicates a Pivotal Role for Palmitoylation in Diseases and Disorders of the Nervous System and Cancers. *PLoS Comput. Biol.* **11**, e1004405 (2015).
330. Naumenko, V. S. & Ponimaskin, E. Palmitoylation as a Functional Regulator of Neurotransmitter Receptors. *Neural Plast.* **2018**, 5701348 (2018).
331. Matt, L., Kim, K., Chowdhury, D. & Hell, J. W. Role of Palmitoylation of Postsynaptic Proteins in Promoting Synaptic Plasticity. *Front Mol Neurosci* **12**, 23119 (2019).
332. El-Husseini, A. E.-D. *et al.* Synaptic strength regulated by palmitate cycling on PSD-95. *Cell* **108**, 849–863 (2002).
333. Globa, A. K. & Bamji, S. X. Protein palmitoylation in the development and plasticity of neuronal connections. *Current Opinion in Neurobiology* **45**, 210–220 (2017).
334. Fukata, Y. *et al.* Local palmitoylation cycles define activity-regulated postsynaptic subdomains. *The Journal of Cell Biology* **202**, 145–161 (2013).
335. Zhang, Y. *et al.* Capping of the N-terminus of PSD-95 by calmodulin triggers its postsynaptic release. *EMBO J.* **33**, 1341–1353 (2014).
336. Topinka, J. R. & Brecht, D. S. N-terminal palmitoylation of PSD-95 regulates association with cell membranes and interaction with K⁺ channel Kv1.4. *Neuron* **20**, 125–134 (1998).
337. Fukata, M., Fukata, Y., Adesnik, H., Nicoll, R. A. & Brecht, D. S. Identification of PSD-95 palmitoylating enzymes. *Neuron* (2004).

338. Cho, E. & Park, M. Palmitoylation in Alzheimer's disease and other neurodegenerative diseases. *Pharmacol. Res.* **111**, 133–151 (2016).
339. Bhattacharyya, R., Barren, C. & Kovacs, D. M. Palmitoylation of amyloid precursor protein regulates amyloidogenic processing in lipid rafts. *Journal of Neuroscience* **33**, 11169–11183 (2013).
340. Andrew, R. J. *et al.* Lack of BACE1 S-palmitoylation reduces amyloid burden and mitigates memory deficits in transgenic mouse models of Alzheimer's disease. *Proc. Natl. Acad. Sci. U.S.A.* **114**, E9665–E9674 (2017).
341. Huang, K. *et al.* Huntingtin-interacting protein HIP14 is a palmitoyl transferase involved in palmitoylation and trafficking of multiple neuronal proteins. *Neuron* **44**, 977–986 (2004).
342. Yanai, A. *et al.* Palmitoylation of huntingtin by HIP14 is essential for its trafficking and function. *Nature Neuroscience* **9**, 824–831 (2006).
343. Bennett, M. J. & Rakheja, D. The neuronal ceroid-lipofuscinoses. *Dev Disabil Res Rev* **17**, 254–259 (2013).
344. Jalanko, A. *et al.* Mice with Ppt1Deltaex4 mutation replicate the INCL phenotype and show an inflammation-associated loss of interneurons. *Neurobiology of Disease* **18**, 226–241 (2005).
345. Gupta, P. *et al.* Disruption of PPT1 or PPT2 causes neuronal ceroid lipofuscinosis in knockout mice. *Proceedings of the National Academy of Sciences* **98**, 13566–13571 (2001).
346. Mukai, J. *et al.* Molecular substrates of altered axonal growth and brain connectivity in a mouse model of schizophrenia. *Neuron* **86**, 680–695 (2015).
347. Mukai, J. *et al.* Evidence that the gene encoding ZDHHC8 contributes to the risk of schizophrenia. *Nat Genet* **36**, 725–731 (2004).
348. Mukai, J. *et al.* Palmitoylation-dependent neurodevelopmental deficits in a mouse model of 22q11 microdeletion. *Nature Publishing Group* **11**, 1302–1310 (2008).
349. Li, Y. *et al.* DHHHC5 interacts with PDZ domain 3 of post-synaptic density-95 (PSD-95) protein and plays a role in learning and memory. *Journal of Biological Chemistry* **285**, 13022–13031 (2010).
350. Brigidi, G. S. *et al.* Palmitoylation of δ -catenin by DHHHC5 mediates activity-induced synapse plasticity. *Nature Neuroscience* **17**, 522–532 (2014).

351. Raymond, F. L. *et al.* Mutations in ZDHHC9, which encodes a palmitoyltransferase of NRAS and HRAS, cause X-linked mental retardation associated with a Marfanoid habitus. *Am. J. Hum. Genet.* **80**, 982–987 (2007).
352. Aoto, J., Nam, C. I., Poon, M. M., Ting, P. & Chen, L. Synaptic signaling by all-trans retinoic acid in homeostatic synaptic plasticity. *Neuron* **60**, 308–320 (2008).
353. Soares, C., Lee, K. F. H., Nassrallah, W. & Beique, J.-C. Differential subcellular targeting of glutamate receptor subtypes during homeostatic synaptic plasticity. *Journal of Neuroscience* **33**, 13547–13559 (2013).
354. Sanderson, J. L., Scott, J. D. & Dell'Acqua, M. L. Control of Homeostatic Synaptic Plasticity by AKAP-Anchored Kinase and Phosphatase Regulation of Ca²⁺-Permeable AMPA Receptors. *Journal of Neuroscience* **38**, 2863–2876 (2018).
355. Wolf, M. E. Synaptic mechanisms underlying persistent cocaine craving. *Nat Rev Neurosci* **17**, 351–365 (2016).
356. Esteban, J. A. *et al.* PKA phosphorylation of AMPA receptor subunits controls synaptic trafficking underlying plasticity. *Nature Neuroscience* **6**, 136–143 (2003).
357. Hu, H. *et al.* Emotion enhances learning via norepinephrine regulation of AMPA-receptor trafficking. *Cell* **131**, 160–173 (2007).
358. Qian, H. *et al.* β 2-Adrenergic receptor supports prolonged theta tetanus-induced LTP. *Journal of Neurophysiology* **107**, 2703–2712 (2012).
359. Sun, X., Zhao, Y. & Wolf, M. E. Dopamine receptor stimulation modulates AMPA receptor synaptic insertion in prefrontal cortex neurons. *Journal of Neuroscience* **25**, 7342–7351 (2005).
360. Diering, G. H., Gustina, A. S. & Huganir, R. L. PKA-GluA1 Coupling via AKAP5 Controls AMPA Receptor Phosphorylation and Cell-Surface Targeting during Bidirectional Homeostatic Plasticity. *Neuron* 1–16 (2014).
doi:10.1016/j.neuron.2014.09.024
361. Zhang, M. *et al.* Adenylyl cyclase anchoring by a kinase anchor protein AKAP5 (AKAP79/150) is important for postsynaptic β -adrenergic signaling. *Journal of Biological Chemistry* **288**, 17918–17931 (2013).
362. Kay, H. Y., Greene, D. L., Kang, S., Kosenko, A. & Hoshi, N. M-current preservation contributes to anticonvulsant effects of valproic acid. *J. Clin. Invest.* **125**, 3904–3914 (2015).

363. Smith, K. E., Gibson, E. S. & Dell'Acqua, M. L. cAMP-dependent protein kinase postsynaptic localization regulated by NMDA receptor activation through translocation of an A-kinase anchoring protein scaffold protein. *Journal of Neuroscience* **26**, 2391–2402 (2006).
364. Grosshans, D. R., Clayton, D. A., Coultrap, S. J. & Browning, M. D. LTP leads to rapid surface expression of NMDA but not AMPA receptors in adult rat CA1. *Nature Neuroscience* **5**, 27–33 (2002).
365. Brandao, K. E., Dell'Acqua, M. L. & Levinson, S. R. A-kinase anchoring protein 150 expression in a specific subset of TRPV1- and CaV 1.2-positive nociceptive rat dorsal root ganglion neurons. *J. Comp. Neurol.* **520**, 81–99 (2012).
366. Kim, B. G., Dai, H.-N., McAtee, M., Vicini, S. & Bregman, B. S. Labeling of dendritic spines with the carbocyanine dye Dil for confocal microscopic imaging in lightly fixed cortical slices. *Journal of Neuroscience Methods* **162**, 237–243 (2007).
367. Meyer, S. A. *et al.* Super-resolution imaging of ciliary microdomains in isolated olfactory sensory neurons using a custom two-color stimulated emission depletion microscope. *J Biomed Opt* **21**, 66017 (2016).
368. Crosby, K. C. *et al.* Nanoscale Subsynaptic Domains Underlie the Organization of the Inhibitory Synapse. *CellReports* **26**, 3284–3297.e3 (2019).
369. Paul, G., Cardinale, J. & Sbalzarini, I. F. Coupling Image Restoration and Segmentation: A Generalized Linear Model/Bregman Perspective. *Int J Comput Vis* **104**, 69–93 (2013).
370. Rizk, A. *et al.* Segmentation and quantification of subcellular structures in fluorescence microscopy images using Squassh. *Nat Protoc* **9**, 586–596 (2014).
371. Kollerker, A. *et al.* Glutamatergic plasticity by synaptic delivery of GluR-B(long)-containing AMPA receptors. *Neuron* **40**, 1199–1212 (2003).
372. Norris, C. M., Korol, D. L. & Foster, T. C. Increased susceptibility to induction of long-term depression and long-term potentiation reversal during aging. *The Journal of Neuroscience* **16**, 5382–5392 (1996).
373. Ashby, M. C. *et al.* Removal of AMPA receptors (AMPA receptors) from synapses is preceded by transient endocytosis of extrasynaptic AMPARs. *Journal of Neuroscience* **24**, 5172–5176 (2004).
374. Kim, S. *et al.* Network compensation of cyclic GMP-dependent protein kinase II knockout in the hippocampus by Ca²⁺-permeable AMPA receptors. *Proc. Natl. Acad. Sci. U.S.A.* **112**, 3122–3127 (2015).

375. O'Brien, R. J. *et al.* Activity-dependent modulation of synaptic AMPA receptor accumulation. *Neuron* **21**, 1067–1078 (1998).
376. Turrigiano, G. G., Leslie, K. R., Desai, N. S., Rutherford, L. C. & Nelson, S. B. Activity-dependent scaling of quantal amplitude in neocortical neurons. *Nature* **391**, 892–896 (1998).
377. Iwata, K., Sun, Q. & Turrigiano, G. G. Rapid synaptic scaling induced by changes in postsynaptic firing. *Neuron* **57**, 819–826 (2008).
378. Lee, K. Y. & Chung, H. J. NMDA receptors and L-type voltage-gated Ca²⁺ channels mediate the expression of bidirectional homeostatic intrinsic plasticity in cultured hippocampal neurons. *Neuroscience* **277**, 610–623 (2014).
379. Hou, Q., Zhang, D., Jarzylo, L., Huganir, R. L. & Man, H.-Y. Homeostatic regulation of AMPA receptor expression at single hippocampal synapses. *Proc. Natl. Acad. Sci. U.S.A.* **105**, 775–780 (2008).
380. Maghsoodi, B. *et al.* Retinoic acid regulates RARalpha-mediated control of translation in dendritic RNA granules during homeostatic synaptic plasticity. *Proc. Natl. Acad. Sci. U.S.A.* **105**, 16015–16020 (2008).
381. Frey, U. & Morris, R. G. M. Synaptic tagging and long-term potentiation. *Nature* **385**, 533–536 (1997).
382. Frey, U. & Morris, R. G. Synaptic tagging: implications for late maintenance of hippocampal long-term potentiation. *Trends in Neurosciences* **21**, 181–188 (1998).
383. Coultrap, S. J. *et al.* Autonomous CaMKII mediates both LTP and LTD using a mechanism for differential substrate site selection. *CellReports* **6**, 431–437 (2014).